MODELING AND SIMULATION OF HYBRID DISTILLATION COLUMN

A DISSERTATION

*Submitted in partial fulfillment of the
requirements for the award of the degree*
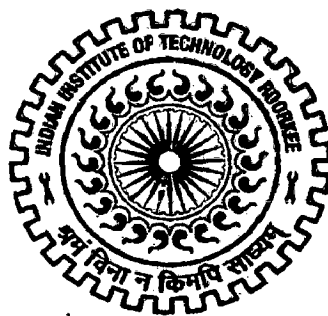of
MASTER OF TECHNOLOGY
in
CHEMICAL ENGINEERING
(With Specialization in Computer Aided Process Plant Design)

By

SUKALYAN GHOSH

DEPARTMENT OF CHEMICAL ENGINEERING
INDIAN INSTITUTE OF TECHNOLOGY ROORKEE
ROORKEE - 247 667 (INDIA)
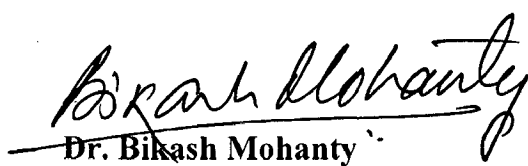JUNE, 2007

CANDIDATE'S DECLARATION

I here by declare that the work which is being presented in the thesis report entitled **"MODELING AND SIMULATION OF HYBRID DISTILLATION COLUMN"**, in partial fulfillment of the requirement for the award of the degree of Master of Technology in Chemical Engineering with specialization in Computer Aided Process Plant Design, submitted in the Department of Chemical Engineering ,Indian Institute of Technology Roorkee, Roorkee, is an authentic record of my own work carried out during the period form May 2006 to July 27, 2007, under the supervision of **Dr. Bikash Mohanty**, Professor, Department of Chemical Engineering ,Indian Institute of Technology Roorkee, Roorkee.

Date: 27/6/07

Place: Roorkee

(Sukalyan Ghosh)

CERTIFICATE

This is to certify that the above statement made by the candidate is correct to the best of my knowledge.

Dr. Bikash Mohanty

Professor

Dept. of Chemical Engineering

Indian Institute of Technology Roorkee

Roorkee – 247667, Uttaranchal

India

ACKNOWLEDGEMENTS

ABSTRACT

Distillation is an energy intensive process and is extensively used in process industry to separate liquid mixtures. For industries dealing with liquid products such as alcohol, ether, and close boiling liquid mixtures like propane-propylene, benzene – cyclohexane, etc the problem is more acute. If one focuses on world scenario of fuels he will find than with the depletion of petroleum products ethyl alcohol is being projected as the next generation fuel. Its large-scale production at low cost will help us to cut down our fuel bills.

The increasing worldwide competitiveness in production has forced industry to improve current process design. Consequently, the development of new process design and reorganization of present process designs with the possible integration of new technologies is a growing importance to industry.

Pervaporation / Vapor-permeation with distillation in form of a hybrid separation unit are one such developing technology that can be used for various industrial applications. An analysis shows that the operating cost of the Pervaporation unit are about 66% less than the costs of the entrainer based distillation process (in the case of dehydrating ethanol from 94 to 99.8 wt%). The same fact is also true for isopropanol production. Further, it has also been found than cost savings in the case of a 100,000 kg/day plant are claimed to be about 48% less in overall cost compared to azeotropic distillation in the case of dehydration of isopropanol from 85 to 99.0 wt%.

This Thesis work focuses on Pervaporation based hybrid processes. Hybrid configurations and their economic evaluation available till now are also present in this work. A critical review, of various types of membrane, membrane – modules has also been made a part of this thesis. Based on the vapor liquid equilibrium in membrane unit the selection criterion between pervaporation – distillation and vapor-permeation-distillation are also included. A simple steady state pervaporation model is developed using log mean diffusivity coefficients and simulated in visual Basic 6.0. Based on this model "user defined unit" is developed in HYSYS 3.0 and for dehydration of ethanol from 20 wt% to 95.53wt % hybrid system is designed similar to I – 211A configuration

except that permeate is not recycled back to column. It is found that the proposed model and its log mean approximation of diffusivity can be used successfully to calculate the composition and flux for lower and higher ethanol content feed.

COTENTS

Title	Page No.

LIST OF FIGURES

LIST OF TABLES

NOMENCLATURE

Abbreviation

$D-P$	Dubinin – Polanyi (equation)
D-R	Dubinin-Radushkevich (equation)
$ENSIC$	Engaged Specie Indused Clustering Model
IPA	Iso-propanol
PAN	Polyacrylonitrile
$PDMS$	Polydimethylsiloxane
PEI	Polyetherimide
PI	Process Intensification
$POPMI$	4, 4'-oxydiphenylene pyromellitimide
$PPCSD$	Pseudophase – Change Solution – Diffusion
PV	Pervaporation
PVA	Polyvinylalcohol
TIP	Thermodynamics of Irreversible Process
$UNIFAC$	UNIQUAC Functional-Group Activity Coefficients
$UNIQUAC$	UNIversal QUasi Chemical Theory
VEL	Vapor Liquid Equilibrium
VOC	Volatile Organic components
VP	Vapor Permeation

Symbols

a	Activity
a	Constants for prediction of interaction parameter from lattice graph theory
a_{ij}	Parameter to predict solvent – solvent interaction τ_{ij} for UNIQUAC model
b	Constants for prediction of interaction parameter from lattice graph theory
b_{ij}	Parameter to predict solvent – solvent interaction τ_{ij} for UNIQUAC model

c	Constants for prediction of interaction parameter from lattice graph theory
c_i	Concentration of component i
c_{ij}	Parameter to predict solvent – solvent interaction τ_{ij} for UNIQUAC model
d_{ij}	Parameter to predict solvent – solvent interaction τ_{ij} for UNIQUAC model
f	Fugacity
f_s, f_g'	Partition function for adsorbed molecule and partition function per unit volume for free gaseous molecules
i	Component i
j	Component j
k	Component k
k	Boltzmann constant
k_p, k_s	Affinity between solvent – solvent and solvent – polymer species according to ENSIC model
m	Saturation limit in terms of molecules per cavity
m_i	Mobility of species i
n	Number of components
p	Pressure
q	Relative surface of molecule (UNIQUAC)
q^*	Relative surface of molecule (UNIQUAC)
r	Relative volume of molecule (UNIQUAC)
v_i	Mean velocity of component i
x	Mole fraction of component in liquid phase
y	Mole fraction of component in vapor phase
w	Weight fraction
w'	Weight fraction in membrane
z	Membrane thickness
B	Constant (Pore Flow Model)
D	Diffusivity coefficient

D^0_{ij}	Maxwell – Stefan interaction parameter
$\tilde{D}_{ij}$	Effective diffusion coefficient dependent on concentration
$\overline{D}_{ij}$	Averaged diffusion coefficient
E	Activation energy
H	Henry's law constant
J	Flux
K	Constant (Maxwell – Stefan interaction parameter calculation)
L	Phenomenological constants
M_i	Molecular weight of component i
P	pressure
R	Universal Gas law Constant
T	Temperature
V_i	Partial molar volume of component i
Z	Coordination number (UNIQUAC)

Greek Letters

α	Selectivity of membrane
β	Selectivity of membrane
β_s	Volume of a sorbate molecule
γ	Plasticization coefficient
γ_i	Activity coefficient of component i
δ	Thickness of membrane
ε	Porosity of Zeolite matrix
θ_i	Surface fraction of component i in mixture (UNIQUAC)
θ_i^*	Surface fraction of component i in mixture (UNIQUAC)
κ	Constants for free volume diffusion model
M_i	Chemical potential of component i
σ	Concentration coefficient
τ_{ij}	Interaction parameters for UNIQUAC theory
χ	Adjustable parameter (Flory – Huggins Theory)
ϕ	Volume fraction of component i in mixture (UNIQUAC)

ξ	Ratio of molar volume of penetrant and polymer unit
$\bar{\rho}$	Average dinsity
ϑ	Average jumping frequency
∇	Difference operator
Γ	Matrix of thermodynamic factors
Ω	Jumping distance of penetrant

Subscripts

1	Component 1
2	Component 2
c	Crosslinks
f	Feed
fp	Free volume for polymer
g	Gas
i	Component i
j	Component j
l	Liquid
p	Permeate/polymer
per	Permeate
sat	Saturated
t	Total
r	Retentate
M	Membrane
V	Vacant

Superscript

s	Surface
C	Combinatorial
R	Residual
T	Thermodynamic

CHAPTER 1

INTRODUCTION

Process Intensification (PI) refers to the technologies and strategies that enable the physical sizes of conventional process engineering unit operation to be significantly reduced. The goal is to bring down the plant size by 10-1000 times [1] by replacing large, expensive and energy-intensive equipment or processes with ones that are smaller, less costly and more efficient [2]. Hybridization of multiple unit operations and processes is thus a part of process intensification as it helps in reducing equipment size and cost.

Distillation – a unit operation is the most commonly used method for separation of mixtures of the compounds when there is a difference in relatively volatility. However, many industrially important liquid mixtures are difficult or even impossible to separate by simple continuous distillation because the phase behavior contains an azeotrope, a tangent pinch, or overall low relative volatility. In such a situation, the logical solution is to combine distillation with one or more complementary separation technologies such as pervaporation, stripping, absorption etc. to form a hybrid. The overall separations task is divided amongst various technologies in such a way that each operates in the region of the composition space where it is most effective [3].

Membrane technologies have recently emerged as an additional category of separation processes in addition to the well-established mass transfer processes, which offer advantages over existing mass transfer processes. Such advantages can comprise high selectivity, low energy consumption, moderate cost to performance ratio, compact and modular design, etc. [4]. Pervaporation (PV) / Vapor permeation (VP) is an interesting membrane separation alternative, because it offers less energy consumption than distillation. It is not influenced by equilibrium between components, makes azeotrope breaking easier than by a sequence of distillation columns. In pervaporation, separation is based on a selective transport through a dense layer associated with evaporation of the permeants at down streamside. The phase changing is usually obtained by lowering the partial pressure of the permeants at the downstream side of the

1

membranes to the vacuum [5]. However, the energy consumption in pervaporation is lower because it requires energy only for the vaporization and expansion of the components that selectively have been transported through the membrane. This energy is removed from the sensible heat carried by the liquid, inducing a drop in the retentate temperature and, consequently, in the flux. The retentate temperature drop increases the required membrane area for a specific removal duty. Usually, auxiliary equipment like heat exchangers are necessary. In vapor permeation, feed is in vapor form and due to partial pressure gradient components are selectively transport through dense membrane. Capital cost in pervaporation or vapor permeation is high due to maximum capacity of a module is low and for the cost of the membranes, the modules and the auxiliary equipment. One advantage with distillation is that it needs low capital investment than membrane separation process. Hybrid membrane-distillation process exploits the advantages of distillation and membrane operations, while overcoming the disadvantages of both [4].

While in the field of distillation, for example, various types of distillation processes, selection of column, modeling and simulation are widespread and steady state and dynamic models are available on different scales (models for VLE, mass transfer, tray hydraulics, or whole column), the detailed review of membrane processes has attracted comparatively little interest [6]. Thus to bridge the gap, in this thesis work, Pervaporation and vapor permeation process are reviewed. A simple pervaporation model is taken and simulated in Visual Basic 6.0 and HYSYS 3.0. User defined unit for pervaporation is developed in HYSYS – 3.0 using Micro Language Editor.

HYBRID DISTILLATION & INDUSTRIAL APPLICATION

2.1. Hybrid process

A hybrid process is defined as a process package consisting of generally different, unit operations, which are interlinked and optimized to achieve a predefined task [4].There are two types of hybrid process namely, Type R (reactor) and Type S (Separator). Different types of hybrid processes are shown in Fig 1.
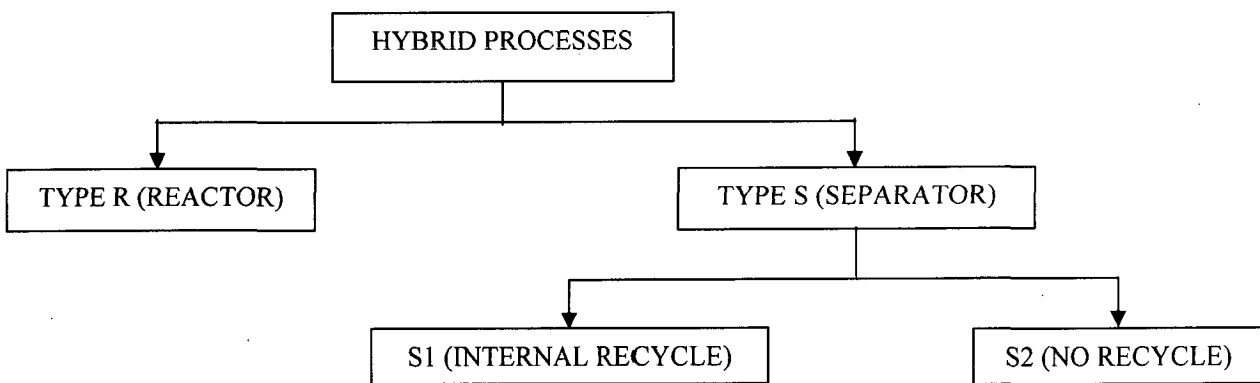
Fig. 2.1: Different types of hybrid processes

Type R (reactor): Hybrid processes which are an offspring of two different processes are referred as to Type R (Reactor). Combination of pervaporation unit with reactor comes under this class [4].

Type S (Separator): Hybrid processes consisting of processes which are "essentially performing the same function" are known as Type S (Separator). Combination of pervaporation with any separation unit comes under this class [4].

With regard to Type S hybrid process, the component parts serve a common purpose (e.g. separation of A and B) and there are a maximum of two output streams (one rich in A, the other rich in B) and the common purpose could not be achieved by either component alone. For example, extractive distillation, where a second distillation column recovers the extractive agent for recycle to the first column but in total, there are only two

3

output streams. But series-processes like a cascade of distillation columns such as a de-methaniser, a de-ethaniser and a de-propaniser is not a hybrid process because multiple products are produced in this process. Type S hybrid process is subdivided into two classes namely S1 and S2, as defined below.

Type S1 (internal recycle): An interlinked inter-dependent combination achieving a binary split is referred as Type S1 hybrid process [4].

Type S2 (no recycle): A combination of consecutive separation processes achieving a split that neither could achieve alone is referred as Type S2 hybrid process [4].

Hybrid separation process

Type S1 (internal recycle)   Type S2 (no recycle)
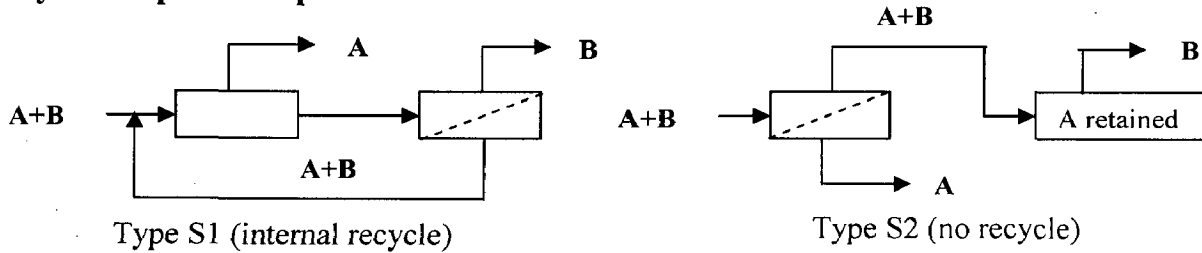
Series processes (not Hybrid processes)

Cascade   Multistage unit operation
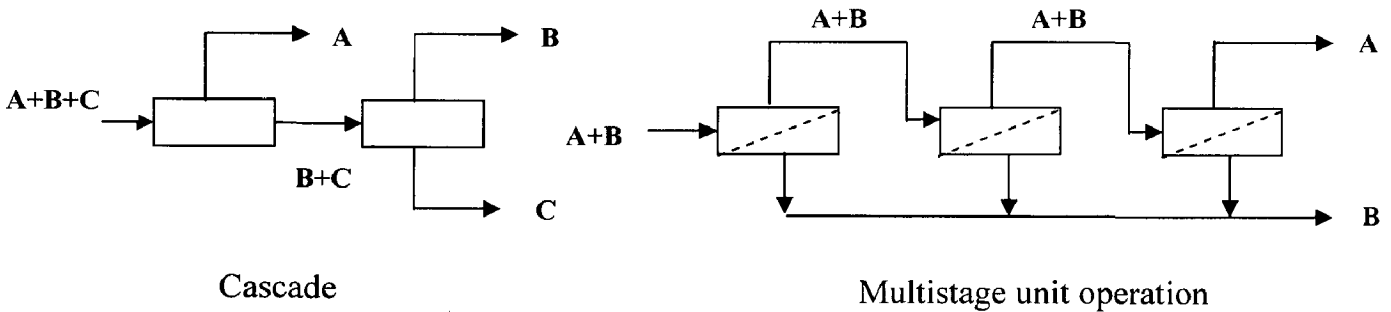
Fig. 2.2: Hybrid processes (Types S1 and S2) and non Hybrid Series Processes

2.2. Different Process Configuration for Hybrid Distillation

Thomas G.Pressly and Ka M. Ng (1998) [3] classified distillation – membrane hybrid for binary mixtures based on the complexity of configurations and phase behavior. They identified three general types of systems as candidates for hybrid application.

Type I.   Systems with a difficult region near one of the pure components are in this class. This difficult region can either be a tangent pinch or an azeotrope, for example, the acetic acid –water system.

4

Type II. Systems with an azeotrope at an intermediate concentration are belong to this class, for example ethanol –water system.

Type III. System has a difficult region that spans the whole composition space in the form of an overall low relative volatility are belong to this class, for example, the propylene-propane system.

They classified the system according to systems type and complexity with the help of a group of alphabets such as: *T-fmdL*

where,

T   Type of system (as discussed earlier)

f   Number of degrees of freedom (is the difference of the number of the system variables, and combined number of the specified variable for the configuration, mass balance equation, and the constraints of equating concentration across any stream split.)

m   Number of membranes

d   Number of distillation column

L   Letter designation for configuration having the same number designation (i.e., a distillation column and a membrane is configured in two way with 3 degree of freedom and both are dealing with system Type I, then the configuration number will be I-311 same for the two. Then these two configurations are assigned with letter A and B arbitrarily to identify them).

They classified the hybrid process in fifteen configurations which are presented in Table 1 with their effects on operating curves in McCabe – Thiele diagram and field of applications (merits). The configurations from Table 1 are displayed in Fig. 12, in order of complexity.

Table 2.1: Process Alternatives and Description

Configuration	Effects and merits
I-211A	Truncates operating line in the top section of the column
I-311A	Truncates operating lines; appropriate for concentration below azeotropic point
Pseudo I-311A	Similar to configuration I-311A; useful for membrane of low separation factor
I-311B	Truncates and lowers the operating lines; only effective for concentrated feed or a membrane with a high separation factor
I-411A/ III-411B	Lowers the operating lines in middle/top; not appropriate for azeotropic systems
I-521A	Truncates and lowers the operating lines; primarily for membranes of low separation factor
I-621A	Truncates and lowers the operating lines at the top and slightly below; the permeate from the lower membrane to the upper set at the same concentration as the distillate
II-512A	Truncates the operating lines at the top at the first column
II-612A	Truncates the operating lines; when azeotropic concentration is far from either product concentration
II-612B	Only appropriate if the feed is near the azeotropic composition
II-822A	Similar to configuration II-612A, with the second column assisted by using another membrane to further truncate and lower the operating lines; good for systems with a large region of low relative volatility around the azeotrope
II-822B	Configuration II-822A with the retentate from the second membrane fed into the first column; again, good for a region of low relative volatility around the azeotrope
III-311A	Operating lines are lowered in the region around the feed, resulting in a reduction in reflux ratio and the number of stages
III-511A	Lowers the operating lines in the middle of the column greatly
III-521A	Lowers and truncates the operating lines on the top and bottom of the column

I-211A I-311A Pseudo I-311A

I-311B I-411A/III-411B I-521A

I-621A II-512A II-612A

II-621B II-822A II-822B

III-311A III-511A III-521A
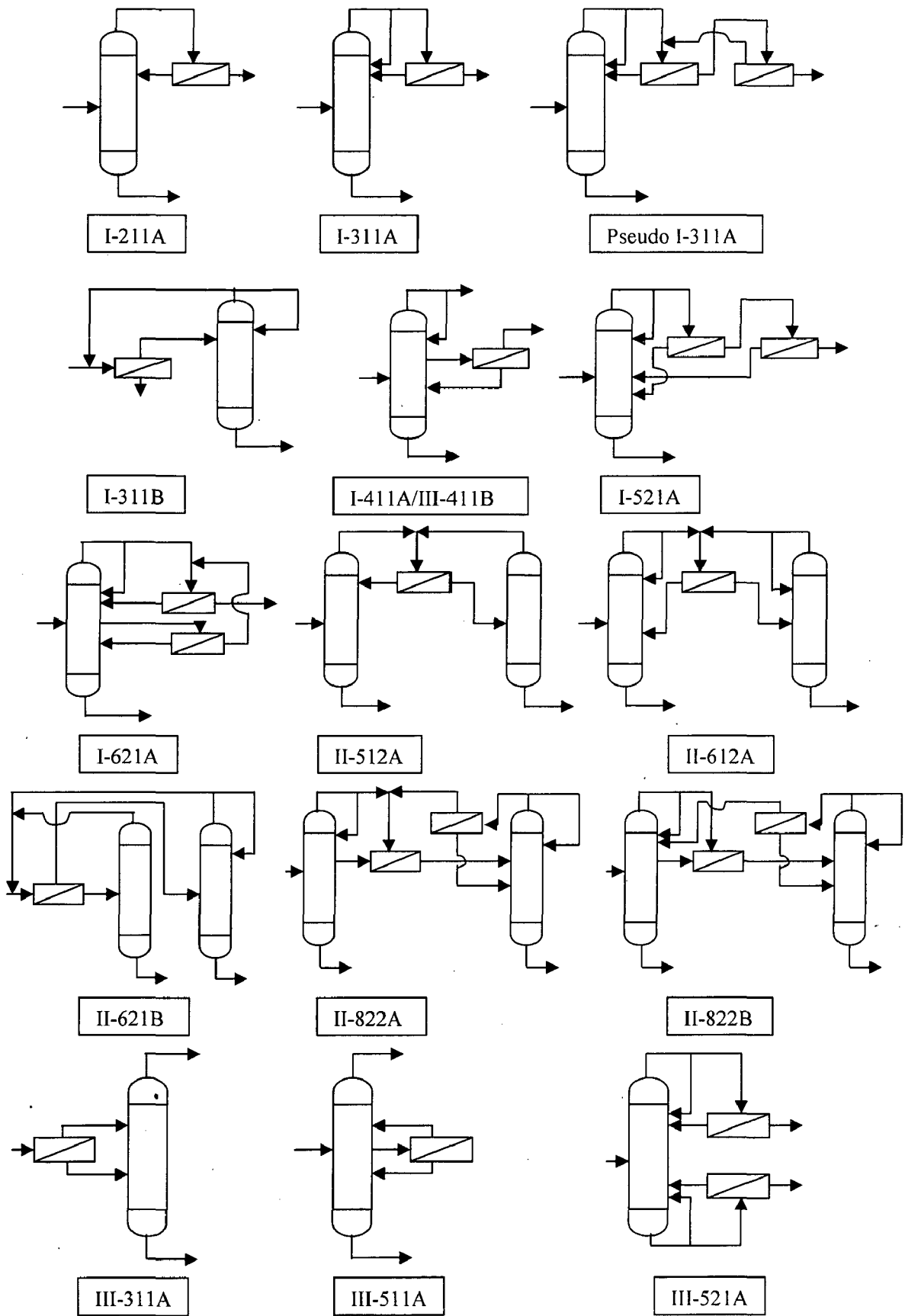
Fig. 2.3: Different Hybrid process configurations

7

2.3. Application of Hybrid Distillation Process

On pervaporation-distillation hybrid process the first paper was being published for the dehydration of isopropanol-ethanol mixtures by Binning and James in 1958 [25]. It took, however, until the late 1980's for the process to be regarded with some importance as an attractive alternative (especially with distillation as the first step) for several separation processes. In 1983 a first 1200 l/d dehydration plant started its operation for the dehydration of ethanol-water mixture in Brazil [7]. In 1988 the first plant started for dehydration of ether [7]. According to the most recent global analysis on pervaporation by Néel and to technical brochures of Sulzer Chemtech, 90% of the pervaporation systems that have been commercialized world – wide were produced by GFT or associates. Between 1984 (corresponding to the beginning of pervaporation industrialization by GFT) and 1996, 22 pervaporation unit for ethanol dehydration and 16 pervaporation units for isopropanol dehydration were commercialized [26].

The hybrid process can be applied for the separation of low volatility and azeotropic mixture. Generally, two applications of distillation-pervaporation hybrid processes can be found:

i)   Dehydration of organic mixtures using hydrophilic membranes, and

ii)   Separation and concentration of organic mixtures using organophilic membranes

All pervaporation-distillation hybrid processes can be defined as Type S1 hybrid processes since they include an internal recycle between pervaporation and distillation. A large number of researchers have focused the applicability of hybrid distillation on various systems. Their works give the economical evaluation as well as the model of the process and optimized design for more profitable situation. Existing and potential applications of pervaporation combined with distillation are summarized in Table 2.2 Many of these applications are still under development and, therefore, under continuous optimization. Few of the processes are described below.

Ethanol-Production Process

The pervaporation-distillation hybrid process is employed to separate ethanol-water mixtures by splitting its azeotrope and then to dehydrate the ethanol.

Tusel and Ballweg [27] patented a system (I - 521A) for dehydration of alcohol from 80 wt% ethanol to 99.8 wt% ethanol. An alternative process layout in I-311A configuration is proposed by Tusel and Brüschke [28], Cogat [29] and Fleming [30]. Economic evaluation of a commercial ethanol dehydration plant producing 6 m^3 per day is given by Sander and Soukup [31]. They pointed out that for concentrating ethanol from 94 to 99.8 wt % in hybrid process with three pervaporation unit in series give 66% less operating cost than conventional entrainer distillation.

Frank [32] analyzed two different cases (concentrating ethanol from 7 to 99.8 wt% and 7 to 99.95 wt% ethanol) using similar process layout (I − 311A) for the production of 5000 kg/h anhydrate ethanol. In both cases distillation process is used to concentrate ethanol from 7 to 95% and remaining dehydration is done in pervaporation unit. In the first case, investment cost is similar to conventional process but overall cost is 16% less due to saving in steam requirement. They also showed that the thermal energy cost is 60 to 70% of overall cost and by decrease in steam costs and using an integrated energy system could place conventional process in a more favorable position. In second case for achieving higher purity investment cost 50 % higher (due to larger membrane area) than the first process, and they concluded that for purifying ethanol higher than 99.8 wt% conventional process is more economical than hybrid process.

Guerreri [33] modified two conventional ethanol dehydration plants producing 50,000 t/year ethanol (99.9 wt% purity) by introducing pervaporation unit. The first configuration is combination of fractional distillation and azeotropic distillation with benzene as entrainer. This process is changed by replacing azeotropic distillation unit with a pervaporation unit using hydrophilic polyvinylalcohol/poly − acrylonitrile (PVA/PAN) membranes. They found that the conventional process need 13% less capital investment than hybrid process whereas 14% operating cost can be save by hybrid process. Applying an improved energy recovery system within the hybrid process may increase investment costs slightly but it will save another 6% in operating cost. The second process, a combination of vacuum distillation and azeotropic distillation, is changed by replacing azeotropic unit by pervaporation unit. They found that conventional process (investment cost is 40% higher than first conventional process) needs 8% less capital investment whereas 36% operating cost can be save by hybrid process.

Brüschke and Tusel [34] proposed a plant configuration (II-612A) and concluded that such hybrid system could save 28% investment costs and 40% operating cost for concentrating ethanol 94 to 99.85 wt%. There are numerous results that claim the opportunity of hybrid process as an alternate process [35 -37].

Isopropanol-production process

The first integration of a distillation-pervaporation hybrid process into the isopropanol (IPA) production was suggested by Binning and James [25]. They proposed I-311A configuration to concentrate isopropanol (less than 0.5 wt % water). For a feed rate 34,000 kg/day containing 14 wt % water, the proposed configuration could save 31% investment cost and 15 to 16 % (of investment cost) operation cost than conventional two column azeotropic process with hexane entrainer.

A pervaporation-distillation hybrid process with the hydrophilic pervaporation unit installed between two distillation columns (configuration II-612A) to dehydrate IPA was discussed by Stelmaszek [38] and Gooding and Bahouth [36]. An economical comparison of different process variations showed that the hybrid process proposed reduced IPA production costs by about 5% compared to azeotropic distillation with benzene as entrainer [38]. They also found that with I-311A configuration IPA production costs reduced by about 36% compared to the conventional process [37].

More recently, a distillation – pervaporation hybrid process was suggested to dehydrate an IPA-water mixture, is in I-311A configuration [39-41]. By retrofitting of an existing azeotropic/ extractive distillation system is also economical as pervaporation unit lower the water load and give the freedom to choose the economic entrainer [30, 42]. Veerle Van Hoof et al. [43] the performance of conventional dehydration process and different hybrid system consisting of distillation followed by pervaporation as well as distillation followed by pervaporation followed by a second distillation. They pointed out that the hybrid system distillation–pervaporation with ceramic membranes was the most interesting process from economic point of view and could lead to a saving in total costs of 49% compared to azeotropic distillation.

Table 2.2: Existing and potential hybrid distillation processes.

Sl. No.	Investigator	Earlier process	System /Capacity/Configuration	Output achieved	Saving made	Remarks	Ref.
1	Tusel and Ballweg	Azeotropic distillation	System: Ethanol – water mixture (80 wt% ethanol) Configuration: I – 521A	99.8 wt% ethanol		Cheaper than conventional process due to energy saving and for the avoidance of entrainers for distillation.	27
2	Tusel and Brüschke, Cogat and Fleming	Azeotropic distillation	System: Ethanol – water mixture Configuration: I – 311A	99.5 – 99.95 wt % ethanol		Saving of investment cost as well as operating cost due to reduction in energy consumption, reduction in waste water treatment and the absence of entrainer	28-30
3	Sander and Soukup	Azeotropic distillation	System: Ethanol – water mixture (95 – 96 wt% ethanol) Capacity : 6 m³ per day Configuration: Three pervaporation unit in series used for final polishing of distillate.	99.9 vol% ethanol	Operating cost saving : 66%	Improve marketability of product ethanol (free from entrainer contamination);	31
4	Frank	Azeotropic distillation	System: Ethanol – water mixture (7 wt% ethanol) Capacity : 5000 kg/h Configuration: I – 311A	99.8 wt% ethanol	Operating cost saving: 16% less	Decrease in steam cost could place rectification in a more favorable position	32
5	Frank	Azeotropic distillation	System: Ethanol – water mixture (7 wt% ethanol) Capacity : 5000 kg/h Configuration: I – 311A	99.95 wt% ethanol	Investment cost increase by 50% Operating cost increase by 9%	Dehydration under 2000 ppm was not considered economically feasible in hybrid process	32
6	Guerreri	Azeotropic distillation	System: Ethanol - water mixture Capacity : 50000 tpa Configuration: azeotropic column replaced by pervaporation unit	99.9 wt% ethanol	Investment cost increase by 15 % Operating cost increase by 14 %		33

Sl. No.	Investigator	Earlier process	System /Capacity/Configuration	Output achieved	Saving made	Remarks	Ref.
7	Guerreri	Vacuum distillation then Azeotropic distillation (40% higher investment cost than fractionation and azeotropic distillation)	System: Ethanol - water mixture Capacity : 50000 tpa Configuration: Azeotropic column replaced by pervaporation unit; hydrophilic polyvinyl alcohol / poly — acrylonitrile (PVA/PAN) membrane used	99.9 wt% ethanol	Investment cost increase by 8.7 % Operating cost saving 36 %	Applying an improved energy recovery system within the hybrid process may increase investment costs slightly but it will save another 6% in operating cost.	33
8	Brüschke and Tusel	Azeotropic distillation	System: Ethanol — water mixture (94 wt% ethanol) Configuration: II – 612A	99.85 wt% ethanol	Investment saving: 28% Operating savin : 40%		34
9	Chamberlain et al.	Multicompo-nent distillation	System: Mixture of isoamyl alcohol, isobutanol, ethanol and water. Configuration: I – 311A	99 wt % isoamyl alcohol, 30 wt% isoburano-l 76 wt% ethanol	Operating cost saving : 16%		44
10	Binning and James	Two column azeotropic distillation	System: Mixture of isopropanol, ethanol and water (14 wt% water) Capacity:34,000 kg/day Configuration: I – 311A	Isopropanol (less than 0.5 wt% water)	Investment cost saving: 31 % Operating cost saving:15 to 16% (of investment cost)		25
11	Stelmaszek;	Two column azeotropic distillation with benzene as entrainer	System: Mixture of isopropanol and water (36.4 wt% isopropanol) Configuration: II - 612A	anhydrate isopropanol	Production cost saving : 5%		38
12	Stelmaszek	Two column azeotropic distillation with benzene as entrainer	System: Mixture of isopropanol and water (36.4 wt% isopropanol) Configuration: I - 311A	anhydrate isopropanol	Production cost saving: 36%		38

12

Sl. No.	Investigator	Earlier process	System /Capacity/Configuration	Output achieved	Saving made	Remarks	Ref.
13	Gooding and Bahouth	Two column Azeotropic distillation	System: Mixture of isopropanol and water (5 wt% isopropanol) Configuration: II - 612A	99.5 mole% isopropanol			36
14	A. Shanley et al. and A.H.A. Brüschke	Two column Azeotropic distillation	System: Mixture of isopropanol and water (85 wt% isopropanol) Configuration: I - 311A	99 wt% isopropanol	1) Investment cost saving: 10% (compare to single rectification or pervaporation alone) Operating cost saving: 25% (for production rate 500 kg/h) 2) Investment cost saving: 20%(compare to single rectification or PV alone) Operating cost saving: 45% (for production rate 2000 kg/h) 3)operating cost saving: 48% (for production rate 100,000 kg/day)		34, 40-41
15	Arnold	Extractive distillation with ethylene glycol as entrainer	System: Mixture of isopropanol and water Capacity : 500 kg/h Configuration: I - 612A Membrane : Hydrophilic plasma – polymerized membrane PERVAP – 1137 (Sulzer Chemtech/GFT)	Anhydrate isopropanol	Investment cost is 92% and operating cost is 54% of conventional process. Annual overall cost saving 27%.	Saving increase with increasing production rate from 5000 to 20,000 kg/h .	45
16	Fleming	Two column azeotropic distillation/ extractive distillation	System: Mixture of isopropanol and water. Suggest retrofitting of existing system.			Pervaporation unit take the load of concentrating 85 to 95 wt% which can leads to lower water load in the extractive distillation column and enables the use of an alternate entrainer other than benzene.	30,42

13

Sl. No.	Investigator	Earlier process	System /Capacity/Configuration	Output achieved	Saving made	Remarks	Ref.
17	Bart and Reisl	Azeotropic distillation to separate carboxylic acid ester – water azeotrope and carboxylic acid – methanol azeotrope.	System: Carboxylic acid ester – water azeotrope and carboxylic acid ester – methanol azeotrope Configuration: Hybrid process integrating a PV unit with hydrophilic plasma-polymerized PEPVAP1137 membranes (Sulzer Chemtech/GFT) between two reactive distillation columns to split the azeotropes.	99.9 wt% carboxylic acid ester			46
18	Bergdorf	Two – pressure distillation/ Distillation combined with adsorption using activated carbon as a polishing stage.	System: Dimethyl acetal – water mixture; Configuration: II-612A; an additional liquid – liquid separator is integrated to separate water from permeate.	99.995 wt% dimethyl acetal		Hybrid process is more economical due to reduced distillation temperature and reflux ratio. No needs of additive like adsorption granules for polishing stage.	47
19	Staudt-Bickel and Lichtenthaler	Distillation and liquid – liquid phase separation	System: Methylisobutylketone (MIBK) –water mixture Configuration: Pervaporation unit is integrated to remove water from the bottom product of first distillation column, and the MIBK rich retentate (about 0.1 wt %) water is further processed in second column Membrane : Hydrophilic cross – linked PVA – 1001 (Sulzer Chemtech/GFT)	Anhydrate MIBK		Hybrid process is more economical due to reduce the amount of MIBK – water azeotrope in the distillate (product distillation column); less cooling water is required due to absence of liquid – liquid separator unit.	48-50
20	Shah et al.	Two – pressure distillation process	System: Dimethyl carbonate (DMC) - methanol azeotrope (70 wt% methanol) Configuration: I – 311B Membrane: PAN support layer (Texaco) with PVA selective layer cross – linked with aliphatic dialdehyde	99 wt% Methanol 95 wt% DMC	Investment cost saving: 33% Operating cost saving : 60%		42

14

Sl. No.	Investigator	Earlier process	System /Capacity/Configuration	Output achieved	Saving made	Remarks	Ref.
21	Vier et al.	Two pressure distillation process	System: DMC - methanol azeotrope (20 wt% methanol) Configuration: I – 311A Membrane: Organophilic (methanol – philic) PERVAP 1137 membrane (Sulzer Chemtech/GFT)	Purified methanol and DMC	Investment cost saving: 33% Operating cost saving: 60%	Two – pressure – distillation may become moderately superior if energy costs are substantially decreased by 50% or large feed streams of more than 2000 kg/h have to be process	51-54
22	Davis et al.	Fractionation of propylene and propane	System : Propylene and Propane Capacity : 10,000 bbl/day polymer grade propylene production (case 1) Capacity : 1250 bbl/day chemical grade propylene production (case 2) Membrane : Facilitated transport membrane		Operating cost saving: 20 to 50% Energy saving : 500 and 150 billion BTU per year for case 1 and 2 respectively		55
23	Srinivas Moganti et al.	Fractionatio-n of propylene and propane	System : Propylene and Propane Configuration: III – 311A(case 1) III – 511A (case 2) Membrane : Facilitated transport membrane (Ag carrier)	Purified propylene and propane	Plate number reduced 22.5% (case 1) and 30% (case 2)		56
24	Rautenbach et al. and R. Albrecht	Extractive distillation using furfurol as entrainer	System: Benzene-Cyclohexane (50 mol% cyclohexane) Configuration: Hybrid process with extractive distillation, using furfurol as entrainer and organophilic (benzene-philic) pervaporation; first distillation column is used to separate cyclohexane as top product form furfurol – benzene mixture; top cyclohexane is further purified in pervaporation unit; the bottom product furfurol – benzene is separated in second column. Membrane: Organophilic (benzene-philic)	99.2 mol% cyclohexa-ne and 99.5 mol% benzene	Overall cost saving : 20%		57-59

15

Sl. No.	Investigator	Earlier process	System /Capacity/Configuration	Output achieved	Saving made	Remarks	Ref.
25	Chen et al.	Hüls – process (two high – pressure columns between 6 and 12 bar)	Process: "Total recovery improvement for MTBE" or TRIM™ System: Methanol – MTBE and methanol – C₄ azeotrope Layout 1 Similar to I – 311B but the only difference is the top product instead of recycling, fed to a methanol recovery unit to purify it. Purified MTBE obtained as bottom product. Layout 2 Configuration: I – 411A/　　　　　　　　　I – 411B; Top product of the distillation column is fed to methanol purifying unit and MTBE obtained from bottom of the de – dutanizer.	Purified MTBE	Layout 1 Investment cost saving: 10 to 15% Layout 2 Investment cost saving: 20%	Rretrofitting of an existing system is economical, and it could increase production by 5%	60-61
26	Kanji and Makoto	Hüls – process (two high – pressure columns between 6 and 12 bar)	System: Methanol – MTBE and methanol – C₄ azeotrope Configuration: I -311A Membrane: Organophilic (lower alcohol – philic) aromatic asummetric membrane ; separation factor 200	Purified MTBE		More economical than conventional process without PV and the TRIM™ process	62
27	Streicher et al.	Hüls – process (Two high – pressure columns between 6 and 12 bar)	System: Methanol – MTBE and methanol – C₄ azeotrope Configuration: Pervaporation unit is integrated to separate methanol C₄'s between the two distillation columns (de-butaniser and C₄ purification column) Membrane: Organophilic (methanol –philic) plasma – polymerized PERVAP 1137 membrane (Sulzer Chemtech/GFT)	Purified MTBE	Steam saving: 30% (for 50000 kg/h production)		63
28	Rautenbach and Vier	Hüls – process (Two high – pressure columns between 6 and 12 bar)	System: Methanol – MTBE and methanol – C₄ azeotrope Configuration: Pervaporation unit was used to separate a side stream from distillation column Membrane: Organophilic (methanol –philic) plasma – polymerized PERVAP 1137 membrane (Sulzer Chemtech/GFT)	Purified MTBE		Energy requirement is reduced	52
29	Hömmerich	Hüls – process (Two high – pressure columns between 6 and 12 bar)	System: Methanol – MTBE and methanol – C₄ azeotrope Configuration: Pervaporation unit is integrated in front of distillation column	Purified MTBE	Operating cost reduced by 10 % (Hüls – process) and 20% (side stream approach (6 bar distillation and pervaporation unit)		64 -6(

16

Sl. No.	Investigator	Earlier process	System /Capacity/Configuration	Output achieved	Saving made	Remarks	Ref.
30	Uwe Hömmerich, Robert Rautenbach	Hüls – process (Two – high – pressure columns between 6 and 12 bar)	System: Methanol – MTBE and methanol – C$_4$ azeotrope Configuration: Distillation with pervaporation and distillation with vapor permeation	Purified MTBE		Distillation with vapor permeation configuration is the most economic between all alternative process	67
31	Streicher et al.	Two – column distillation	System: Ethanol, isobutene and Ethyl tert-butyl ether (ETBE) Membrane: Organophilic (ethanol – philic) membranes (PERVAP 1051 and PERVAP 2051 by Sulzer chemtech /GFT)	Purified ETBE	Operating cost saving 60%		63
32	Vier	Two – column distillation	System: Ethanol, isobutene and ETBE Configuration: Pervaporation unit is integrated to separate distillation column bottom product. Membrane: Organophilic (ethanol – philic) membranes (PERVAP 2051 by Sulzer chemtech /GFT)	Purified ETBE (less than 1 wt% ethanol) Purified ethanol (less than 5 wt% ETBE)	Operating cost saving 30 – 50 %		53
33	Luo et al.	Two – column distillation	System: Ethanol (10 wt%), isobutene and ETBE Configuration : I – 311A Membrane: 30 wt% cellulose acetate butyrate and 70 wt% cellulose propionate (CAP) organophilic (ethanol – philic) membranes	Purified ETBE and purified ethanol (99.34 wt%)		Ethanol recovery increased (ethanol recovered 99.34 wt% and 55.2 wt% in hybrid and conventional process respectively)	68
34	Yang and Goto	Reactive distillation of ethanol and tert – butyl alcohol using the cation – exchanger resin Amberlyst 15 as catalyst	System: ETBE, ethanol, tert –butyl alcohol and water Configuration: pervaporation unit is integrated to the reactive distillation column to anhydrate the bottom product ; ETBE obtained as top product from distillation column.			Dehydration of bottoms (reactive distillation column) by pervaporation shifts the reaction equilibrium and the fraction of ETBE product in the top product is nearly doubled	69

PERVAVORATION PROCESS AND MEMBRANE

3.1. Pervaporation / Vapor permeation

Pervaporation, Vapor Permeation and Gas Permeation are very closely related processes where the driving force for the transport of species or components through the membrane is a gradient in the chemical potential or simply gradient in partial pressure of the components. The separation is governed by the physical-chemical affinity between the membrane material and the species to pass through and thus, by sorption and solubility phenomena. The transport through the membrane is affected by diffusion and the differences in the diffusivities of the different components in the membrane are important for the separation efficiency [7].

3.2. Pervaporation

In pervaporation the liquid feed mixture is heated to the highest temperature compatible with its own stability, the stability of the membrane and all other parts (e.g. gaskets) in the system. The partial vapor pressures of the component at the feed side are fixed by nature of components, composition and the temperature of feed, whereas the total pressure is of no influence, as long as the liquid mixtures can be regarded as incompressible. On the permeate side all non condensable gases are removed by means of vacuum pump and the permeated vapors are condensed at a sufficiently low temperature as shown in Fig. 3 .
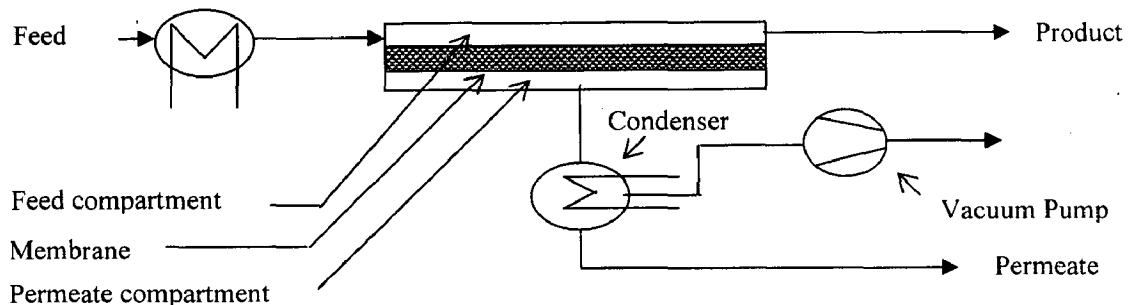
Fig. 3.1: Basic principle of pervaporation.

There are several factors which affect the pervaporation process performance. Some of these factors are:

- **Feed composition and concentration:** A change in feed concentration directly affects the degree of swelling which causes to change in solubility coefficient and diffusivity of components through the membrane. So the permeation characteristics are dependent on feed composition and concentration of component. Fig. 4 shows the influences of benzene feed concentration (wt %) in benzene – cyclohexane mixture on selectivity (i.e., the ratio of the better permeable component to the lesser permeable component in the permeate dividing by the respective ratio in the feed) and flux [8].

Benzene in feed (wt%)
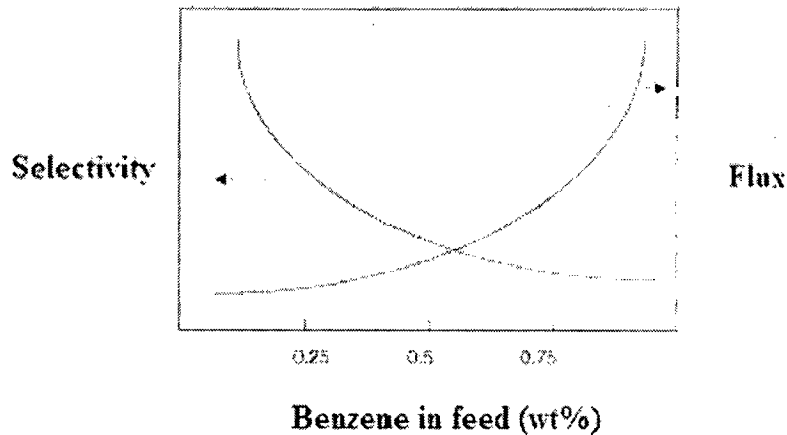
Fig.3.2: Effect of feed concentration on organic–organic pervaporation separation of benzene–cyclohexane mixture. [8]

- **Feed and permeate pressure:** The main driving force in pervaporation is the gradient in activity coefficient, simply the difference in partial vapor pressures of the components. This gradient is maximum when the permeate pressure is zero or the feed pressure is too high. The influences of downstream pressure (permeate pressure) on flux and selectivity for ethanol – benzene pervaporative separation are shown in Fig. 5 [8].

Downstream pressure (kPa)
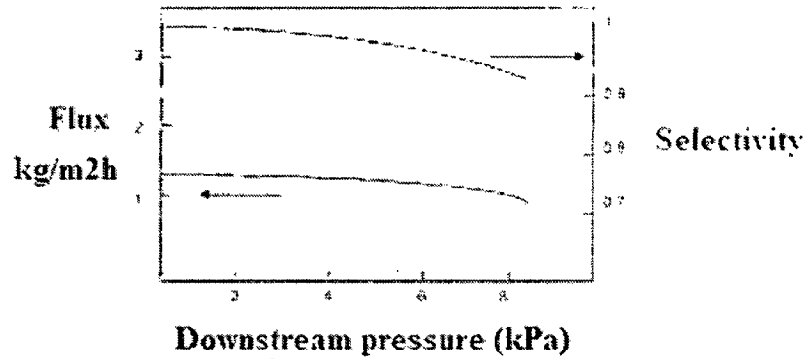
Fig. 3.3: Effect of pressure on pervaporation (for ethanol/benzene system) [8]

- **Temperature:** when the temperature of the feed increases, the permeation rate generally follows an Arrhenious – type law. The selectivity is strongly dependants on temperature. In most of the cases, flux is increased with temperature whereas selectivity is decreased with temperature as shown in Fig. 6 [8].

1/T
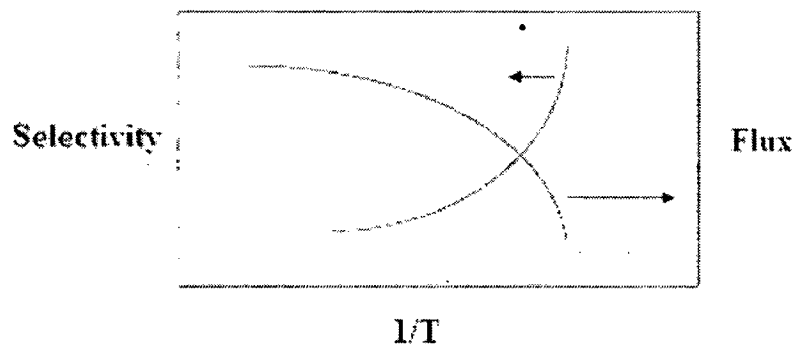
Fig.3.4: Trend of flux and selectivity with varying temperature for benzene/cyclohexane mixture (temperature is in degree centigrade) [8]

- **Concentration and heat/ temperature – polarization:** When gases are produced during electrolysis, these accumulate on and around the electrodes of the electrolytic cell reducing the flow of electric current. This phenomenon is referred to as polarization.

A similar phenomenon, concentration polarization, occurs in pervaporation when the membrane is permeable to molecules of **A**, but relative impermeable to molecule **B**. Thus, molecules of **B** carried by bulk flow to the upstream surface of the membrane where they accumulate, causes their concentration at the surface of the membrane to increase and to form a "polarization layer." As a worst case scenario, the concentration on the membrane surface can be 100 times lower than in the bulk [8]. The equilibrium concentration of **B** in this layer reached when its back-diffusion to the bulk fluid (in retentate side) equals to its bulk flow toward the membrane. The polarization effect can particularly serious if the concentration of **B** attains its solubility limit next to the membrane surface. A precipitate of jel may then form, the result being fouling on the membrane surface or within membrane pores. The component that is enriched in permeate may also be depleted in the boundary layer causing reduction in flux and selectivity [9]. A sketch of a boundary layer and the occurring concentration profiles is presented in Fig 7.
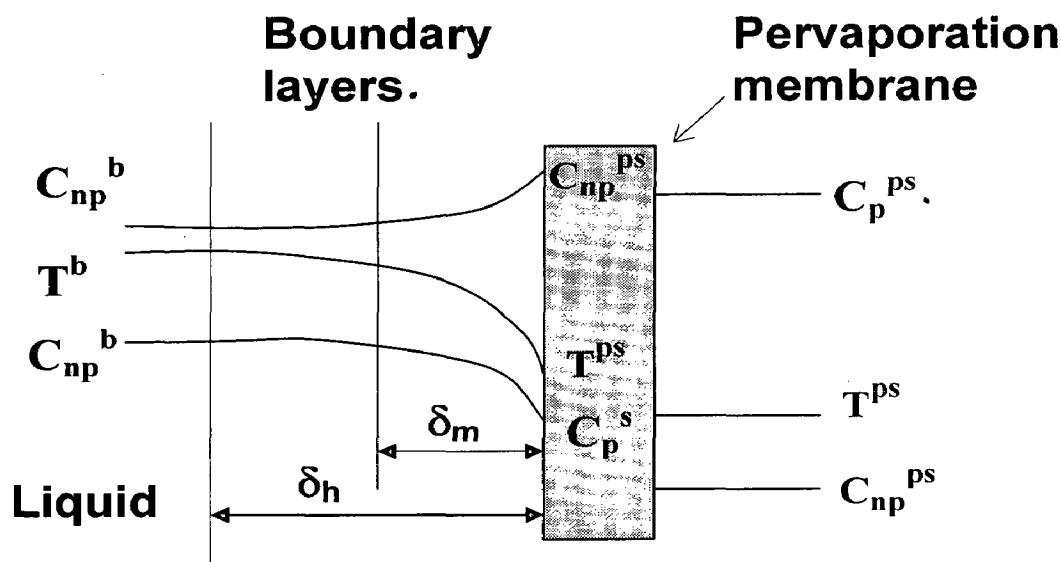
Fig. 3.5: Concentration (C) and temperature (T) polarization on a pervaporation membrane.

In Fig. 7, "p" and "np" indicate the permeating (component A) and non-permeating component (component B), respectively. Subscripts "b" and "s" are

locations in the liquid at the bulk and the membrane surface. The superscript "ps" indicates the permeate side. δ is the thickness of the mass (m) and heat (h) boundary layers.

The effect of concentration polarization in pervaporation processes is presented in Fig.8. In this figure, the concentration polarization modulus (defined as the ratio of concentrations between the membrane surface and the bulk) is presented as a function of the Peclet number for mass transport of the component that preferentially permeates. Several curves are shown, each corresponding to a constant value of the enrichment factor (defined as the ratio of concentrations between the permeate and the retentate on the membrane surface). The region where pervaporation processes operates is shown, based on typical values of Peclet number and enrichment factor [8].
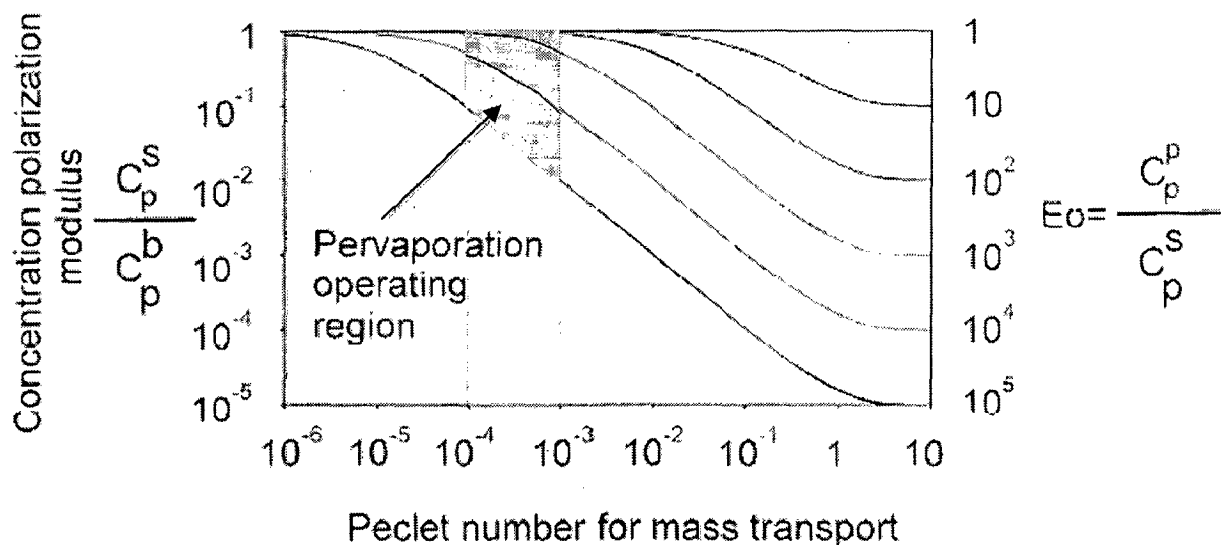
Fig. 3.6: Concentration polarization modulus as a function of the Peclet number at several enrichment factors. Gray areas correspond to ranges of values usually obtained in pervaporation processes.

As the loss of heat and the temperature reduction occur inside the membrane or at the permeate side the heat has to be transported by heat conduction through at least part of the membrane. The feed side surface will then be at a lower temperature than the bulk of the liquid flowing over it. Thus, temperature gradients develop perpendicular to the

membrane surface as well as in the direction of flow (Fig. 7). Following the term "concentration polarization", this effect is referred to as "heat polarization" or "temperature polarization" [7]. This temperature drop reduces the driving forces of mass transfer and changes the intrinsic properties of membrane with respect to permeating component and as a result, there is a drop in flux and selectivity. Fig.9 shows the influences of temperature drop on water-driving force (defined as the ratio of the driving force at a given temperature to the driving force at the bubble point temperature) for dehydration of organic component using hydrophilic membrane.
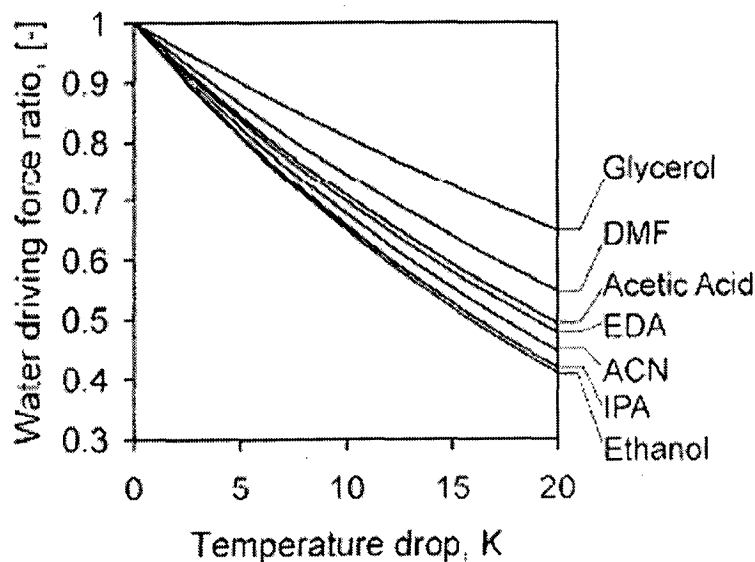
Fig. 3.7: Effect of the temperature drop on the water driving force, relative to the driving force at saturated conditions at 1.013 bar for water – organic mixtures containing 5 wt. % water. (Abbreviations: Dimethyl formamide (DMF), Ethylene diamine (EDA), Acetonitrile (ACN) and isopropyl alcohol) (IPA) [8].

By maintaining high Reynolds numbers at the membrane surface and frequent remixing of the feed stream (by vibration of membrane module), both polarizations can be reduced. Hydrodynamic pressure losses for the transportation of feed and energy costs for pumping will limit the applicability of high Reynolds number [7].

Different means have been proposed to overcome the effects of this heat loss: (i) Direct heating of the membrane from the permeate side by steam; (ii) Electrical heating of the membrane; (iii) Heating of the liquid flowing over the membrane by additional heat

exchanger; (iv)For practical applications the total membrane area required for a specific separation is split into several so-called stages which are arranged in series, with an intermediate heat exchanger between each two stages.

3.3. Vapor permeation

In vapor permeation the liquid feed mixture to be separated is preheated and totally evaporated; the saturated vapor, at least the better permeable component is kept as close to saturation, is fed to the membrane system. The whole membrane area is arranged in one stage, and will in general operate at the same temperature. By means of a pressure controller the vapor is kept under constant pressure. Recovery of the heat of evaporation from the product is possible in principle, but usually not economical except that a part of it can be used to preheat feed [7].

Superheating of the vapor should be strictly avoided as: (i) When a vapor is superheated the partial pressures of its components are not increased; (ii) The activity coefficients (or fugacity coefficients) will drop; (iii) The density of the vapor decreases and fewer molecules get in contact with the membrane per unit of time. This effect will result in a flux reduction [7].

When saturated vapor is fed to vapor permeation unit during stat up (and also shut – down) of the installation, some portion of vapor is condensed on the membrane to heat the cool membrane and module. Besides these, heat losses are affected more by the physical arrangement of the installation. There are two more sources of heat losses caused by the laws of thermodynamics:

1. The vapor is expanded from the high pressure at the feed side to the low pressure at the permeate side. This will cause a Joule – Thompson effect, which in general will lead to a slight temperature drop from the feed to the permeate side and cool the membrane. Although this effect will reduce the temperature by one to three degrees centigrade for most of the mixtures treated in practical application, it will lead to condensation of a small part of the vaporous feed [7].

2. If a mixture is fed at a composition equivalent to a minimum boiling point azeotrope to a vapor permeation unit, and one of the component from the mixture is removing then boiling point of the mixture at feed side increases at constant pressure at which

the vapor permeation unit is being operated. The mixture is moving from azeotropic point to liquid region in T – x –y diagram while it flows over the membrane from inlet to outlet. This is being shown for a water – n – propanol system in Fig. 10. At this condition, a part of vapor is condensed. Liquid and vapor exists in equilibrium (two-phase region; point B in Fig. 10). The respective composition of liquid and vapor are given by the tie line (line VCL in Fig. 10) passing through that point in two phase region and the vapor leaving the vapor permeation unit is at higher temperature than azeotrope boiling temperature (eventually at the boiling temperature of the component which is less permeating) at that pressure. This effect is negligible in the dehydration of azeotropic ethanol where the difference between the boiling point of the azeotrope and that of the pure alcohol is only a few tenth of a degree. For water-n-propanol system shown in Fig. 10, this temperature can be as high as $10°C$, and the effect is even higher for other systems [7].
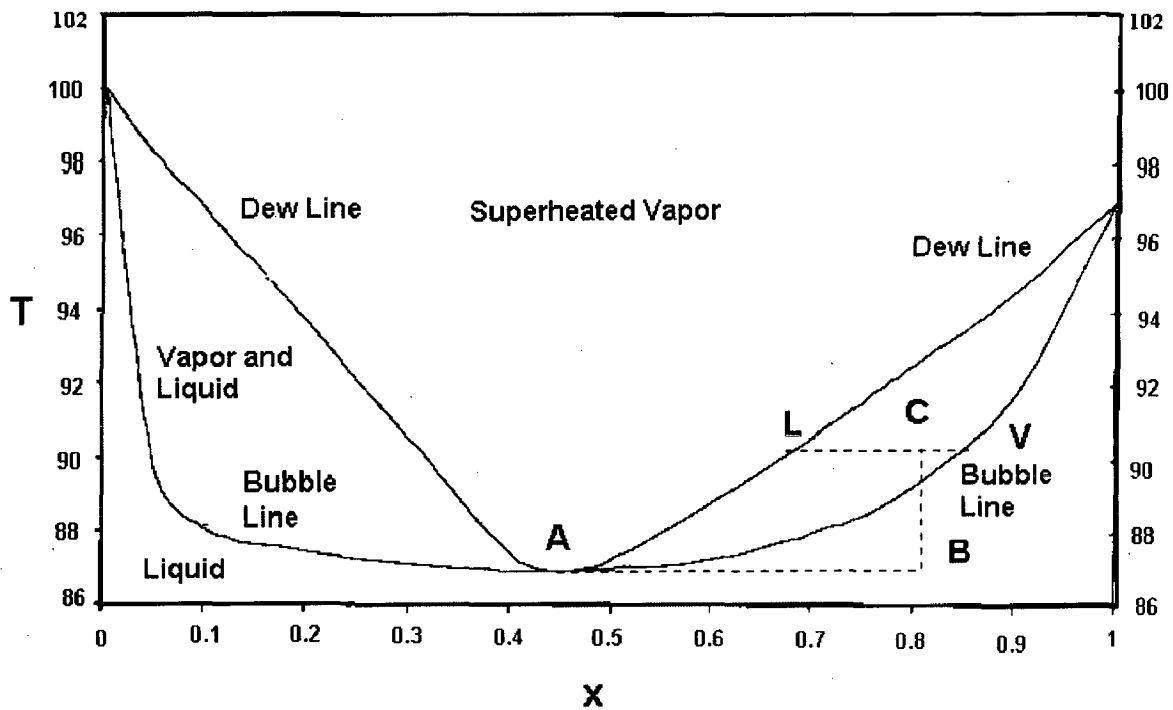
Fig. 3.8: Dew and bubble point of water – n – propanol (T- temperature, $°C$; x – mole fraction of n – propanol)

Vapor permeation is preferred when:

- The feed is already available in the vapor phase, e.g. from a distillation column at the specified temperature (e.g. 95°C to 105°C).

- Dissolved or undissolved solids are present in the original feed (e.g. the feed is a mother liquor), and an additional purification step by evaporation has to be performed anyway.

- The plant capacity is small but a large concentration change is required.

- The additional heat consumption of the plant is not an issue.

Vapor permeation offers the advantage of:

- Simple plant arrangement, all membrane area in one stage.

- No need for intermediate heat exchangers, the interconnecting piping, and controls.

- No heat polarization occurs as the evaporation enthalpy has already been supplied to the feed.

- The total membrane area is operated at a higher temperature, and less membrane area is required.

- Polluted feed streams, containing impurities, can be processed in one plant.

Guidelines for selection of Hybrid Pervaporation – Distillation or Hybrid Vapor permeation – distillation

J. Fontalvo et al. (2005) used membrane driving force at several pressures as a criterion, which can assist to decide which process is more convenient for a specific application, taking water – acetonitrile system as an example [10]. Fig. 11 presents the driving force available for pervaporation and vapor permeation at 1 and 10 atm at different feed water concentration for water – acetonitrile mixture.
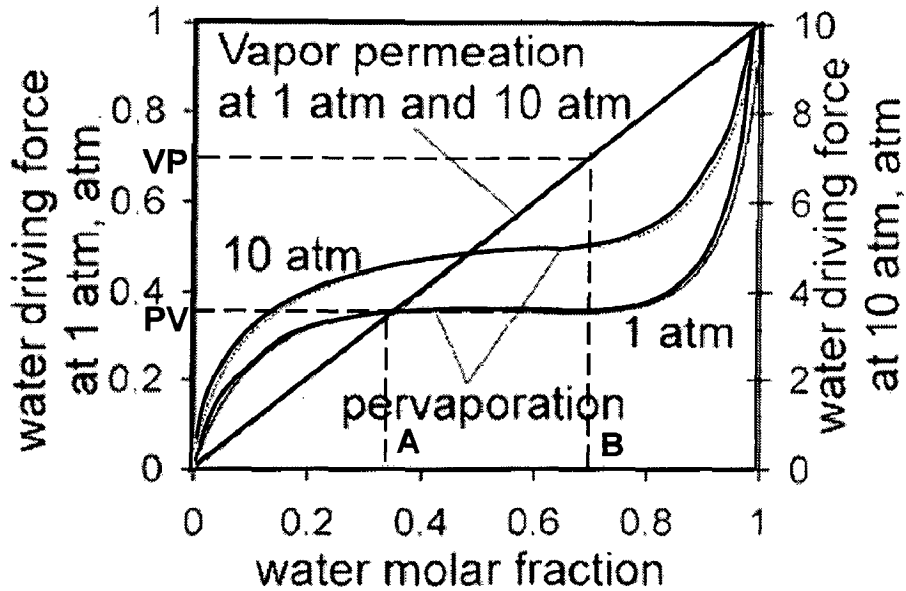
Fig. 3.9: Water driving force for pervaporation and vapor permeation as function of the water concentration at 1 and 10 atm. Driving force is calculated as the difference in water partial pressure between permeate and retentate at bubble point (PV) and dew point (VP).

Following three facts can be distinctly visualized from Fig .11:

i)   Water driving forces corresponding to point B for pervaporation and vapor permeation at 1 atm are PV and VP respectively and VP is greater than PV. This indicates the fact that vapor permeation has a higher driving force for water (better permeating) removal than pervaporation in the range of water concentrations higher than the azeotropic point (point A to 1 for 1 atm pressure in Fig. 11). So vapor permeation is more efficient for better permeating component at concentration higher than the azeotropic point because it requires less membrane area (as driving force is high) than pervaporation and the energy consumption is also lower due to the availability of vapor from the distillation column.

ii)   In the range of water concentration lower than azeotropic point (point 0 to A for 1 atm pressure in Fig. 11) driving force for water removal is high for pervaporation than vapor permeation and it increases with pressure. So for the removal of better permeating component at low concentrations (less than azeotropic concentration),

pervaporation is preferable, especially at high pressure where it requires a smaller membrane and low energy consumption than vapor permeation.

iii) At the azeotropic point (point A for 1 atm pressure in Fig. 11), the driving forces are equivalent for vapor permeation and pervaporation. So for just splitting the azeotropes membrane area requirement is same (as driving force is same) but vapor permeation is preferable because vapor is available at the top of the distillation column (no need of total condensation of vapor) resulting in lower energy consumption with similar capital cost.

2.4. Methods for Reduction of Permeate Side Vapor Pressure

Different means have been proposed in order to reduce the permeate side partial vapor pressure. These are:

i) All permeating vapor is removed by means of a vacuum pump. Applicable when- the volume of permeating vapor is relatively small, and the permeate side pressure is not too low.

ii) The permeated vapor is condensed at sufficiently low temperatures. This is the most cost effective way to maintain the partial vapor pressure at the permeate side at the required low value. Condensation temperatures may be reached simply with cooling water. In some application cooling water is used and in other applications cooling media with temperature as low as -20°C are required.

iii) The permeate side of the membrane is swept with an inert gas in which the partial vapor pressure of the critical (preferential permeating) component is kept sufficiently lower than that on the feed side. This procedure is often discussed in the literature but not yet really introduced into practical application (with the exemption of air drying by means of membranes where part of the produced dry air is used as a sweeping gas).

2.5. Membranes

Membranes used for separating the four major categories of organic–organic mixtures viz., polar/non-polar mixtures, aromatic/alicyclic mixtures, aromatic/aliphatic mixtures,

and aromatic isomers are made of materials that are organic as well as inorganic in nature. A considerable amount of background information related to the developments in the field, and the current trends of industrial pervaporation are given by B. Smitha et al. (2004) [11]. Depending on the feed component that is preferentially permeated, membranes are classified as:

1. **Hydrophilic membranes.** The target compound water is separated from an aqueous-organic feed mixture by being preferentially permeated through the membrane. Membrane materials are: e.g., Polyvinyl alcohol (PVA),   Polyvinyl alcohol / Polyacrylonitrile (PVA/PAN), Polyetherimide (PEI),   4, 4'-oxydiphenylene pyromellitimide (POPMI) [4].

2. **Organophilic membranes.** The organic target compounds are separated from an organic-organic feed mixture by being preferentially permeated through the membrane. Membrane materials are typically Polydimethylsiloxane (PDMS) and Polyvinyl alcohol / Polyacrylonitrile (PVA/PAN) [4].

Pervaporation uses different types of membranes depending upon the material from which these are constructed. These are: **Organic membranes** - also called polymeric membranes, and inorganic membranes - also called **Ceramic membranes.**

At present, most pervaporation membranes that are used in industrial applications are of the polymeric type and are made from natural or synthetic polymers (macromolecules). A wide variety of synthetic polymers have been developed and commercialized since 1930. But it is not before 1982 that the first pervaporation membrane useful for the removal of water from organic liquids on industrial scale was developed and introduced into market by a small German company, GTF (Gesellschaft für Trennverfahren) [12 - 14]. Synthetic polymers are produced by polymerization of monomer by condensation (step reaction) or addition (chain reaction), or by the copolymerization of two different monomers. The resulting polymer is categorized as:

i)   A long linear chain, such as polyethylene;

ii)   A branched chain, such as polybutadiene;

iii)   A three dimensional, highly cross linked structure, such as phenol – formaldehyde;

iv)   A moderate cross – linked structure, such as butyl rubber.

Polymer membranes can be characterized as dense or micro porous. For dense membranes, pores of microscopic dimensions may be present, but they are generally less than a few Angstroms in diameter, such that most, if not all, diffusing species must dissolve into the polymer and then diffuse through the polymer between the segments of macromolecular chains. Diffusion can be difficult, but highly selective for glassy polymers. If the polymer is partly crystalline, diffusion will occur almost exclusively through the amorphous regions. In that case diffusion area decreases and diffusion path increases depending on the crystalline regions presents in polymeric membrane [9].

A micro porous membrane contains interconnected pores that are small (of the order 0.001-10 μm), but larger in comparison to the size of the molecules to be transferred. The pores are formed by a variety of proprietary techniques, some of which are descried by Baker et al. [15]. Such techniques are especially valuable for producing symmetric, micro porous, crystalline membranes. Permeability for micro porous membranes is high but selectivity is low, for small molecules. However, when molecules both smaller and larger than the pore size are the feed to the membrane, the molecules may be separated almost perfectly by size [9]. A major drawback of these polymeric membranes is their limited solvent and temperature stability [16 – 18]

For hydrophilic and organophilic membrane both a composite membrane structure (Fig.3.10) is preferred, allowing for very thin defect free separation layers, but with sufficient chemical, mechanical, and thermal stability. Due to the composite structure flat sheet configurations are preferred. The substructure of both types of flat sheet pervaporation membranes is very similar: A porous support membrane with an asymmetric pore structure is laid onto a carrier layer of a woven or non-woven textile fabric and a basic ultra filtration membrane is formed. On the free side of this asymmetric porous substructure the pores have diameters in the order of 20 to 50 nanometers which widen up to the fabric side to the micrometer range. On this substructure a thin dense layer (in the range of 0.5 to 10 μ thick) is coated which has a very good separation capacity. Different coating techniques are in use, most commonly a solution of the respective polymer in an appropriate solvent is spread on the porous substructure by evaporation of that solvent the dense separating layer is form.

Dense Separating layer	0.5-1 μm
Porous support	70-100μm
Carrier non – woven fabric	100 μm
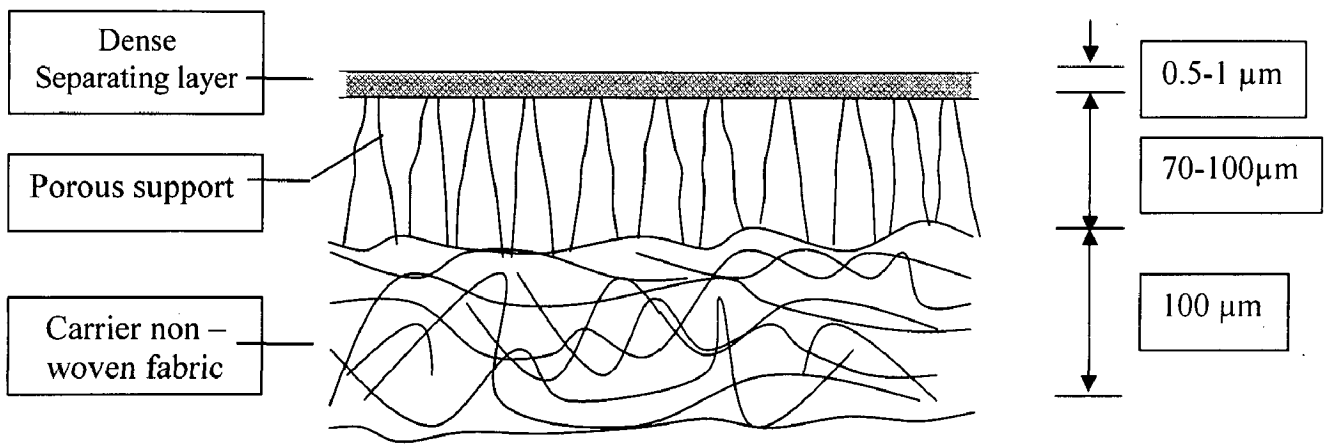
Fig.3.10: Cross-section of a composite membrane.

Generally, ceramic membranes are solvent and temperature stable, can be used in a broad pH range and have both high selectivity and permeability. Asymmetric, micro porous α – aluminium tubes with 40 - 50 A^o pores at the inside surface and 100,000 A^o pores at the outside [9]. Zeolite membranes have also been used for pervaporation both industrially and in laboratory studies. The industrial use of ceramic membranes could lead to a higher product quality and could broaden the application range of pervaporation [4]. Ceramic membranes are polycrystalline zeolite layers deposited on porous inorganic supports, and they offer several advantages over polymeric membranes:

- Zeolite membranes do not swell, whereas polymeric membranes do.

- Zeolites have uniform, molecular-sized pores that cause significant differences in transport rates for some molecules, and allow molecular sieving in some cases

- Most zeolite structures are more chemically stable than polymeric membranes, allowing separations of strong solvents or low pH mixtures.

- Zeolites are stable at high temperatures (as high as 1270K for some zeolites) [19]

The membrane shapes e.g., flat asymmetric or thin – film composite, tubular, hollow fiber, monolithic are incorporated into compact commercial modules and cartridges. Design of modules for pervaporation and vapor permeation processes had been based on the experience gained in those for water treatment by membranes, like Ultra-filtration and Reverse Osmosis. However, significant modifications had to be made due to the specific requirements of pervaporation and vapor permeation processes. Whereas, in the water treatment the portion of the feed volume passing into permeate is

small, in pervaporation and vapor permeation the volume of permeate is much larger than that of the feed as permeates are in vapor form.

Pressure losses at the feed side have to be reduced to a minimum in order of several millibar only in vapor permeation. In pervaporation feed side pressure losses are not that important, but in multistage arrangements will eventually limit the number of applicable stages. The partial vapor pressure at the permeate side has to be reduced in both processes to fairly low values, especially when low final concentrations of the better permeating component have to be reached in the retentate. Therefore, any pressure losses, even in the range of a few millibar have to be avoided at the permeate side [7].

As any feed mixture will contain organic components at high concentration, mostly at elevated temperatures, chemical and mechanical stability of all module components, like spacer, gaskets, potting material and glues is critical. So far mainly four different types of modules are in use on an industrial scale namely plate module [6], spiral wound module [20], envelope module [7] and tubular module [21, 22]. A vibrating membrane module currently marketed which can minimize the polarization problem also available in literature [23, 24].

2.6. Characterization of membranes [2]

The performance of a membrane is general characterized by its flux and its selectivity. For practical reasons fluxes for pervaporation membranes are just given in either kg/m^2h or in $mole/m^2h$, either as total flux of all components or separated into partial fluxes of different components. As the flux depends on the composition of the feed for hydrophilic membranes the concentration of the water in the feed of the respective measured value has to be indicated. For comparison of different membranes very often the so-called "Pure Water Flux" is calculated by dividing the actual flux by the water concentration of the feed. As stated above the "Pure Water Flux" is depending exponentially on temperature.

Selectivity is indicated in different ways. Most commonly found in literature is the so-called α-value (Eq.3.1). This is calculated as the ratio of the better permeable

component (water) to the lesser permeable component (organic) in the permeate dividing by the respective ratio in the feed.

$$\alpha = \frac{(c_{water} / c_{org})_{Permeate}}{(c_{water} / c_{org})_{Feed}} \qquad (3.1)$$

Although the α-value looks fairly simple it is not very informative. For most dehydration membranes the composition of permeate is constant over a very brad range of feed compositions. As a consequence the α-value is not a constant but varies considerably, depending to which feed composition it is related.

Secondly membrane selectivity is characterized by the so-called β-value or enrichment factor (Eq.3.2 and 3.3). This is simply the concentration of water in the permeate divided by that in the feed.

$$\beta = \frac{c_{Water\ in\ Permeate}}{c_{Water\ in\ Feed}} \qquad (3.2)$$

$$\alpha = \beta \frac{c_{Org\ in\ Permeate}}{c_{Org\ in\ Feed}} \qquad (3.3)$$

Again this numerical value is informative for only one feed concentration and not very useful if different membranes have to be compared.

2.7. Modules [2]

Design of modules for pervaporation and vapor permeation processes had been based on the experience gained in those for water treatment by membranes, like Ultra-filtration and Reverse Osmosis. However, significant modifications had to be made due to the specific requirements of pervaporation and vapor permeation processes. Whereas in the water treatment the portion of the feed volume passing into permeate is small, in pervaporation and vapor permeation the volume of permeate is much larger than that of the feed.

Pressure losses at the feed side have to be reduced to a minimum in vapor permeation. Otherwise the process would no longer operate at constant pressure, but the feed vapor could reach a region where superheated conditions would exist. Consequently pressure losses in vapor permeation modules have to be as low as several millibars only.

In pervaporation feed side pressure losses are not that important, but in multistage arrangements will eventually limit the number of applicable stages.

The partial vapor pressure at the permeate side has to be reduced in both processes to fairly low values, especially when low final concentrations of the critical component have to be reached in the retentate. Therefore any pressure losses, even in the range of a few millibar have to be avoided at the permeate side.

As any feed mixture will contain organic components at high concentration, mostly at elevated temperatures, chemical and mechanical stability of all module components, like spacer, gaskets, potting material and glues is critical. So far mainly four different types of modules are in use on an industrial scale.

3.7.1. Plate Modules

Plate modules are mainly used for dehydration applications with permeate channels as open as applicable. A rectangular support plate is provided on both sides with gaskets, which partially cover slots in the plat, acting as distribution channels. On each gasket a membrane is placed, its feed side facing the plate. The permeate side of each membrane is supported by a perforated plate, between two perforated plates a grid or spacer is placed. A membrane, one side of the support plate, and a gasket form a feed chamber, two perforated plates and the space between them a permeate chamber. Each feed chamber is thus adjacent to a permeate chamber, each permeate chamber has a feed chamber at each side. Alternating feed and permeate chambers are arranged in a module.

The module package is hold together by means of flanges and bolts. The thickness and weight of bolts and flanges limits the maximum internal pressure for such modules to 6 to 10 bar. In order to keep weight and handability and weight of the modules within a reasonable range, the maximum size of these modules does not exceed 30 to 40 m^2 of membrane area or less than 100 support plates.

Stainless steel is used as a construction material for support plates for the membranes and for spacers. Chemically stable elastomers, like EPDM or perfluorinated polymers are used as gasket material. More widely used is expanded graphite, due to its excellent chemical and thermal resistance. Preferentially the permeate channels are open over the circumference or the module which are assembled inside special vacuum vessel.

Intermediate heat exchangers and the permeate condenser are sometimes installed inside the vacuum vessel, mostly these items are sometimes installed inside the vacuum vessel, mostly these items are installed outside for easier access and maintenance.

Usually all membranes in a module are arranged for parallel flow of the feed. The feed channel, between membrane and supporting plate, has a height between 0.5 to 1 mm, linear flow rates are in the order of cm per minute. Serial flow would be desirable in order to allow for higher linear flow velocities and higher Reynolds numbers, but then feed side pressure losses will become too high.

Alternative designs are very similar to plate heat exchangers, in which the supported membrane replaces the heat exchanger plates. These modules may be open or closed to the outside at the permeate side, with internal ducts for feed and retentate, and, when closed, for permeate removal. It has been proposed to integrate plate exchangers or pre-heater and permeate condenser into such modules.

3.7.2. Spiral wound Modules

Spiral wound modules with stainless steel central tubes, but otherwise similar to those known from the conventional membrane processes ultra-filtration or Reverse Osmosis, are in use, mainly for organophilic membranes. Due to the larger molecular weight of the substances removed through organophilic membranes the volume of the vaporous permeate is much smaller, even at the same permeate side pressure , and the total permeate side pressure can be usually higher than in dehydration applications. Thus pressure losses in the permeate channels are less critical than in water removal. As organophilic application operate at lower temperatures and low concentrations of organic solvent in the feed, polymers materials can be used as spacer or glue. One or several of the spiral wound modules are housed inside a pressure tube and assembled in conventional skids, very similar as in water treatment.

Similar considerations are valid for organic-organic separation. Spiral wound modules have thus be used in pilot plants for the removal of methanol and ethanol from dry organic mixtures or for the removal of aromatic from aliphatic components. Stability of the material for the feed side spacer and the glue are problems still to be solved.

3.7.3. Envelope Modules

A special modules design which is a hybrid between a plate module and a spiral module has been developed by the research institute GKSS in Germany. Here two membrane sheets are welded together (by heat or ultrasonic welding) to a sandwich structure with a permeate spacer between the two membranes. A multitude of these sandwiches, each with a central hole are arranged on a central perforated tube which removes the permeate. Each membrane sandwich is sealed from the feed to the permeate side by means of a gasket. Around the central hole a perforated ring is inserted into the permeate spacer in order to have an unhindered flow of permeate in to the permeate tube. Feed spacer keeps the membrane sandwiches apart from each other. Feed flow over all sandwiches in a module can be in parallel, by means of additional separation plates any number of the sandwiches can be arranged in groups, with the flow parallel in each group, but in serial for the groups. The central tube with membrane sandwiches around is housed inside a feed vessel, usually of stainless steel. Originally these modules were developed for water treatment, but are now widely used with organophilic membranes in the recovery of organic vapors especially gasoline vapors from gas streams.

3.7.4. Tubular Modules

As stated above, inorganic (ceramic) membranes are produced mainly as tubes. The obvious module is therefore a tube bundle very similar to a tubular heat exchanger. The detailed arrangement depends on the fact whether the separating layer of the membrane is on the inside or on the outside of the tube.

In the first case a bundle of membrane tubes is connected on both ends into tube sheets, each individual tube sealed and fixed. The feed is more or less evenly distributes and directed into the inner lumen of the tubes. Well defined flow regimes and high Reynolds numbers can be obtained at the feed side, controlling polarization effects like in water treatment application. Depending on the inner diameter of the tube the ratio of feed volume to membrane surface is rather high, and the feed stream cannot be heated inside the module. At high linear velocities this may require partial recirculation of the feed or very small modules in series with the respective intermediate heat exchangers. The

MODELING OF HYBRID DISTILLATION COLUMN

4.1. Introduction

Today modeling and numerical simulation of chemical engineering processes is widespread in the process industries. For many processes models are available through simulators like ASPEN PLUS, PRO/II, or HYSYS. However, these simulators provide steady-state models only. While steady-state models can be applied in process design, dynamic models are needed to investigate aspects of process control, disturbance rejection, or optimization of process transients (such as startup optimization). Consequently, dynamic modeling has received an increasing interest in the last decade [70].

While in the field of distillation, for example, modeling and simulation are widespread and steady-state and dynamic models are available on different scales (models for VLE, mass transfer, tray hydraulics, or whole column), the detailed modeling of membrane processes has attracted comparatively little interest. Often, empiric models are fitted to experimental data for on a special membrane [53]. And even detailed models [71] cover steady-state conditions only. However, for the integrated design of pervaporation plants, which covers aspect of feasibility, economics, and control, not only steady-state but also dynamic models are needed. In particular pervaporation processes are known to exhibit a very slow dynamic behavior, and it may take several minutes or hours in order to reach steady state [72]. This phenomenon has been reported by different sources as a problem when measuring steady-state fluxes. In most cases, only qualitative information is available. Recently, quantitative dynamic experimental data have been published by Rautenbach and Hommerich (1998) [73]. These data show that the dominant time constant of the mass transfer through the membrane has same order of magnitude as dominating time constant of the membrane separator, when modeled with a steady- state mass –transfer model [74]. Thus, it is clear that mass-transfer dynamics will affect the dynamic behavior of the whole process and must not be neglected. In this

chapter we describe some well known mathematical model proposed by reseachers of pervaporation only not for distillation because modeling and simulation are widespread and steady-state and dynamic models are available on different scales.

4.1. Generalized Dense Membrane Transport Models
4.1.1. Thermodynamics of Irreversible Processes (TIP)

The driving force for permeation of pure component through a dense membrane is the chemical potential gradient of the species across the thickness of the membrane. The transport model equation for dense membrane-based processes related the chemical potential driving force to the flux for each species. The simplest transport equation can be written as

$$J_i = -L_i \frac{d\mu_i}{dz}$$ (4.1)

Where, J_i is the flux of species, L_i is a phenomenological constant and μ_i is the chemical potential of species i at distance a in the membrane active layer. The phenomenological constant L_i in Eq. 4.1 may be depending on the concentration of the permeating species [75 – 76]. It is obvious from Eq. 4.1 that the flux of component i depends only on its chemical potential gradient. However, this may not be always true. In certain cases, coupling of fluxes occurs, that is, the flux of species i depends on the chemical potential gradient of all the components in the system. The coupling effect can be modeled by thermodynamics of irreversible processes. The model starts from the basic premise that any transport process is an irreversible process and as the component permeates through the membrane there is a continuous generation of entropy [77]. The flux of component i on the basis of this model can be written as

$$J_i = -\sum_j L_{ij} \frac{d\mu_i}{dz}$$ (4.2)

Where L_{ij} is a constant representing the effect of component j on permeation of component i. The chemical potential of any species i in an isothermal system may be expressed as

$$d\mu_i = RTd \ln(a_i) + V_i dP$$ (4.3)

Where a_i is the activity, V_i is the molar volume of component i, T and P are the temperature and pressure of the system. Substituting Eq. 3.3 in Eq. 3.2, we have

$$J_i = -\sum\left(L_{ij}RT\frac{d\ln(a_i)}{dz} + L_{ij}V_i\frac{dP}{dz} \right)$$

(4.4)

Eq. 4.4 is a generic equation that can be used to model the permeation process through any dense membrane. The disadvantage of the TIP theory is that the term L_{ij} is only a phenomenological constant with no real physical significance and for most modeling exercises, it would have to be treated as an adjustable thermodynamic considerations and does not take into account the kinetic effects such as diffusion, which are an integral part of any permeation process.

4.1.2. Maxwell-Stefan Transport Model

The transport of multicomponent mixtures has also been described by the Maxwell-Stefan equation [78 – 81]. This equation takes into account the interactions between all the diffusing species in the mixtures. The equation is written as follows:

$$-\nabla\mu_i = RT\sum_{k=1,k\neq i}^{n} x_k\frac{(v_i-v_k)}{D_{ik}} \qquad i = 0, 2.......n$$

(4.5)

Where x_k is the mole fraction of species k in the mixture, v_i and v_k are the velocities of components i and k in the mixture respectively and D_{ik} is the Maxwell-Stefan i-k pair diffusivity. D_{ik} is a measure of the interaction between components i and k in the mixture. The flux of species i (J_i) can be written in terms of the velocity as

$$J_i = C_i x_i v_i$$

(4.6)

Eq. 3.5 can be written in terms of the component fluxes as

$$-\frac{x_i\nabla\mu_i}{RT} = \sum_{k=1,k\neq i}^{n} \frac{(x_k J_i - x_i J_k)}{C_i D_{ik}} \qquad i = 0, 2.......n$$

(4.7)

It is conventional to express the left hand side of the Eq. 4.7 in terms of mole fraction gradients by introducing a $(n-1)$ by $(n-1)$ matrix of thermodynamic faction denoted by $[\Gamma]$.

$$\frac{x_i\nabla\mu_i}{RT} = \sum_{k=1}^{n-1}\Gamma_{ik}\nabla x_k \qquad i = 0, 2.......n$$

(4.8)

$$\Gamma_{ik} = \delta_{ik} + x_i \frac{\partial \ln \gamma_i}{\partial x_k} \qquad\qquad i = 0, 2.........n-1 \qquad\qquad (4.9)$$

In Eq. 4.9, γ_i is the activity coefficient of species i in solution and δ_{ik} is the Kronecker delta whose values is equal to unity for $i = k$ and null for $i \neq k$. therefore, in matrix notation, Eq. 4.7 can be written as

$$-C_i[\Gamma](\nabla x_i) = [K](J_i) \qquad\qquad i = 0, 2.........n-1 \qquad\qquad (4.10)$$

[K] is the matrix of Maxwell-Stefan pair diffusivities written as shown in Eq. 4.11 an Eq.4.12.

$$K_{ij} = \frac{x_i}{D_{in}} + \sum_{k=1, k\neq i}^{n} \frac{x_k}{D_{ik}} \qquad\qquad i = 0, 2.........n-1 \qquad\qquad (4.11)$$

$$K_{ij} = -x_i\left(\frac{1}{D_{ik}} - \frac{1}{D_{in}}\right) \qquad\qquad i = 0, 2.........n-1 \qquad\qquad (4.12)$$

4.1.3. Fickian Model

The Fick's law is simply represented as

$$J_i = -D_i \frac{dC_i}{dz} \qquad\qquad (4.13)$$

Where D_i is the diffusion coefficient of species i and dC_i/dz is the concentration gradient of species i. Fick's law has been commonly used to model diffusive processes and it has also found application in membrane process. In most cases, the diffusion coefficient is not a constant, but strongly depends on the feed composition, temperature, interaction between components and membrane swelling (for polymeric system). For polymeric membranes, the membrane undergoes maximum swelling on the feed side. The concentration gradient gives rise to a swelling gradient across the membrane thickness. In case of moderately to highly swollen membranes, a Hittorf frame of reference wherein the membrane material is considered stationary with respect to the frame of reference is preferred over the Fick's system [57, 82 – 84].

$$J_i = -\left(\frac{D_i}{1 - \phi_i}\right)\frac{dC_i}{dz} \qquad\qquad (4.14)$$

Where ϕ_i is the volume fraction of component i in the polymer matrix.

4.2. Pervaporation Transport Models

The transport theories described in the previous section are general models, which can be applied to various membrane transport processes. In order to apply these models to pervaporation process, an understanding of the various possible mechanisms of transport is necessary. Depending on the mechanism and the related assumptions, the mathematical treatment and the final form of the above models will apply.

4.2.1. Solution – Diffusion Model

According to the solution- diffusion model, the transport process in pervaporation essentially can be visualized to occur by the following series of steps:

1) Transport of the species from the bulk liquid to the feed-membrane interface.

2) Preferential sorption of the species at the feed-membrane interface.

3) Diffusion of the species through the membrane.

4) Desporption and evaporation of the species at the membrane-permeate interface.

Step 1 depends on the cross- flow velocity of the feed across the membrane surface. The design module nowadays is such that a high cross-flow velocity is almost always maintained across the membrane as a result which the mass transfer resistance of the first step is negligible. However, the first step becomes critical when the species to be transported across the membrane are present in very small proportions in the feed a and the selective sorption of the membrane for the same species is very high (the concentration polarization effect). An appropriate example of such a situation would be the removal of VOC's from aqueous solutions by organophilic membrane using pervaporation [85]. Step 4 is a very rapid step when permeate pressures are low. However the permeate pressures approach the partial vapor pressure of the permeating species, the permeate pressure approach the partial vapor pressure of the permeating species, the permeate flux does become dependent on the rate of vaporization [86].

The solution – diffusion model is the most widely accepted model for the pervaporation process [87 – 88]. The model states that steps 2 and 3 mentioned above are generic to all pervaporation processes. Steps 1 and 4 on the other hand are dependent on

43

the process conditions. The model assumes that the pressure and temperature variation through the membrane is negligible. There is a step change in both the pressure and the temperature at the permeate interface. Fig. 4.1 shows a schematic of the chemical potential/gradients existing in the pervaporation process according to the solution-diffusion model.

Feed Interface
$\mu_{i,f} = \mu_{im,f}$ or
$a_{i,f} = a_{im,f}$

Feed

Permeate Side

Membrane Active Layer

Permeate Interface
$\mu_{i,f} = \mu_{im,f}$ or

Feed Pressure - P_f

Constant Pressure - P_f throughout Membrane

Feed

Permeate Side

Permeate Pressure – P_p

Membrane Active Layer
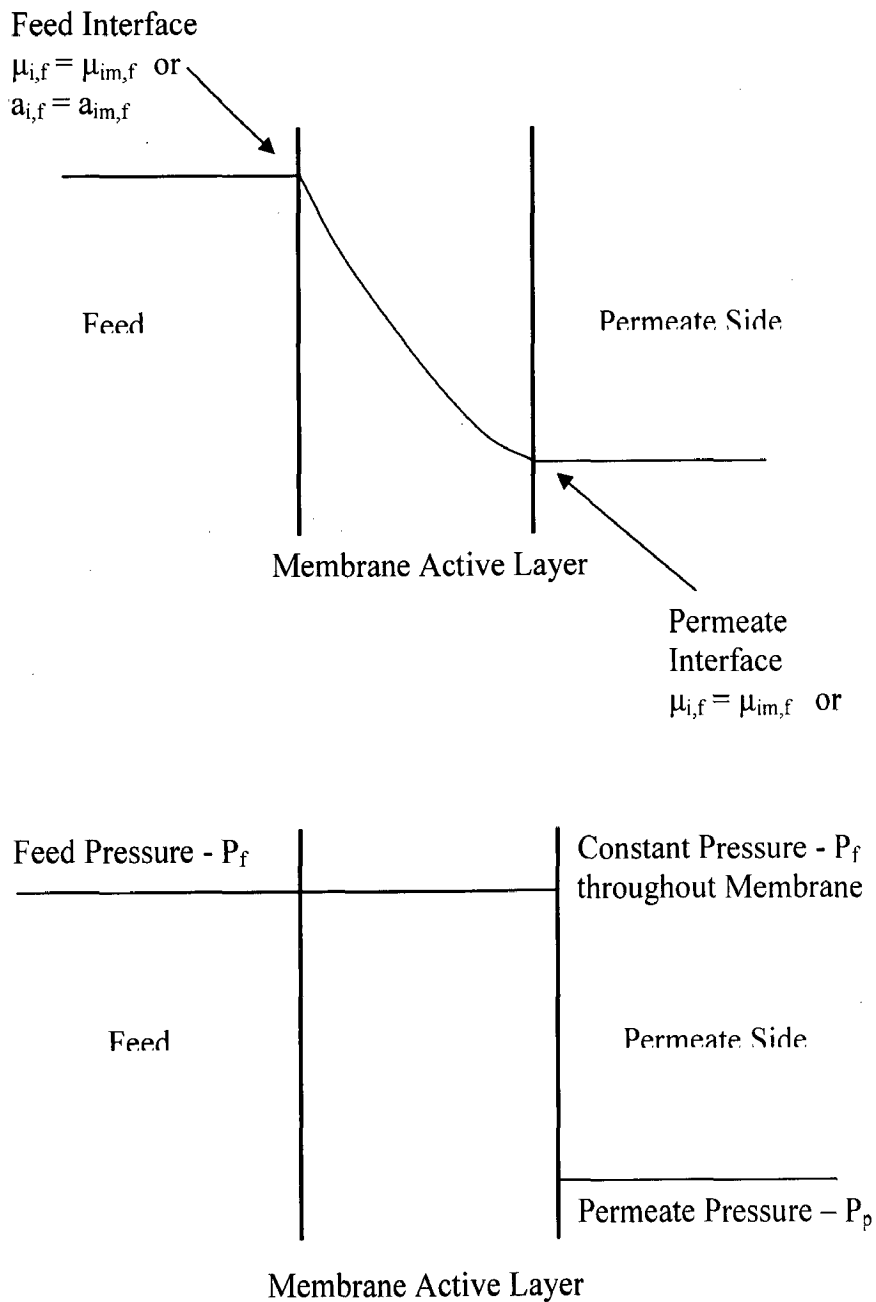
Fig. 4.1: Chemical Potential and Pressure Profiles across Pervaporation membrane according to Solution-Diffusion model

One of the common assumptions of the solution-diffusion model is that the pressure across the membrane thickness is a constant. The relevance of this assumption to the pervaporation process is that the vaporization of the species occurs on the permeate interface of the membrane. Within the membrane, no phase change is possible since the pressure is constant. However, in reality, this may not be true i.e. the pressure may vary gradually across the membrane thickness. Katoaka et al. (1991) [88] have assumed a linear pressure profile across the membrane thickness and simulated the effect of the variables such as feed and permeate pressure on the pervaporation performance. Their simulation results showed that both reverse osmosis and pervaporation show identical flux and separation behavior at very high feed pressures (>100 atm). Also, the simulations showed that a higher pervaporation flux and lower selectivity wuld be observed for a linear pressure profile as compared to a flat pressure profile. The solution –diffusion requires knowledge about the sorption of the various species on the membrane and the diffusion of the same through the membrane. Several researchers [89 – 92] have developed into such theoretical aspect of solution-diffusion model for liquid permeation through dense membrane.

4.2.2. Pore Flow Model

Sourirajan and Matsuura (1985) [93] were among the first ones to propose the pore flow or preferential sorption-capillary flow model to explain the transport mechanism and analyze the data for reverse osmosis and gas separation processes. The model was successful in explaining the negative rejection observed for reverse osmosis membranes. The model basically assumes the existence of micropores in the membrane material through which permeation of the liquid species takes place. At the mouth of the pore on the feed-membrane interface, preferential sorption of one of the species takes place. There is a sharp change in the comcentration gradient at this point because the feed components come under the influence of a strong force field present in the pores. The liquid then flows through the pores via a capillary flow mechanism. Sourirjan et al. (1987) [94] have extende the pore –flow model to model pervaporation membranes. According to the newely proposed mechamism, feed liquid enters the membrane pores on the feed side. At a certain thickness (z_i) in the membrane, the liquid undergoes a phase

45

change to the vapor phase. The vapor phase then traverses along the remaining length (z_v) of the pore and emerges on the permeate side. Fig. 4.2 shows a schematic of the pervaporation process in a membrane pore. Thus the pervaporation process can be considered as a combination of liquid transport (reverse osmosis) and vapor transport (gas separation) in series.
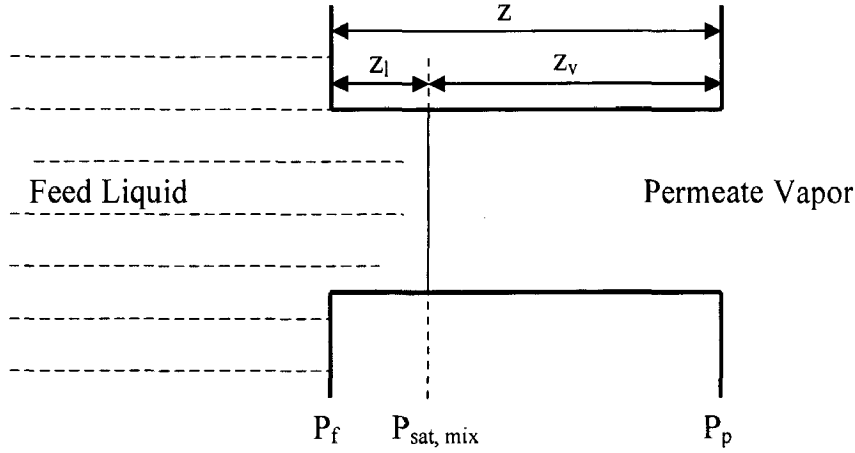
Fig. 4.2: Schematic of Pervaporation Process in Membrane Pore [95].

Based on the above model, the total flux equation [95] appears as

$$J_i = \left[\frac{Q}{z}\left(P_f - P_{sat,mix}\right) + \frac{B_i}{z}\left(P_{i,sat}^2 - P_{i,p}^2\right) + \frac{B_j}{z}\left(P_{j,sat}^2 - P_{j,p}^2\right) \right]\left(y_i M_i + y_j M_j\right) \quad (4.15)$$

In the above Eq.4.15 , Q, B_i, B_j are constant, z is the thickness of membrane, P_f is the feed pressure at pore inlet, $P_{i,p}$ is the partial pressure of component i on permeate side, $P_{i,sat}$ is the partial pressure of component i on feed side, y_i is the permeate mole fraction of component i and M_i is the molecular weight of component i. it is apparent from Eq. 4.15 that the total flux according to the pore-flow model depends on the pressure gradient across the membrane. The ratio B_j/B_i decides the selectivity of the membrane for a particular component. For example, for ethanol-water mixture at 40°C, the authors have shown that if a ration of 0.001 is assumed then water is strongly enriched in the permeate whereas for a ration of 10, it is fount that ethanol preferentially permeates through the membrane. In contrast, according to the solution –diffusion model, the total flux depends on the concentration gradient across the membrane. Okada et al. (1991) [95] have extended the above model to predict ethanol/water-silicone membrane system quite well.

However, it failed to do so for the ethanol/water-PVA membrane system. The reason for this is the fact that the pore flow model fails to take into account membrane swelling and hence pore enlargement at high water concentration.

4.2.3. Thermodynamic Vapor Liquid Equilibrium (VLE) Model

Wijmans and Baker (1993) [96] visualized the pervaporation process as two separate steps, a vapor liquid equilibrium step followed by a vapor permeation step. In the first part, the liquid feed is assumed to be in equilibrium with a hypothetical feed vapor which is in contact with the membrane. The hypothetical feed vapor is then assumed to sorb and permeate through the membrane. Fig. 4.3 shows a pictorial representation of the hypothesized process.
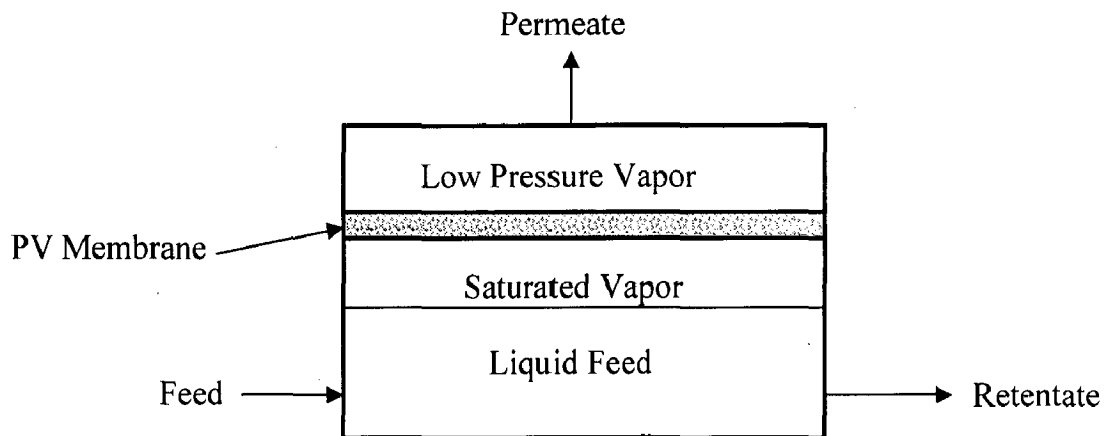
Fig. 4.3: Visualization of Thermodynamic Vapor Liquid Equilibrium Model for the Pervaporation Process (Adapted from Wijmans and Baker, 1993)

Wijmans and Baker have used the following equation for flux:

$$J_i = -\left(\frac{L_i RT}{x_i} \frac{d \ln a_i}{d \ln x_i} \right) \frac{dx_i}{dz}$$

(4.16)

It has been assumed in the thermodynamic VLE model that the term in the brackets is a constant and can be equated to the diffusion coefficient D_i. Integrating equation 4.16 over a membrane thickness z, we have,

$$J_i = \frac{D_i}{z} \left(x_{if,m} - y_{ip,m} \right)$$

(4.17)

Where $x_{if,m}$ and $x_{ip,m}$ are the mole fractions of species i on the membrane feed surface, on the feed and the permeate side respectively. To find the value of $x_{if,m}$, let us

imagine a situation wherein the component in the feed is in equilibrium with a hypothetical vapor which in turn is in equilibrium with the component i on the membrane surface. Thermodynamically this situation is not different from the actual situation. Now equating the chemical potential of the component i in the hypothetical vapor with that the surface of the membrane, we have

$$\mu_{i,sat} + RT\ln\left(\gamma_{if,v} x_{if,v}\right) + RT\ln\frac{P}{P_{i,sat}} = \mu_{i,sat} + RT\ln\left(\gamma_{if,m} x_{if,m}\right) + V_i\left(P - P_{i,sat}\right) \qquad (4.18)$$

Where $\gamma_{if,v}$ and $\gamma_{if,m}$ are the activity coefficients and $x_{if,v}$ and $x_{if,m}$ are the mole fraction of the component i in the hypothetical vapor and the membrane respectively. Simplifying Eq. 4.18, we have

$$x_{if,m} = \frac{x_{if,v}\gamma_{if,v}P}{\gamma_{if,m}P_{i,sat}\exp\left[\left(P - P_{i,sat}\right)/RT\right]} \qquad (4.19)$$

Assuming that the exponent term (Polynting factor) is 1, we have

$$x_{if,m} = \frac{\gamma_{if,v}}{\gamma_{if,m}P_{i,sat}}P_{if,v} \qquad (4.20)$$

Where $P_{if,v}$ is the partial pressure of the component i in the hypothetical vapor phase. The term $\gamma_{if,v}/(\gamma_{if,m}P_{i,sat})$ is termed as Henry's constant. Now for equilibrium

$$P_{if,m} = P_{i,f} \qquad (4.21)$$

Where $P_{i,f}$ is the partial pressure of component i in the feed. Hence, we have

$$x_{if,m} = H_i P_{i,f} \qquad (4.22)$$

Using similar type of equation for the permeate side, we have

$$x_{ip,m} = H_i P_{i,p} \qquad (4.23)$$

Substituting Eq. 4.22 and 4.23 in Eq. 4.17, we have

$$J_i = \frac{D_i H_i}{z}\left(P_{i,f} - P_{i,p}\right) \qquad (4.24)$$

The inherent assumptions about the sorption and diffusion coefficients made in the above equation are that the diffusion coefficient D_i is constant and sorption in the membrane follows the Henry's law. Based on these assumptions the normalized flux and permeability of the membrane would be assumed to be a constant. For the ethanol/water –PVA membrane system however, Wijmans and Baker (1993) [96] observed that the

water permeability varied by an order of magnitude (from *0.001* to *0.01* cm³ (STP)/cm³-s-cmHg) as the feed water concentration was increased from *10* to *100* wt%.

Thus it is obvious that the above model cannot be used for systems involving significant membrane swelling and non-ideal effects. However, the above model can be useful to explain the flux trend over small range of feed concentrations where variations in membrane swelling and coupling effects can be neglected.

4.2.4. Pseudophase – Change Solution – Diffusion (PPCSD) Model

Shieh and Hung (1998) [97] have proposed a modified version of the solution - diffusion model. Similar to the pore flow model, this model takes into account the fact that the phase change occurs within the membrane. However, permeation both in the liquid and vapor zone takes place by the solution-diffusion mechanism. The mass transport process thus is a combination of liquid and vapor permeation mechanisms in series. Also, contrary to the assumption of the solution-diffusion model, the pressure across the membrane is not a constant. Based on the PPCSD model, the final form of the flux equation for a pure component is very similar to that of the pore flow model.

$$J_i = \left[\frac{B}{z}\left(P_f - P_{sat}\right) + \frac{C}{z}\left(P_{sat}^2 - P_p^2\right) \right] \tag{4.25}$$

Although the equation is similar, it should be noted that the value of the constant **B** and **C** is different from the pore-flow model. The authors also assume that the solubility of the component depends linearly on the feed concentration whereas the diffusivity varies linearly with the sorbed concentration. The PPCSD model has been successfully used to predict the permeation of pure hexane through polyethylene membranes at various permeate pressures. It is observed experimentally that the pervaporation flux is dramatically affected when the permeate pressure approaches the saturation pressure. The PPCSD model can predict this sharp variation quite accurately.

4.2.5. Dusty Gas Model for Zeolite Micropores

The transport mechanism through zeolite micropores is different from that through the polymeric membranes. Within zeolite micropores, the surface forces are

extremely dominant and any adsorbed molecule can not escape from the strong force field of the pore irrespective of its position. The steric effects are critical and the diffusion through a zeolite micropore is considered to be an activated process wherein the diffusing species undergoes a series of jumps between regions of low energy potential. Karger and Ruthen (1992) [98] have considered the diffusing molecules within a zeolite micropore to form a single adsorbed phase. Diffusion of this adsorbed phase through the zeolite cages is called ether configuration diffusion, intra-crystalline diffusion, micropore diffusion or simply surface diffusion. The dusty gas model has been used to model the bulk and Knudsen diffusion through zeolite micropores [99 - 103] have extended the dusty gas model approach to the description of the surface diffusion of species within the micropores. According to this approach, the sites within the micropores of the zeolite cage are considered to be the $n+1^{th}$ species in the system. The diffusing species are assumed to hop from one site to the other. Fig. 4.4 shows a pictorial representation of the surface diffusion of adsorbed species on the zeolite surface.
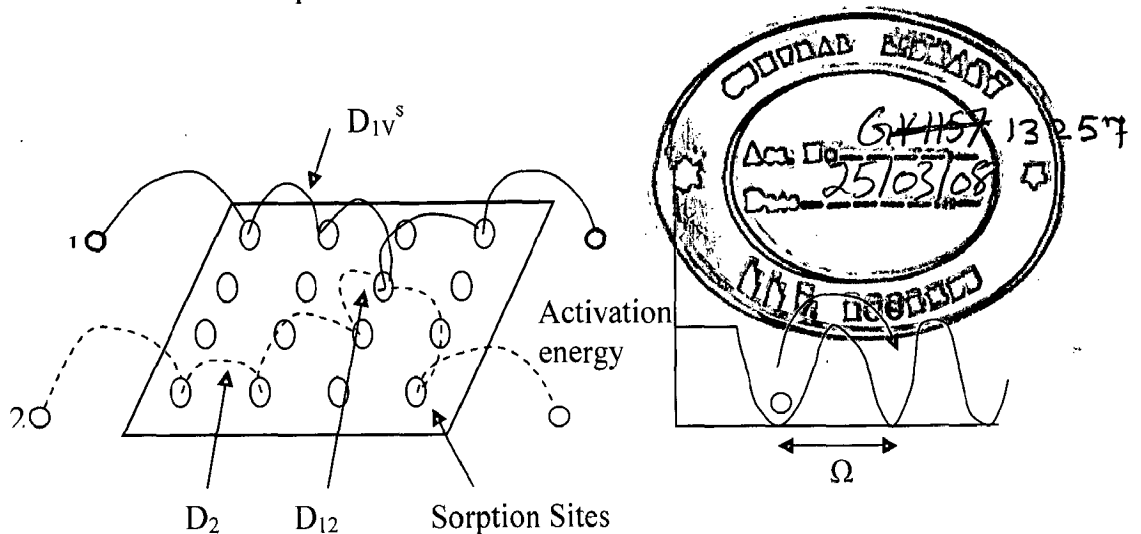
Fig. 4.4: Surface Diffusion of Adsorbed Species on Zeolite Sites by Hopping Mechanism (Adapted from Krishna and Wesselingh, 1997)

Eq. 4.5 can be used to model this system with inclusion of an additional term for the $n+1^{th}$ species.

$$-\nabla\mu_i = RT\sum_{k=1}^{n}\theta_k\frac{(v_i-v_k)}{D_{ik}^s}+RT\theta_{n+1}\frac{(v_i-v_{n+1})}{D_{i,n+1}^s}, \qquad i = 0, 2........n \qquad (4.26)$$

In the above equation, x_k has been replaced by θ_k, which represents the fractional site occupancy of species k. the term θ_{n+1} represents the fraction of the vacant sites present in the system. $D_{i,n+1}{}^s$ represents the Maxwell-Stefan pair diffusivity of species i with respect to the vacant sites. It is conventional to express the Maxwell-Stefan pair diffusivity in terms of the surface diffusivity $(D_{iV}{}^s)$ as

$$D_{iV}^s = \frac{D_{i,n+1}^s}{\theta_{n+1}}$$ (4.27)

Although this model has been conventionally used to describe the permeation of gaseous species through zeolite cages, it is thought that this model can be extended to the transport of liquid mixtures as well.

4.3. Sorption

It has already been mentioned that knowledge of sorption of all species in the membrane material is essential to predict the pervaporation behavior. The sorption usually strongly depends on the material-solvent interactions, degree of cross-linking, feed concentration and temperature. Ideal sorption can be expected when the interactions between the penetrating component is weak. This is mainly observed for sorption of gases in polymer. If ideal sorption is assumed, the concentration of a component in the membrane at equilibrium is linearly proportional to its concentration in the feed. Also the concentration of other components in the feed, does not affect the sorption of the primary or main component. Although some researchers [96 – 97, 104] have used ideal sorption for pervaporation modeling, this is generally not a good assumption due to the stronger interaction of liquids with polymeric ceramic materials. Researchers have therefore proposed various models to predict the sorption of multicomponent liquid mixtures in pervaporation membranes.

4.3.1. Flory-Huggins Theory

The sorption of multi-component mixtures in polymers can be explained by Flory-Huggins [105] thermodynamics wherein the activity of a species in the polymer can be expressed as a function of the volume fraction of species, the molar volumes of

the component and the Flory-Huggins interaction parameters. The Flory-Huggins theory takes into account both enthalpic and entropic effects into the free energy of mixing (ΔG_m). For a three component system comprising of two solvents and a polymer, the free energy of mixing is given by the following equation.

$$\Delta G_m = RT\left(x_1 \ln\phi_1 + x_2\phi_2 + \chi_{12}x_i\phi_j + \chi_{1p}x_i\phi_p + \chi_{2p}x_2\phi_p\right) \qquad (4.28)$$

Where x and ϕ are the mole fraction and volume fraction respectively and χ's are the adjustable parameters. Subscripts *1*, *2* and *p* denote solvent *1*, *2* and the polymer respectively. Differentiation of Eq.4.28 with respects to the mole fraction yields the equations for activity prediction of solvents *1* and *2* in the polymeric system as a function of the volume fractions.

$$\ln a_1^m = \ln\phi_1 + \phi_2\left(1-\frac{V_1}{V_2}\right) + \phi_p\left(1-\frac{V_1}{V_p}\right) + \left(\chi_{12}\phi_2 + \chi_{1p}\phi_p\right)\left(\phi_2 + \phi_p\right) - \chi_{2p}\phi_2\phi_p\frac{V_1}{V_2} \qquad (4.29)$$

$$\ln a_2^m = \ln\phi_2 + \phi_1\left(1-\frac{V_2}{V_1}\right) + \phi_p\left(1-\frac{V_2}{V_p}\right) + \left(\chi_{12}\phi_1 + \chi_{2p}\phi_p\right)\left(\phi_1 + \phi_p\right) - \chi_{1p}\phi_1\phi_p\frac{V_2}{V_1} \qquad (4.30)$$

In the above equations, a^m is the activity in the membrane and χ_{12}, χ_{1p} and χ_{2p} are the binary interaction parameters.

The value of the parameters χ_{1p} and χ_{2p} can be experimentally determined by pure component swelling experiments whereas the value of χ_{12} can be determined by fitting vapor-liquid equilibrium (VLE) data to the Flory-Huggins binary equation [106]. Attempts have also been made to theoretically calculate the value of the solvent-polymer binary interaction parameters [107]. As shown in Eq.31, the interaction parameter is considered to be summation of two terms; the enthalpic $\left(\chi_h\right)$ and the entropic term $\left(\chi_s\right)$.

$$\chi = \chi_s + \chi_h = \chi_s + \frac{V_s}{RT}\left(\delta_s - \delta_p\right)^2 \qquad (4.31)$$

For PDMS based mixtures, the entropic term $\left(\chi_s\right)$ is usually set equal to *0.45* [108] while the enthalpic $\left(\chi_h\right)$ is obtained from the solubility parameters of the solvent and the polymer. The Flory-Huggins theory has been very successful in predicting the sorption of organic apolar solvents in rubbery polymers. Some typical examples are chloroform-

PDMS and carbon tetrachloride-PDMS system. However, poor agreement between theoretical and experimental results is observed in the case of associated or polar solvents

Variable interaction parameters have been used to extend the predictability of the Flory-Huggins theory to polar systems as well. Kennedy (1980) [109] has proposed the use of a quadratic, empirical relationship which has three adjustable parameters.

$$\chi = \chi_0 + \chi_1\phi_p + \chi_2\phi_p^2 \tag{4.32}$$

The use of above correlation resulted in a significant improvement for prediction of alcohol isotherms in PDMS. Koningsveld and Kleintjens (1971) [110] have proposed a different form of the interaction parameter and volume fraction dependence, based on the lattice graph theory.

$$\chi = a + \frac{b(1-c)}{(1-c\phi_p^2)} \tag{4.33}$$

In the above equation, a is an empirical entropy correction term, $c \approx \frac{2}{Z}$ (Z is the lattice coordination number which is usually set to 10) and b is given by

$$b = \frac{(Z-2)\Delta\omega}{RT} \tag{4.34}$$

Where $\Delta\omega$ is the difference between the interaction free enthalpy of unlike neighbors. The drawback of the Koningsveld-Kleintjens approach is that the value of the parameters a, b and c cannot be predicted but has to be determined by fitting experimental data.

4.3.2. Flory-Rehner Theory

Flory and Rehner (1943) [111] have proposed an additional term in the Flory-Huggins equation, to take into account the elastic forces contribution for a cross-linked polymer. The Flory-Rehner equation for a simple, binary polymer-solvent system is written as

$$\ln a_s^m = \left[\ln\phi + \left(1 - \frac{V_s}{V_p}\right)\right] + \chi\phi_p^2 + \left[\frac{V_s\rho_p}{M_c}\left(\phi_p^{1/3} - \frac{\phi_p}{2}\right)\right] \tag{4.35}$$

53

Where M_c denotes the molecular weight between two cross-link points and ρ_p is the polymer density. The elastic term calculation assumes that the coiling of the chain is unaffected by the presence of neighboring polymer molecules, which is true only for dilute or highly swollen polymer solutions. Thus the above equation underestimates the elastic contribution, especially in the case of crystalline polymers [112 – 113]. It can be seen from Eq.4.35 that as the value M_c tends to infinity, the predicted activity tends to approach the values predicted by Flory-Huggins theory. In fact, when the value of M_c tends to infinity, the equation simplifies to the Flory-Huggins equation. This trend is expected because a high value of M_c implies a lower degree of cross-linking and the polymer properties would tend towards that of an uncrosslinked polymer.

4.3.3. UNIQUAC/UNIFAC Model

The use of group contribution models such as UNIQUAC (UNIversal QUasi Chemical Theory) and UNIFAC (UNIQUAC Functional-Group Activity Coefficients) has become popular in recent years for prediction of component solubilities in polymers. UNIQUAC is an acronym for universal quasi-chemical equation or molel [114 – 116]. This model is used to correlate and predict liquid-vapor and liquid-liquid equilibria, i.e., solution properties such as activity coefficients, partition coefficient, Henry's law constant. The term UNIFAC is an acronym for UNIQUAC Functional-Group Activity Coefficients, and combines the concept that a liquid mixture is composed of a solution of functional groups with an extension of the UNIQUAC model applies essentially to compounds themselves, UNIFAC nidek was initially proposed to provide a new group contribution method for predicting the activity coefficients in liquid mixtures of nonelectrolytes. Oishi and Prausnitz (1978) [117] applied the UNIFAC model to polymeric solutions (dilute concentrations of polymer) after adding a term for free volume correction and observed a good agreement for a variety of solvent-polymer systems. Goydan et al. (1989) [118] extended Oishi and Prausnitz's UNIFAC model to predict sorption of organic compounds in polymers and obtained fairly accurate results.

Heintz and Stephan (1992, 1994) [119 – 120] have modeled the sorption of highly non-ideal systems such as alcohol-water mixtures in PVA, using the UNIQUAC theory. UNIQUAC theory states that the activity of component i (a_i) in a system is the sum of a

54

combinatorial part (a_i^C) mainly due to differences in molecular size and shape and a residual part (a_i^R) reflecting energetic interactions. According to the UNIQUAC theory, the activity of component i in a multi-component liquid mixture containing n species, can then be expressed as

$$\ln a_i(x_1,....x_i,...x_n) = \ln\phi_i + \frac{Z}{2}q_i\ln\left(\frac{\theta_i}{\phi_i}\right) + l_i - \sum_{j=1}^{n}\phi_j\frac{r_i}{r_j}l_j - q_i^*\ln\sum_{j=1}^{n}\theta_j^*\tau_{ji} + q_i^*$$

$$-q_i^*\sum_{j=1}^{n}\frac{\theta_j^*\tau_{ij}}{\sum_{k=1}^{n}\theta_k^*\tau_{kj}}$$

(4.36)

Where

$$\phi_i = \frac{r_i x_i}{\sum_{j=1}^{n} r_j x_j}$$

(4.37)

$$\theta_i = \frac{q_i x_i}{\sum_{j=1}^{n} q_j x_j} = \frac{\left(\frac{q_i}{r_i}\phi_i\right)}{\sum_{j=1}^{n}\left(\frac{q_j}{r_j}\phi_j\right)}$$

(4.38)

$$\theta_i^* = \frac{q_i^* x_i}{\sum_{j=1}^{n} q_j^* x_j} = \frac{\left(\frac{q_i^*}{r_i}\phi_i\right)}{\sum_{j=1}^{n}\left(\frac{q_i^*}{r_j}\phi_j\right)}$$

(4.39)

$$l_i = \frac{Z}{2}(r_i - q_i) - (r_i - 1)$$

(4.40)

In Eq.4.36 to 4.40, θ and θ^* are the surface fractions of the various components in the mixture, r, q and q^* and l are parameters related to the size and shape of molecule, Z is the coordination number. τ_{ij} and τ_{ji} are binary interaction parameters describing the intermolecular interactions between the various components. These parameters are generally obtained by fitting the VEL data of the liquid mixture to the above equation. For polymeric systems, it is easier to express a_i as a function of the volume fractions ϕ_i in the system. The main reason for this is the fact that the mole fraction of the polymer is

generally very small compared to the solvent species, due to its high molecular weight. For polymeric systems (m refers to the polymer), Eq. 4.36 takes the form

$$\ln a_i (\phi_1,....\phi_i,...\phi_n,\phi_m) = \ln \phi_i + \frac{Z}{2} q_i \ln\left(\frac{\theta_i}{\phi_i}\right) + l_i - \sum_{j=1, j\neq m}^{n} \phi_j \frac{r_i}{r_j} l_j$$

$$- r_i \phi_m \left(\frac{Z}{2}\left(1 - \frac{q_m}{r_m}\right) - 1\right) - q_i^* \ln \sum_{j=1}^{n} \theta_j^* \tau_{ji} + q_i^* - q_i^* \sum_{j=1}^{n} \frac{\theta_j^* \tau_{ij}}{\sum_{k=1}^{n} \theta_k^* \tau_{kj}}$$

(4.41)

The solvent-membrane parameter τ_{im} in Eq. 4.41, is generally estimated by fitting Eq. 4.41 to the pure component vapor sorption data. The last two terms in Eq. 4.36 and 4.41 (terms containing q^* and θ^*) have been specifically added to take into account the hydrogen bonding present in the system. The inclusion of these terms aids the prediction of sorption isotherms for highly associating non-ideal system. In fact due to the presence of the modified surface parameters (q^* and θ^*), Eq.4.36 to 4.41 represents UNIQUAC-HB (UNIQUAC-Hydrogen Bonding) model [121 – 122]. Heintz and Stephan (1994) [119] successfully modeled the sorption of alcohols from aqueous-organic mixtures using the above theory. For example, they predicted a maximum methanol sorption of *0.3* was also predicted using the same theory. These values match well with the observed experimental values. Also, since methanol is more polar than ethanol its sorption value would be expected to be higher than ethanol. This trend is reasonably predicted by UNIQUAC theory. Besides Heintz and Stephan, Jonquieres et al. (2000) [123] have used this approach to model other non-ideal ternary systems such as ethyl acetate-ethanol in polyurethanemide (PUI) membranes. The strong synergy effects observed for the swelling of PUI membranes could be effectively modeled by this method. The model has also shown superior capabilities in predicting the solubilities of the other systems such as chclohexane/benzene and cyclohexane/ toluene in a polyurethane membrane [124]. The only drawback of the UNIQUAC model is that it requires knowledge of the pure component vapor sorption isotherm and the VLE data for the liquid mixtures to generate the values of the binary interaction parameters. Very often, such data is hard to find in literature making the applicability of this model difficult.

4.3.4. Engaged Specie Induced Clustering Model (ENSIC)

The ENSIC model is a semi-empirical, mechanistic model that has been proposed by Favre et al., (1993, 1996) [125 – 126]. The model considers the probability of insertion of a solvent/vapor molecule in a polymer matrix already containing some preciously sorbed species. Two parameters are used to define the interactions in the system: k_s, which define the affinity between the solvent species being sorbed and the solvent species already sorbed and k_p, which determines the affinity between the solvent species and the polymeric species. This theory bridges the gap between the simple one parameter theories like Flory- Huggins and the more sophisticated multiparameter theories like UNIQUAC.

Based on the assumption of lattice framework of the penetrant-polymer system (i.e. the same volume of polymer segment and penetrant cell as in the Flory-Huggins theory) and an ideal gas phase, the final expression for the ENSIC model appears as

$$\phi_s = \frac{e^{(k_s - k_p)a_s} - 1}{(k_s - k_p)/k_p} \tag{4.42}$$

Eq. 4.42 can be used to describe both concave (i.e. Langmuir type) and convex (Flory Huggins type) behavior, depending on the respective values of k_s and k_p. When the affinity of the solvent being sorbed for the polymeric segments is higher than its affinity for the sorbed species, i.e., $k_p \gg k_s$, then the model shows Langmurian type behavior. On the other hand when the solvent/solvent affinity is stronger than the solvent/polymer affinity, the model exhibits Flory-Huggins type of behavior. When k_s is equal to k_p, the model follows Henry's law, i.e., the sorption of the solvent is directly proportional to its activity in the vapor phase. This model is especially attractive for cases where there is a strong affinity between the solvent specie, leading to formation of solvent clusters in the polymer phase. Several other researchers have indirectly observed the information of solvent clusters in polymer. For example, Yasuda (1962) [127], while studying the sorption of water in polymers, observed a deviation from the linear behavior to BET type III isotherm, which is indicative of solvent clustering. Nguyen et al. (1996) [128] have found evidence of both water and alcohol clustering in membranes by using interface

(IR) spectroscopy. Rogers (1965) [129] and Favre et al. (1994) [130] have observed that the diffusion coefficient of certain penetrants through the polymer matrix decreases with an increase in the volume fraction of the penetrant, which is indirect proof of the solvent clustering phenomenon. The strength of the ENSIC model thus lies in the fact that it can give a mechanistic insight into the solvent clustering effect. Jonquieres et al. (1998) [131] have used the ENSIC model to predict the pure vapor sorption of ethanol and ethyl acetate in polyurethanimides (PUI) and have obtained an excellent fit. The residual sum of squares (RSS) for ethanol and ethylacetate sorption in PUI was found to be less than 0.4. The R-squared value for the fit was found to be *0.998*. The fit was better than that obtained by Flory-Huggins theory. However, the drawback of this model is that it is difficult to extent to multicomponent system.

4.3.5. Sorption in Zeolites

Ceramic pervaporation membranes are typically made from one of five different types of zeolites: zeolite A, X, Y, silicate and ZSM-5. These zeolites are mainly classified based on their cage size and hydrophilicity. Both the hydrophilicity and the cage size are varied by changing the ratio of the various oxides (Na_2O, SiO_2 and Al_2O_3) in the membrane. Typically, the zeolite tends to be more hydrophobic if the SiO_2 content is higher. Also when sodium is present as the counterion in the membrane lattice, then the zeolites are named as NaZ, NaX and NaY. Sorption of most species in molecular sieves can be considered as a physical sorption process due to the fact that no electron transfer is involved in the process. Normally, any physical adsorption process includes both van der Waals dispersion-repulsion forces and electrostatic forces comprising of polarization, dipole and quadrupole interaction. However, since the zeolite have an ionic structure, the electrostatic forces become very large in the adsorption of polar molecules like H_2O. The effect is manifested in the fact that the heat of adsorption of water on zeolitic adsorbents is usually high (*25-30* kcal/mole) [132]. The heat of adsorption is a direct measure of the strength of bonding between the sorbate and surface thus proving that there is a very strong interaction between water and the ionic species in the zeolite cage. In fact, the heat of adsorption values (for water sorption on zeolites), are of the order of the chemisorption process which is again indicative of strong ionic interactions. Researchers [133] have

evaluated the contribution of elextrostatic forces in the adsorption of various polar molecules in the NaX zeolite, through heat of adsorption experiments. They found that the contribution of electrostatic forces to the heat of adsorption for H_2O, NH_3, CH_3OH and C_2H_5OH were **80%**, **80%**, **72%** and **63%** respectively. Equilibrium sorption data for zeolites are commonly presented as isotherms plotting the adsorbed concentration versus partial pressure for gases or concentration for liquids. Although a detailed theoretical analysis for complex polar molecules is difficult, the structural regularity of molecular sieves makes possible the prediction of sorption isotherms for simple adsorbates such as the rare gases.

4.3.5.1. Henry's Law

Most adsorption systems exhibit linear behavior in the low concentration range. The Henry's law constant (H) is defined as 'the ration of the partition functions for adsorbed and gaseous molecules duly corrected for the difference in potential energy' [134]. Mathematically, it can be expressed as

$$H = \frac{f_s}{f_g' kT} \exp\left(\frac{u_g - u_s}{kT}\right)$$ (4.43)

In the above equation, f_s and f_g' are the partition functions for adsorbed molecule and partition function per unit volume for free gaseous molecule respectively. u_g and u_s represent the free energy of the gaseous molecule in the free gaseous and the sorbed state respectively whereas k is the Boltzmann constant. For a monoatomic species or polyatomic species in which the rotational and internal freedom are not modified by sorption, the term on the right hand side of Eq. 4.43 can be written as

$$\frac{f_s}{f_g'} \exp\left(\frac{u_g - u_s}{kT}\right) = Z_l = \int_V \exp\left[-\frac{u(r)}{kT}\right] dr$$ (4.44)

Z_l is known as the configuration integral for an occluded molecule and $u(r)$ is the potential energy of adsorbed molecule (relative to the gas phase) as function of position within the cavity. The Henry's constant H decreases exponentially with temperature according to the Arrhenius law,

$$H = H_0 \exp\left(\frac{-\Delta q_s}{RT}\right)$$ (4.45)

Where Δq_s represents the heat of sorption of the sorbate on the zeolite. The heat of sorption can also be theoretically expressed as a function of the configuration integral.

$$\frac{-\Delta q_s}{RT} = 1 - \int_V \frac{u(r)}{Z_i kT} \exp\left[-\frac{u(r)}{kT}\right] dr$$ (4.46)

It is possible to know the position of each ion in the zeolite lattice by X-ray crystallographic studies and hence on can calculate $u(r)$ by summing the dispersion, repulsion and polarization energies of interaction of the sorbate molecule with each ion in the lattice. From evaluation of $u(r)$ and the configuration integral, one can then calculate the heat of sorption Δq_s and the Henry's constant H. Derrach and Ruthven (1975) [135] have performed such theoretical computations for sorption of inert gases in zeolites A and X and obtained fairly accurate results.

Extension of the above theory to more complex molecules however, is quite difficult. For molecules with strong dipole or quadrupole moments, the electrostatic interactions must also be included in the above calculations. It is also necessary to take sorbate-sorbate interactions and molecular rotation into account. Researchers obtained poor agreement between theory and experiment when an attempt was made to calculate the Henry's law constant and the heat of sorption for CO_2 in zeolite 5A. Hence, the use of adsorption isotherms to model adsorption on zeolites has become more popular.

4.3.5.2. Langmuir Adsorption Isotherm

This model assumes that the zeolite crystal lattice contains a fixed number of distinct, identical adsorption sites (θ_t) on which the species get adsorbed. If no interaction between adsorbed molecules on neighboring sites is assumed, then the simple Langmuir equation can be written as

$$\theta_s = \frac{sP_g}{1 + sP_g}$$ (4.47)

Where θ_s is the site occupancy of the sorbate, P_g is the pressure of the free sorbate in the gaseous phase and s is a constant. The Langmuir constant s also has a simple temperature dependence as the Henry's constat.

$$s = s_0 \exp\left(\frac{-\Delta q_s}{RT}\right) \qquad (4.48)$$

The Langmuir equation fails to take into account the interaction between adsorbed molecules and the heterogeneity of the adsorption sites. As a result, it has been used to model only a few systems such as Kr-5A [135] and C_3F_8-13X [136] over a limited range of concentrations ($\theta_s < 0.5$). Some modified expressions have been suggested to take care of the above limitations but only with limited success [136 – 137].

4.3.5.3. Statistical Thermodynamics Model

For most molecular sieves, the assumption of fixed number of adsorption sites is erroneous. This is because the zeolitic materials do nat show an exact saturation limit for the sorbate but rather the saturation sorbate concentration increases slowly an exact saturation limit for the sorbate but rather the saturation sorbate concentration increases slowly with applied pressure and decreases at elevated temperatures. It is thus obvious that the sorbate displays bulk fluid-like properties mainly such as an increase in concentration as higher pressures (compressibility) and lower temperature (thermal expansion) [138 – 139]. It is therefore thought that one can view the process of zeolite sorption simply as the filling of intracrystalline zeolite micropores by the condensed adsorbate. This has been proven by the fact that the sorption capacity of the zeolite can be estimated as a ratio of the intracrystalline volume and the molecular volume of the saturated adsorbed [140].

The concept of pore filling of zeolite micropores has been used to develop a simple statistical isotherm mainly applicable to zeolites types A, erionite and chabazite, in which the intracrystalline space is divided into discrete cavities interconnected through small windows. It is assumed that the potential energy is uniform throughout a single cavity and there is a significant energy barrier between two cavities. This assumption ensures that an adsorbed molecule stays confined within a given cavity. It is free to move

within the cavity but cannot hop from one cavity to another. A second assumption made is that there is no intermolecular attraction and when a cavity contains more than one molecule, the interaction can be accounted for by a reduction in the free volume. The configuration integral for a cavity containing n molecules (Z_n) becomes

$$Z_n = \frac{Z_1^n}{n!}\left(1 - \frac{n\beta_s}{V_s}\right)^n$$ (4.49)

$$Z_1 = HkT$$ (4.50)

Where Z_1 is the configuration integral for a cavity containing one molecule, β_s is the volume of a sorbate molecule and V_z is the volume of the zeolite cavity. The expression for the equilibrium isotherm [141 – 142] can then be written as:

$$q = \frac{HP_g + \left[HP_g\left(1 - \frac{2\beta_s}{V_z}\right)\right]^2 + \ldots\ldots + \dfrac{\left[HP_g\left(1 - \frac{m\beta_s}{V_z}\right)\right]^m}{(m-1)!}}{1 + HP_g + \dfrac{1}{2!}\left[HP_g\left(1 - \frac{2\beta_s}{V_z}\right)\right]^2 + \ldots\ldots + \dfrac{\left[HP_g\left(1 - \frac{m\beta_s}{V_z}\right)\right]^m}{m!}}$$ (4.51)

Where the saturation limit in terms of molecules per cavity is given by $m \leq V_z/\beta_s$. All the parameters in the above equation except H are known, which can be estimated from initial slope of the low concentration region of the isotherm. Eq. 4.51 has been found to fit the isotherms for several light hydrocarbons in zeolite 5A sieve well [142]. The model has also been used to correlate equilibrium data for CO_2 in different zeolites [143]. However, the model does give a good fit for sorption of polar molecules in the zeolite cages. Polar molecules tend to undergo sorption at localized sited within the zeolite cages and therefore the assumption of a uniform field for such systems in inappropriate.

4.3.5.4. Adsorption Potential Theories

Due to the limited applicability of the model isotherm equations, several generalized thermodynamic models have been developed. One example of this approach is the application of Polanyi potential theory to zeolitic adsorbents [144]. It is assumed

that the adsorbed fluid is similar to the saturated liquid adsorbate. The equilibrium data is correlated in terms of the adsorption potential (ε_p) which is defined as the difference in the free energy between the adsorbed fluid and the pure saturated liquid sorbate.

$$\varepsilon_p = RT \ln\left(\frac{f}{f_s}\right) \approx RT \ln\left(\frac{P_g}{P_{sat}}\right) \qquad (4.52)$$

In Eq. 4.52, P_g represents the equilibrium pressure of the species in equilibrium with the zeolite and P_{sat} refers to the saturation or vapor pressure of the species at that temperature. According to the potential theory, a plot of the volume of fluid adsorbed versus the adsorption potential (ε_p) should yield a temperature invariant characteristic curve. This trend can be expressed in form of the Dubinin-Radushkevich (D-R) equation.

$$\frac{q}{q_{sat}} = \exp\left[-\left(\frac{\varepsilon_p}{\varepsilon_p{}'}\right)^2\right] \qquad (4.53)$$

In the above equation, $\varepsilon_p{}'$ is a constant which depends on the characteristics of the sorbate-sorbent system. The characteristic curve for any system can be established by fitting date from an isotherm covering a wide range of pressures or from isotherms at several temperatures. With the help of D-R equation, one can then predict the isotherm at any other temperature.

The D-R equation is a modification of the Dubinin-Polanyi equation (D-P) which took into account only the dispersion-repulsion forces and the temperature invariance was thus introduced into the theory. The theory does not incorporate electrostatic interactions (dipole and quadruple force), which are temperature dependent. However, it has been observed that over small temperature ranges (*25* to *125°C*), the D-R equation can still be used to model the sorption of polar compounds such as NH_3, H_2O, and CO_2 in *4A* and 13X zeolites [145]. A severe limitation of the D-P and the D-R equation is that these cannot be reduced to the Henry's law at low sorbent concentration. However, these equations for provide a common correlation for a wide range of equilibrium data and prediction of isotherms at different temperatures.

4.4. Diffusion

The diffusion of the various species through the dense membrane is generally the rate-controlling step in the pervaporation process. The diffusion process through the membrane is a very complex phenomenon, namely due to the coupling effect of the diffusing species, the plasticizing effect of the diffusing species in case of polymeric materials and the dependence of the diffusion coefficient on the concentration of the diffusing species. A variety of different models, both fundamental and semi-empirical have been proposed to explain the diffusion of a component through the membrane.

4.4.1. Free Volume Model

The diffusion of molecules through polymer networks basically occurs due to the passage of these molecules through the voids and intermolecular spacing between the polymer chains. Thus the diffusion of the various permeants occurs through the "free volume" of the polymer and the diffusion coefficient of the permeant can be expressed as a function of the fractional free volume of the polymer and two adjustable parameters, which are representative of the permeant-polymer interactions [146 – 148]. The thermodynamic diffusion coefficient (D_{iT}) of component i through a polymer film can be expressed as

$$D_{iT} = RTC_i \exp\left(\frac{E_i}{V_{fp}}\right) \tag{4.54}$$

Where C_i and E_i are constants and V_{fp} is the free volume of the polymer. Yeom and Huang (1992a) [149] obtained good agreement between calculated and experimental diffusivities for permeation of benzene, toluene, hexane and heptane through polyethylene films using Eq.4.54. Fang et al. (1975) [150] have extended the free volume theory to explain the diffusion of gases and liquid mixtures through polymer networks. Yeom and Huang (1992b) [151] have also proposed an equation for diffusion of a binary mixture through a membrane. This model assumes that the total free volume of the system is the sum of the free volume of the polymer and the increase in free volume due

to the plasticozing actions of the two components. Mathematically, the thermodynamic diffusivity (D_{iT}) can then be written as

$$D_{iT} = RTC_i \exp\left\{-\left[\frac{f(0,T)}{E_i} + \frac{\kappa_i(T)}{E_i}\phi_i + \frac{\kappa_j(T)E_j}{E_i}\phi_j\right]^{-1}\right\}$$ (4.55)

Where $f(0, T)$ is the free volume fraction of the dry polymer and $\kappa(T)$ is proportionality constant. An inherent assumption in Eq. 4.55 is that the free volume parameters [C_i, E_i, E_j, $f(0, T)$, $\kappa(T)$] for single component systems remain unchanged in the binary mixture.

The strengths of Vrentas and Duda's free volume model [152 – 153] and Pae-Datyner's molecular model [154] have been combined together in Doong and Ho's model [155]. According to this model, single penetrant diffusivity in a polymer can be given as

$$D_i = \frac{1}{6}\Omega^2 \vartheta \exp\left(-\frac{w_1\vartheta_1^* + w_2\vartheta_2^*\xi}{V_{fp} + \sigma w_1}\right)$$ (4.56)

Where Ω is the jumping distance of the penetrant, ϑ is the average jumping frequency, V_{fp} is the free volume of the polymer (per gram) and w_i is the weight fraction of species i in the polymer. ξ is the ratio of the molar volume of the penetrant V_1^* at 0 K to the molar volume of the polymer jumping unit V_2^* at 0 K. σ is the concentration coefficient of the penetrant to increase the free volume of the penetrant-polymer system. The three adjustable parameters in the above model are Ω, V_2^* (or ξ) and σ. Eq. 4.56 can also be generalized to multicomponent system [156].

$$D_i = \frac{1}{6}\Omega_i^2 \vartheta_i \exp\left(-\frac{\vartheta_i^* M_i \sum_{j=1}^{n} w_j / M_j}{V_{fp} + \sum_{j=1}^{k} \sigma_j w_j}\right)$$ (4.57)

Eq.4.57 could successfully predict the separation of toluene/mesitylene and p-xylene/mesitylene mixtures using polyethylene membranes. The "free volume" model however, has a couple of limitations. It cannot satisfactorily explain the diffusion of molecules through swollen membranes [157]. Also, a lot of experimental data is required to determine the various parameters in the model. Due to these drawbacks, the semi-empirical correlations describing the diffusion of species through the polymer on a macro-level are more popular.

4.4.2. Semi – Empirical Correlations

A variety of semi-empirical diffusivity –concentration relations have been proposed by researchers to model permeation through dense membranes. Lee et al. (1975) [104] have assumed a constant diffusivity to model diffusion through a dense membrane. Kataoka et al. (1991) [88] and Wijmans et al. (1993) [96] have also used a constant diffusivity to develop permeation equations for pervaporation membranes. However, it is well known that the diffusion coefficient of the species through a polymer depends on the concentration of the permeating species. An improved model was proposed by Greenlaw concentration of the permeating species. An improved model was proposed by Greenlaw et al. (1977) [158]. The diffusion coefficient was now assumed to be a linear function of the concentration of the permeating species.

$$D_i = D_i^0 \left(C_i + S_{ji} . C_j \right) \tag{4.58}$$

Where S_{ji} is an empirical constant signifying the coupling or the interaction between the two components. Using Eq.4.58, the researchers predicted the separation of heptane and hexane using polyethylene films.

The Long model [89], which assumes an exponential dependence of diffusivity on concentration, has been conventionally used to model pure component permeation through dense films.

$$D_i = D_i^0 \exp(\gamma_i C_i) \tag{4.59}$$

Based on Eq. 4.59, Suzuki and Onozato (1982) [159] proposed a new model for multicomponent permeation through dense membranes.

$$D_i = D_i^0 \exp(\gamma_i C_i + \gamma_j C_j) \tag{4.60}$$

The parameter γ, in Eq. 4.59, takes into account the plasricizing effect of the species on the polymer matrix. In Eq 4.60, the exponential parts of the expressions for D_i and D_j are the same. This equation has therefore been replaced by the more popular 'six coefficient' model, which has been widely used to model complex, non-ideal ternary systems [131, 153, 160 – 161].

$$D_i = D_i^0 \exp(\gamma_{ii} C_i + \gamma_{ij} C_j) \tag{4.61}$$

A novel approach has also been proposed by Bitter (1984, 1991) [162 – 163] wherein the swollen membrane is treated as a homogeneous liquid mixture consisting of polymer and penetrant. A modified Vigne equation can then be used to calculate the self – diffusion coefficient of component i (D_{im}^*) in the mixture.

$$\ln D_{im}^* = \phi_i \ln D_{ii}^* + \sum_{j=1}^{n} \phi_j \ln D_{ij}^{\infty} \qquad (4.62)$$

In Eq. 4.62, D_{ii}^* is the self-diffusivity of component i, D_{ij}^* is the binary diffusivity of i and j at infinite dilution of i. both these parameters can be obtained from empirical equations for calculating diffusion coefficients as well as desorption experiments. Most of the semi-empirical equations also suffer from the same disadvantage as free volume models in that a number of constants and parameters have to be evaluated experimentally.

4.4.3. Diffusion in Zeolites

Diffusion within the micropores of the zeolite is generally less well understood than macropore diffusion. Zeolite diffusion is fundamentally different from Knudsen and molecular diffusion because the molecule experiences a strong force field within the pore. As a result, zeolitic diffusivities are strongly concentration dependent and they also show an exponential dependence on temperature indicating that the process occurs in an activated fashion. The Fickian diffusivity (D_i) can be expressed as a product of two terms; the thermodynamic or Maxwell-Stefan diffusivity (D_{iT} or $[K]^{-1}$) and the thermofynamic factor ($[\Gamma]$ or $d \ln a_i / d \ln x_i$). For sorption and diffusion of pure gases in zeolites, the equation can be simply represented as

$$D = D_T \frac{d \ln P}{d \ln C} \qquad (4.63)$$

Where P is the pressure of the gas adsorbed on the zeolite and C is the concentration of the adsorbate in the gaseous phase. In an adsorbed phase, ideal behavior is observed in the low concentration limit where $d \ln P / d \ln C$ equals 1. However, at higher concentrations, $d \ln P / d \ln C$ is usually a strong function of concentration. It should be noted that althorgh both the Fickian and thermodynamic diffusivity are concentration

dependent, the concentration dependence of D_T will be less pronounced due to the introduction of the thermodynamic factor.

The model permeation of multicomponent mixtures through zeolite membranes, evaluation of component Maxwell-Stefan surface diffusivities (defined in Eq. 4.27) is important. Several models have been proposed for evaluation of the Maxwell-Stefan surface diffusivity. One model [164] expresses the surface diffusivity as a function of the displacement of the adsorbed species χ and the jump frequency $\vartheta(\theta_i)$ as shown in Eq.4.64.

$$D_{iV}^s = \frac{1}{Z}\Omega^2 \vartheta_i(\theta_t)$$

(4.64)

Where θ_t is the total surface coverage of the species and Z represents the coordination number or the number of nearest neighbor sites. If the jump frequency is independent of the surface coverage, i.e. $\vartheta_i(\theta_t) = \vartheta_i(0)$, it remains a constant and the surface diffusivity is also independent of the surface coverage.

$$D_{iV}^s = \frac{1}{Z}\Omega^2 \vartheta_i(0)$$

(4.65)

Barrer (1978) [165] and Riekert (1971) [166] suggested that the jump frequency would decrease with an increase in the surface coverage of the species. If it is assumed that a molecule will jump only to a vacant site, then the jump frequency and the surface diffusivity can be expressed as

$$\vartheta_i(\theta_i) = \vartheta_i(0)\theta_v, D_{iV}^s = \frac{1}{Z}\Omega^2 \vartheta_i(0)\theta_v$$

(4.66)

Were θ_v is the fraction of vacant sites in the zeolite matrix.

Van der Broeke and coworkers (1995) [167] have proposed a slightly different model to explain diffusion in zeolitic structures with interconnected cages like zeolites A and X. in this model, the jump frequency $\vartheta_i(\theta_t)$ varies with the total site occupancy θ_t in a power law type fashion, as shown in Eq. 4.67

$$D_{iV}^s = \frac{1}{mZ}\Omega^2 \vartheta_i(\theta_t) = \frac{1}{mZ}\Omega^2 \vartheta_i(0)\left[1 - \theta_t^{mZ}\right] = D_{iV}^s(0)\left[1 - \theta_t^{mZ}\right]$$

(4.67)

Where the factor "mZ" represents the maximum number of nearest neighbor sites per cage and $\left(1 - \theta_t^{mZ}\right)$ is the probability that at least one of the sites is vacant. For three

dimensional cage structures such as zeolite A nd X, the suggested values of m and Z are 2 and 4 respectively [164]. For pore-type zeolites such as ZSM-5, values of 1 and 1 have been suggested for m and Z respectively. It is evident from Eq. 4.67 that the surface diffusivity of the species through the pores depends on the number of vacant sites present on the surface. At low surface coverage ($\theta_t = 0 - 0.2$), the value of θ_t^8 is very low and the surface diffusivity is practically independent of the surface coverage. However, at high surface coverage, the value of θ_t^8 cannot be neglected and the diffusivity becomes dependent on the surface coverage. More complicated models taking pore interconnectivity and pore blockage into account have been proposed by researchers [165 – 166].

The term D_{ik}^s in Eq.4.26 represents the adsorbate i-adsorbate k interactions in the zeolite pore. This coefficient can be viewed at the tendency of species k to be replaced by species i at an adsorption site. Obviously, D_{ik}^s is then expected to depend on the jump frequencies of species i and k. the simplest model assumes that the Maxwell-Stefan i-k pair diffusivity is dictated by the lower of the two frequencies.

$$D_{ik}^s = \frac{1}{Z}\Omega^2 \vartheta_k(\theta_t), \qquad \vartheta_k(\theta_t) < \vartheta_i(\theta_t) \tag{4.68}$$

It should be noted that within a single narrow pore of zeolite crystals, the molecular species cannot pass each other. In other words, there is room for only one type of molecular species at a given time. This phenomenon is referred to as single file diffusion. In that case, the i-k pair diffusivity can be ignored. Krishna (1990) [101] has suggested a different procedure for the estimation of the i-k pair diffusivity.

$$D_{ik}^s = \left[D_{iV}^s(0)\right]^{\theta_i/(\theta_i+\theta_k)}\left[D_{kV}^s(0)\right]^{\theta_k/(\theta_i+\theta_k)} \tag{4.69}$$

Eq. 4.69 is an expression of Vignes generalization for diffusion in liquid mixtures. The estimation of the i-k pair diffusivity is experimentally more difficult and hence most models are empirical in natures.

CHAPTER 5

MODELING AND SIMULATION

5.1. Introductions

Pervaporation/vapor permeation based separation processes have become viable enhancement or alternatives in some cases, to the traditional separation techniques for several commercial applications. As more process trains incorporate pervaporation unit like hybrid distillation, there is a growing need to include models of pervaporation unit in process simulation software. These models must include the operating effects of key design parameters, such as stream pressure, compositions, temperatures, membrane area, transport properties, and configuration. The leading process simulators do not have intrinsic, stand-alone models of pervaporation. Nevertheless, process simulators are ideal computing environments for performing phase equilibrium and material and energy balance calculations required by membrane model. Modern simulators have large databases of physical properties and thermodynamic models for predicting a wide range of physicochemical properties for gas and liquid phase mixtures.

The poly(vinyl alcohol)/ poly(acryonitrile) (PVA/PAN) composite membranes are widely used for dewatering organics. A series of experimental solubility data of aqueous/organic mixtures in PVA material are available in literature which makes this membrane most suitable for model calculations. In this work a simple pervaporation unit operation models (steady state) is developed. In HYSYS − 3.0 user defined unit for separation of ethanol-water mixture with PVA membrane is developed using this model and hybrid distillation unit is designed. In the following section the developed pervaporation model and simulation algorithm is given along with the simulation results.

5.2. Assumptions

Some generic assumptions made in the transport modeling of polymeric (PVA/PAN) membrane for removal of water from ethanol-water mixture, have outlined below:

70

- The solution diffusion mechanism is assumed.

- Concentration polarization neglected.

- Resistance of porous support layer is neglected.

- A temperature gradient across the membrane is necessary to allow heat transfer; the temperature cannot be uniform across the membrane. due to the very thin active layer $(\delta \approx 3\mu m)$, however, the temperature difference across the membrane given by Fourier's law,

$$\Delta T \approx \delta \frac{\partial T}{\partial z} = -\delta \frac{Q}{k},$$ (5.1)

is extremely small, even for a high heat flux Q. consequently in the following the temperature in the active layer is considered to be constant and equal to the feed and permeate temperature, and no energy balance is needed.

- The PVA chain can be seen as being build up from ethanol molecules (Stephan, 1996), data taken from component ethanol are used for UNIQUAC model parameter.

- Log mean value of Diffusivity at the feed-membrane interface and membrane-permeate interface is used as average diffusivity in the membrane.

5.3. Model

The partial molar flux J_i of each component i in the active layer is obtained by integrating Fick's law of diffusion:

$$J_i = \frac{\overline{\rho}}{\delta M_i} \int_{w_{iP}'}^{w_{iF}'} D_i \left(w_i', w_j'....w_n' \right) dw_i'$$ (5.2)

where, w_i' is the weight fraction of component i inside the active layer. δ is the thickness of the active layer, $\overline{\rho}$ its density and M_i is the molar weight of component i. w_{iF}' and w_{iP}' are the values of the weight fractions inside the membrane adjacent to the boundary of the feed side and permeate side, respectively, w_{iF}' and w_{iP}' are assumed to be in thermodynamic solubility equilibrium with the corresponding weight fraction w_{iF} and w_{iP} of the bulk phase in the feed and permeate mixture respectively. D_i is the diffusion coefficient of component i in the dense layer. Its value

dependence on the weight fractions of all other components, $1,....i.....n$, in Eq.5.2 indicates possible coupling effects of the diffusivity.

5.2.1. Calculation procedure of mixture solubilities

The conditions for the thermodynamic phase equilibrium between a multicomponent liquid or gaseous mixture is the equality of the chemical potential μ_i in both phases for each component i:

μ_i (Outside the membrane) = μ_i' (inside the membrane) (5.3)

with $\mu_i = \mu_i^0 + RT \ln(a_i)$, Eq.5.3 is equivalent to activities a_i:

a_i (outside the membrane) = a_i' (inside the membrane) (5.4)

The thermodynamic activity a_i of a component i in a multicomponent liquid mixture consisting of n low molecular weight components with the weight fractions $w_1,...w_2,.....w_n$ is given by:

$$\ln a_i(x_1,....x_i,...x_n) = \ln\phi_i + \frac{Z}{2}q_i \ln\left(\frac{\theta_i}{\phi_i}\right) + l_i - \sum_{j=1}^{n}\phi_j\frac{r_i}{r_j}l_j - q_i^* \ln\sum_{j=1}^{n}\theta_j^*\tau_{ji} + q_i^*$$

$$-q_i^*\sum_{j=1}^{n}\frac{\theta_j^*\tau_{ij}}{\sum_{k=1}^{n}\theta_k^*\tau_{kj}}$$

(5.5)

Where

$$\phi_i = \frac{r_i x_i}{\sum_{j=1}^{n}r_j x_j}$$

(5.6)

$$\theta_i = \frac{q_i x_i}{\sum_{j=1}^{n}q_j x_j} = \frac{\left(\frac{q_i}{r_i}\phi_i\right)}{\sum_{j=1}^{n}\left(\frac{q_j}{r_j}\phi_j\right)}$$

(5.7)

$$\theta_i^* = \frac{q_i^* x_i}{\sum_{j=1}^{n}q_j^* x_j} = \frac{\left(\frac{q_i^*}{r_i}\phi_i\right)}{\sum_{j=1}^{n}\left(\frac{q_i^*}{r_j}\phi_j\right)}$$

(5.8)

72

$$l_i = \frac{Z}{2}(r_i - q_i) - (r_i - 1) \qquad (5.9)$$

In Eq.5.5 to 5.9, θ and θ^* are the surface fractions of the various components in the mixture, r, q and q^* and l are parameters related to the size and shape of molecule, Z is the coordination number. τ_{ij} and τ_{ji} are binary interaction parameters describing the intermolecular interactions between the various components. These parameters are generally obtained by fitting the VEL data of the liquid mixture to the above equation. For polymeric systems, it is easier to express a_i as a function of the volume fractions ϕ_i in the system. The main reason for this is the fact that the mole fraction of the polymer is generally very small compared to the solvent species, due to its high molecular weight. For polymeric systems (m refers to the polymer), Eq. 5.5 takes the form

$$\ln a_i{}'(\phi_1, \ldots \phi_i, \ldots \phi_n, \phi_m) = \ln \phi_i + \frac{Z}{2} q_i \ln\left(\frac{\theta_i}{\phi_i}\right) + l_i - \sum_{j=1, j \neq M}^{n} \phi_j \frac{r_i}{r_j} l_j$$

$$- r_i \phi_M\left(\frac{Z}{2}\left(1 - \frac{q_M}{r_M}\right) - 1\right) - q_i^* \ln \sum_{j=1}^{n} \theta_j^* \tau_{ji} + q_i^* - q_i^* \sum_{j=1}^{n} \frac{\theta_j^* \tau_{ij}}{\sum_{k=1}^{n} \theta_k^* \tau_{kj}} \qquad (5.10)$$

The parameter r_i, q_i, q_i^* and the ratio of q_M/r_M of the membrane polymer material can be established from molecular structure data or are available in the literature. The binary interaction parameters τ_{ij} and τ_{ji} for the solvent components can be adjusted to vapor – liquid or liquid – liquid equilibrium data or taken from the literature. τ_{iM} and τ_{Mi} have to be adjusted to the experimental data of the vapor sorption isotherms of the pure components in the membrane polymer material. UNIQUAC model parameters for ethanol – water – PVA system are given in Table 5.1.

considering now a multicomponent liquid mixtures outside the membrane phase having the composition $w_1, \ldots w_i, \ldots w_n$, both a_i on the left side and a_i on the right side of Eq. 5.4, can be substituted by a_i and a_i^* taken from Eq.5.5 and 5.10 respectively, providing a system of n non-linear equations for the unknown values of $w_i{}'$ ($i=1 \ldots n$) of n components in the swollen membrane. in analogous way, the equilibrium solubilities of multicomponent permeate vapor mixture in the membrane polymer can be calculated by replacing left side of Eq.5.4 by the expression for activity an ideal vapor mixture

$$a_i = P_i / P_i^0 . \qquad (5.11)$$

Table 5.1: Input UNIQUAC Parameters to Simulation Model [168 - 169]

Solvent	a_{12}	b_{12}	c_{12}	d_{12}	a_{21}	b_{21}	c_{21}	d_{21}	u_{SM}/R	u_{MS}/R	r	q	q^*
Water	-	-	-	-	-	-	-	-	539.5	-366	0.92	1.47	1
Ethanol	-2.49	756.9	0	0	2.0	-728.9	0	0	632.0	230.9	2.11	1.97	0.92

1 – Water, s – Solvent, M – Membrane;   For PVA material: q/r = 0.934, $q^*/r^* = 0.434$

Computation of Interaction Parameter:

$$\tau_{12} = \exp(a_{12} + b_{12}/T + c_{12}\ln T + d_{12}T)$$ $$\tau_{21} = \exp(a_{21} + b_{21}/T + c_{21}\ln T + d_{21}T)$$

$$\tau_{Ms} = \exp(-u_{Ms}/RT)$$

5.2.2. Calculation procedure of Flux – Maxwell – Stefan model for transport processes of mixtures through dense membrane

From irreversible thermodynamics, the following expression is obtained between driving force and frictional resistances in a multicomponent mixture:

$$\frac{1}{RT}\frac{d\mu_i}{dz} = \sum_{j=1}^{n} x_j \frac{v_j - v_i}{D_{ji}^0}$$ (5.12)

Eq.5.11 is known as the Maxwell – Stefan equation, where μ_i chemical potential of component i and $d\mu_i/dz$ is its local gradient, x_j are the mole fractions of the component $j = 1, 2...n$ and v_j are their local velocities. The reciprocal of D_{ji}^0 has the meaning of a friction coefficient accounting for the frictional effect exerted by component j on component i.

The general expression for the chemical potential μ_i is given by

$$\mu_i = \mu_{io}^{Gas}(T,P^0) + RT\ln f_{io}(T,P^o) + RT\ln a_i(T,P^o) + \int_{P^o}^{P} V_i$$ (5.13)

where $\mu_{io}^{Gas}(T,P^0)$ is the standard chemical potential of pure component i in the ideal gas state, $f_{io}(T,P^0)$ is the fugacity of the real pure fluid at a standard pressure P^0 and temperature T. V_i is the partial molar volume of component i and P the considered value of pressure. a_i is the thermodynamic activity defined by

$$a_i = \frac{f_i(T, P^0)}{f_{io}(T, P^0)} = x_i \gamma_i \qquad (5.14)$$

where $f_i(T, P^0)$ is the fugacity of component i in the mixture and γ_i is the corresponding activity coefficient.

For the special case of the ideal gas mixtures, Eq. 5.13 becomes

$$\mu_i = \mu_{io}^{Gas}(T, P^0) + RT \ln P^0 + RT \ln x_i + RT \ln \frac{p}{p^0} = \mu_{io}^{Gas}(T, P^0) + RT \ln(px_i) \qquad (5.15)$$

and for the case of condensed liquid mixtures one obtains if liquid compressibility is neglected:

$$\mu_i = \mu_{io}^{Liq}(T, p^0) + RT \ln(x_i \gamma_i) + V_i(p - p^0) \qquad (5.16)$$

with

$$\mu_{io}^{Liq} = \mu_{io}^{Gas}(T, P^0) + RT \ln f_{io}(T, P^0) \qquad (5.17)$$

Usually the last term in Eq. 5.17 can be neglected at ambient pressure $(p \approx p^0)$. μ_{io}^{Liq} is the chemical potential of pure liquid at p^0 and T.

In the case where polymer substances are involved, Eq. 5.12 becomes

$$\frac{1}{RT} \frac{d\mu_i}{dz} = \sum_{j=1}^{n} \phi_j \frac{v_j - v_i}{D_{ji}^0} \qquad (5.18)$$

where ϕ_j is the volume fraction of component j,

$$\phi_j = \frac{V_j x_j}{\sum_i V_i x_i} \qquad (5.19)$$

V_i and V_j are the partial molar volumes of the corresponding components. Replacing x_j by ϕ_j exhibits a generalization of the Maxwell – Stefan equation. The physical argument is that ϕ_j rather than x_j is a realistic measure of the probability that the friction influence of component j on component i contributes to the total friction force applied to component i. application of Eq. 5.12 to 5.18 requires the definition of a frame of reference concerning the velocities v_i and v_j which is given by suitable linear combinations of the value v_j values.

We first consider liquid mixtures by combining Eq.5.16 with Eq. 5.18. We account for these components with the condition $v_M = 0$ for the frame of reference (index M denotes the membrane polymer):

$$\frac{d \ln \phi_1}{dz} = \phi_2 \frac{v_1 - v_2}{\tilde{D}_{12}} - \phi_3 \frac{v_1}{\tilde{D}_{1M}}$$

(5.20)

$$\frac{d \ln \phi_2}{dz} = \phi_1 \frac{v_1 - v_2}{\tilde{D}_{21}} - \phi_3 \frac{v_2}{\tilde{D}_{2M}}$$

(5.21)

with

$$\tilde{D}_{ij} = D_{ij}^0 \frac{d \ln a_i}{d \ln \phi_i}$$

(5.22)

where $\tilde{D}_{ij}$ are effective diffusion coefficients generally depends on the concentration of all the components present in the mixture. The frame of reference ($v_M = 0$) chosen in Eq. 5.20 is called Hittorf frame reference. The low molecular weight components 1 and 2 are moving against the background of the fixed membrane polymer component. From this point of view the membrane remains at rest and no swelling of the membrane would be observed when diffusion occurs.

Eq.5.20 has now to be rearranged in order to obtain the diffusive molar fluxes $J_i = c_i v_i$ with the molar concentration c_i given by

$$c_i = \frac{\phi_i}{V_i}$$

(5.23)

solving Eq.5.19 for J_1 and J_2 is a straightforward procedure and leads to the result

$$-J_1 = -c_1 v_1 = \frac{\tilde{D}_{1M}}{\phi_M} \left(\frac{\phi_1 \tilde{D}_{2M} + \phi_M \tilde{D}_{12}}{\phi_M \tilde{D}_{12} + \phi_1 \tilde{D}_{2M} + \phi_2 \tilde{D}_{1M}} \right) \frac{dc_1}{dz} + \frac{\tilde{D}_{1M}}{\phi_M} \left(\frac{\phi_1 \tilde{D}_{2M}}{\phi_M \tilde{D}_{12} + \phi_1 \tilde{D}_{2M} + \phi_2 \tilde{D}_{1M}} \right) \frac{dc_2}{dz}$$

(5.24)

$$-J_2 = -c_2 v_2 = \frac{\tilde{D}_{2M}}{\phi_M} \left(\frac{\phi_2 \tilde{D}_{1M} + \phi_M \tilde{D}_{12}}{\phi_M \tilde{D}_{12} + \phi_1 \tilde{D}_{2M} + \phi_2 \tilde{D}_{1M}} \right) \frac{dc_2}{dz} + \frac{\tilde{D}_{2M}}{\phi_M} \left(\frac{\phi_2 \tilde{D}_{1M}}{\phi_M \tilde{D}_{12} + \phi_1 \tilde{D}_{2M} + \phi_2 \tilde{D}_{1M}} \right) \frac{dc_1}{dz}$$

(5.25)

Obviously, the fluxes depend on the volume fractions and concentration gradients of both components. If $\tilde{D}_{12} \rightarrow \infty$, the second term in Eq.24 and Eq.25 disappears and one obtains

$$-J_i = D_{iM} \frac{dc_i}{dz} \qquad (5.26)$$

with $D_{iM} = \tilde{D}_{iM}/\phi_M$ $\qquad (5.27)$

This is the simple first Fick's law of diffusion in the Hittorf frame of reference where D_{iM} is the diffusion coefficient in the Hittorf system. The fluxes become independent. If Fick's frame of reference would be chosen $v_1\phi_1 + v_2\phi_2 + v_M\phi_M = 0$, $\tilde{D}_{iM}$ instead of D_{iM} appears in Eq.5.25. $\tilde{D}_{12}$ has the meaning of a coupling parameter with the dimension of a diffusion coefficient. $\tilde{D}_{1M}$ and $\tilde{D}_{2M}$ are the diffusion coefficients of component *1* and *2*, respectively, in the polymer. For practical purposes we use the Hittorf system. If weight fraction w_i' instead of volume fraction ϕ_i are introduced, the following equations are obtained from Eq.5.25 and 5.26.

$$-J_1 = D_{1M}\left(\frac{D_{2M}w_1' + D_{12}}{D_{12} + w_1'D_{2M} + w_2'D_{1M}}\right)(\bar{\rho}/M_1)\frac{dw_1'}{dz} + D_{1M}\left(\frac{D_{2M}w_1'}{D_{12} + w_1'D_{2M} + w_2'D_{1M}}\right)(\bar{\rho}/M_1)\frac{dw_2'}{dz}$$

$$(5.28)$$

$$-J_2 = D_{2M}\left(\frac{D_{1M}w_2' + D_{12}}{D_{12} + w_1'D_{2M} + w_2'D_{1M}}\right)(\bar{\rho}/M_2)\frac{dw_2'}{dz} + D_{2M}\left(\frac{D_{1M}w_2'}{D_{12} + w_1'D_{2M} + w_2'D_{1M}}\right)(\bar{\rho}/M_2)\frac{dw_1'}{dz}$$

$$(5.29)$$

where $\bar{\rho}$ is the mean density of the swollen membrane. D_{2M} and D_{1M} are the diffusion coefficient of *2* and *1* in *M* if the Hittorf frame of reference is used and

$$D_{12} = \tilde{D}_{12}/\phi_M \ . \qquad (5.30)$$

Eq. 5.27 and 5.28 in difference from can be written as

$$J_1 = D_{1M}\left(\frac{D_{2M}\bar{w}_1' + D_{12}}{D_{12} + \bar{w}_1'D_{2M} + \bar{w}_2'D_{1M}}\right)(\bar{\rho}/\delta M_1)\Delta w_1' + D_{1M}\left(\frac{D_{2M}\bar{w}_1'}{D_{12} + \bar{w}_1'D_{2M} + \bar{w}_2'D_{1M}}\right)(\bar{\rho}/\delta M_1)\Delta\bar{w}_2'$$

$$(5.31)$$

$$J_2 = D_{2M}\left(\frac{D_{1M}\bar{w}_2' + D_{12}}{D_{12} + \bar{w}_1'D_{2M} + \bar{w}_2'D_{1M}}\right)(\bar{\rho}/\delta M_2)\Delta w_2' + D_{2M}\left(\frac{D_{1M}\bar{w}_2'}{D_{12} + \bar{w}_1'D_{2M} + \bar{w}_2'D_{1M}}\right)(\bar{\rho}/\delta M_2)\Delta w_1'$$

$$(5.32)$$

with

$$\overline{w_i}' = \frac{\left(w_{iF}' + w_{iP}'\right)}{2}$$

(5.33)

$$\Delta w_i' = w_{iF}' - w_{iP}'$$

(5.34)

Model parameters for PVA/PAN membrane are given in Table 5.2

Table 5.2: Model parameters for simulation of PVA/PAN Membranes (PERVAP 1001) [170]

Component	Density (gm/cm^3)	Thickness (m)	D_{ij}^0 (m^2/s)	K_j (m^2/s)	K_{ij}^{Arr} (degree K)
Water (1)	1.0	-	4.2426×10^{-11}	-	22041.4
Ethanol (2)	0.785	-	9.5246×10^{-13}	33.0635	2994.8
PVA/PAN (3)	1.2	1.3×10^{-7}	2.1786×10^{-11}	52.2465	1381.1

$$D_{12}^0 = D_{12}^0 \exp\left[K_{12}^{Arr}\left(\frac{1}{T_0} - \frac{1}{T}\right) \right]$$

(5.35)

$$D_{2M}^0 = D_{2M}^0 (1 + K_2 w_1') \exp\left[K_{2M}^{Arr}\left(\frac{1}{T_0} - \frac{1}{T}\right) \right]$$

(5.35)

$$D_{1M}^0 = D_{1M}^0 (1 + K_1 w_1') \exp\left[K_{1M}^{Arr}\left(\frac{1}{T_0} - \frac{1}{T}\right) \right]$$

(5.35)

$T_0 = 363.15$ K

5.3. Simulation Algorithm

The following algorithm is followed in order to design the pervaporation unit in Visual Basic 6.0 and HYSYS 3.0. The algorithm is divided into three stages namely, calculation of activity in membrane phase adjacent to feed and permeate boundary, calculation of diffusivity and calculation of flux respectively. Fig 5.1 shows the flowsheet of the algorithm.

Stage 1: Calculation of activity in membrane phase adjacent to feed and permeate boundary.

1. Activity of components in feed mixture is calculated using Eq.5.5 to 5.9.

2. Activity of components in membrane phase adjacent to feed mixture (Eq. 5.10), and activity in feed mixture (Step – 1) are substituted in Eq. 5.4 to form two nonlinear equations. These two nonlinear equations are solved by Newton – Raphson method to obtain the weight fraction of components water and ethanol in membrane adjacent to feed. All derivatives are approximated by central difference taking the value of $h = 10^{-7}$.

3. Pure component vapor pressure is calculated by Antonie equation.

4. Activity of components in vapor phase at the permeate pressure is calculated by Eq. 5.12.

5. activity of components in membrane phase adjacent to permeate, is calculated using the value of activity obtained in Step – 4 in similar manner as described in Step – 2 for calculation of weight fraction in membrane adjacent to feed liquid.

Stage – 2: Calculation of diffusivity in membrane phase.

1. D_{ij}^{0} calculated using Eq.5.35.

2. $\tilde{D}_{ij}$ is calculated using Eq. 5.22. In Eq. 5.22 derivative is calculated with central difference approximation with taking the value of $h = 10^{-15}$.

3. D_{iM} and D_{12} are calculated using Eq. 5.27 and 5.30 respectively.

Stage – 3: Calculation of flux

1. Assume the value of weight fraction in permeate vapor ($w_{iP,Ass}$).

2. Calculate the value of weight fraction in membrane phase adjacent to feed (w_{iF}') and the same adjacent to permeate vapor (w_{iP}') using algorithm described in Stage – 1.

3. With these values $\bar{w}_{i}'$ and Δw_{i} are calculated.

4. Diffusivity (D_{iM} and D_{12}) is calculated at the interface adjacent to feed and permeate using the values of w_{iF}' and w_{iP}' respectively using algorithm Stage – 2. Log mean value of these two diffusivities is used as average value of diffusivity in membrane.

5. Fluxes of the components are calculated using Eq.5.31 and 5.32.

6. weight fraction of components in permeate vapor is calculate using the

equation: $$w_{iP,Cal} = \frac{J_i M_i}{\displaystyle\sum_{j=1}^{n} J_j M_j} \qquad (5.36)$$

7. Error $\varepsilon = \left| w_{iP,Ass} - w_{iP,Cal} \right|$ is calculated and if these values are less than 10^{-3} then take that $w_{iP,Cal}$ as required solution otherwise take the value $w_{iP,Cal}$ as new assumed value and go to Step -1.

INPUT PROCESS PARAMETER
x_{iF}, UNIQUAC model parameter,
Density, Temperature

↓

Compute Activity a_i using
Eq. 5.5 to 5.9

↓

Substituting the value of a_i and a_i' (Eq.5.10) in Eq. 5.4, two nonlinear equations are formed; solved by Newton-Raphson method to get the values of w_{iF}'

↓

OUTPUT VARIABLE
w_{iF}'

(a)

INPUT PROCESS PARAMETER, $x_{iP,Ass}$, UNIQUAC model parameter, Density, Temperature, Antonie equation parameter, Permeate Pressure

↓

Compute Activity a_i using
Eq. 5.12

↓

Substituting the value of a_i and a_i' (Eq.5.10) in Eq. 5.4, two nonlinear equations are formed; solved by Newton-Raphson method to get the values of $w_{iP,Cal}'$

↓

OUTPUT VARIABLE
$w_{iP,Cal}'$

(b)

```
┌─────────────────────────────────────────────────────┐
│         INPUT PROCESS PARAMETER                      │
│      Temperature, Interaction parameter              │
└─────────────────────────────────────────────────────┘
                        │
                        ▼
            ┌─────────────────────┐
            │  Compute $D_{ij}^0$ │
            │     (Eq.5.35)       │
            └─────────────────────┘
                        │
                        ▼
┌─────────────────────────────────────────────────────┐
│ Compute $\widetilde{D}_{ij}$ at two interface (membrane – feed, │
│ membrane – permeate) taking $h= 10^{-15}$ (Eq.5.22)  │
└─────────────────────────────────────────────────────┘
                        │
                        ▼
            ┌─────────────────────────┐
            │ Compute $D_{iM}$ and $D_{12}$ │
            │   (Eq.5.27 and 5.30)    │
            └─────────────────────────┘
                        │
                        ▼
        ┌─────────────────────────────────┐
        │     OUTPUT VARIABLE             │
        │     $D_{iM}$ and $D_{12}$       │
        └─────────────────────────────────┘
```
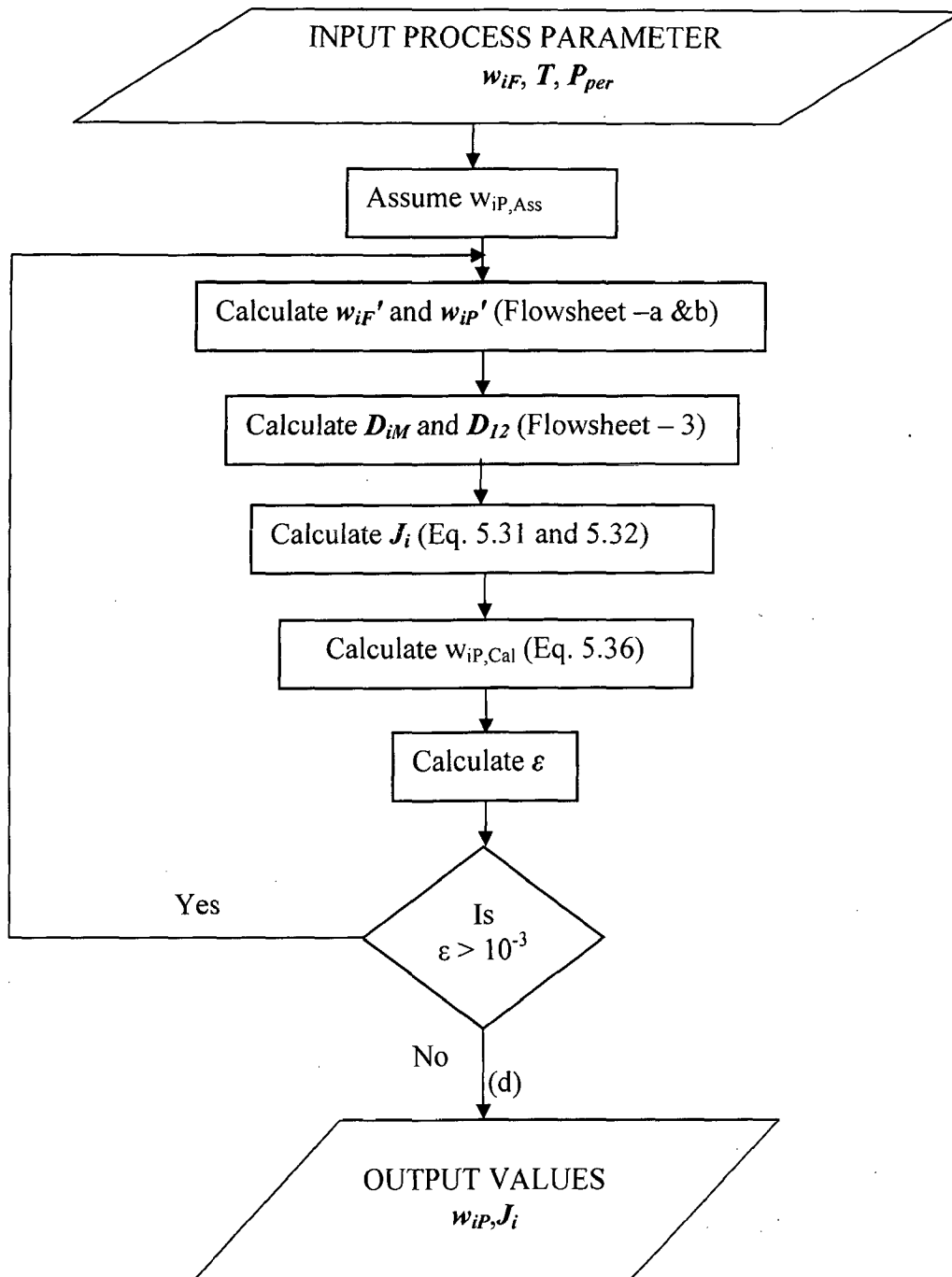
(c)

81

Fig.5.1: Flow sheet for programming : (a) Flow sheet for calculation of w_{iF}'; (b) Flow sheet for calculation of w_{iP}'; (c) Flow sheet for calculation of D_{iM} and D_{12}; (d) Flow sheet for calculation of w_{iP} and J_i;

HYSYS uses Degree of Freedom approach to simulate any unit. For 'user defined' pervaporation unit is so designed that to reduce the degree of freedom to zero, the following process parameter should be mentioned:

1. Totally defined feed stream: Flow rate, Composition, Temperature, Pressure, and Vapor Fraction (any two of Temperature, Pressure, and vapor Fraction).

2. Permeate Stream Pressure and Flow rate

5.4. Simulation Results

To illustrate the steady state behavior of the process, concentration of ethanol and water in membrane adjacent to feed side is calculated at 333 K for different mass fraction of ethanol in feed mixture and plotted (Fig. 5.2). Fig. 5.2 shows the deviation from the experimental value of concentration at 333K. Same weight fractions are plotted against temperature for ethanol mass fraction in feed 0.1, 0.5 and 0.9 respectively (Fig. 5.3). Fig. 5.2 shows that the mass fraction in membrane adjacent to feed liquid deviates from the experimental values for high concentrations of ethanol in feed liquid. Mass fraction in membrane adjacent to feed liquid drops as temperature increases.

Ethanol and Water Concentration

Legend:
- E-W
- Q-W
- E-E
- Q-E

X-axis: Ethanol mass fraction in feed
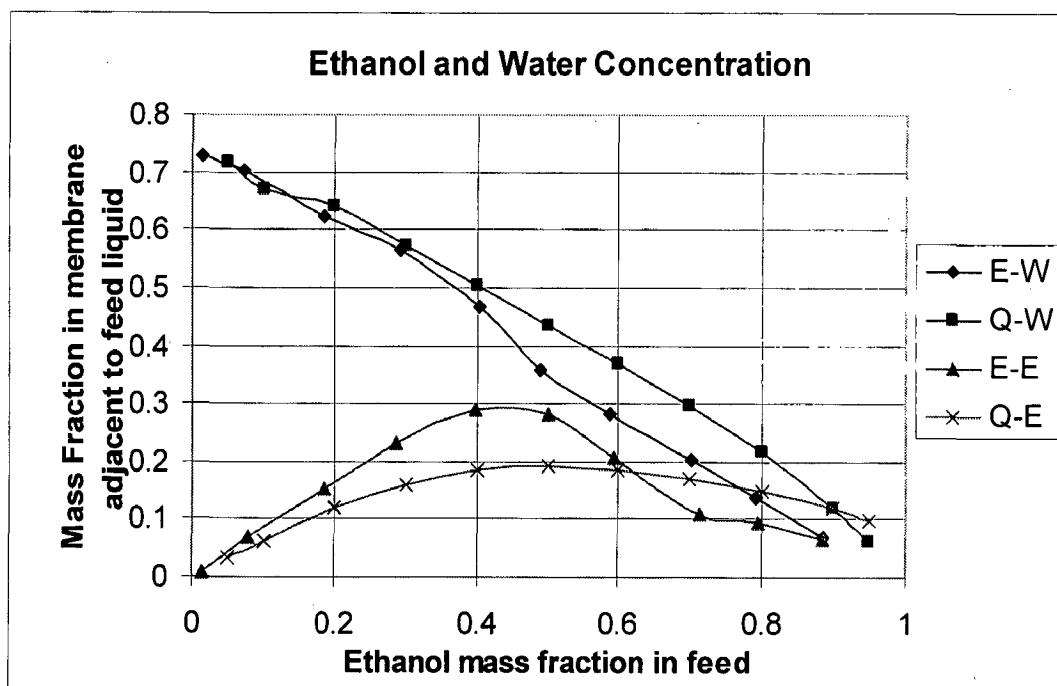Y-axis: Mass Fraction in membrane adjacent to feed liquid

Fig. 5.2: Ethanol and Water mass fraction in membrane phase, at 333 K temperature for different ethanol mass fraction in feed liquid; E – W: Experimental concentration of Water; Q – W: Calculated concentration of Water; E – E: Experimental concentration of Ethanol; Q- E: Calculated concentration of Ethanol.
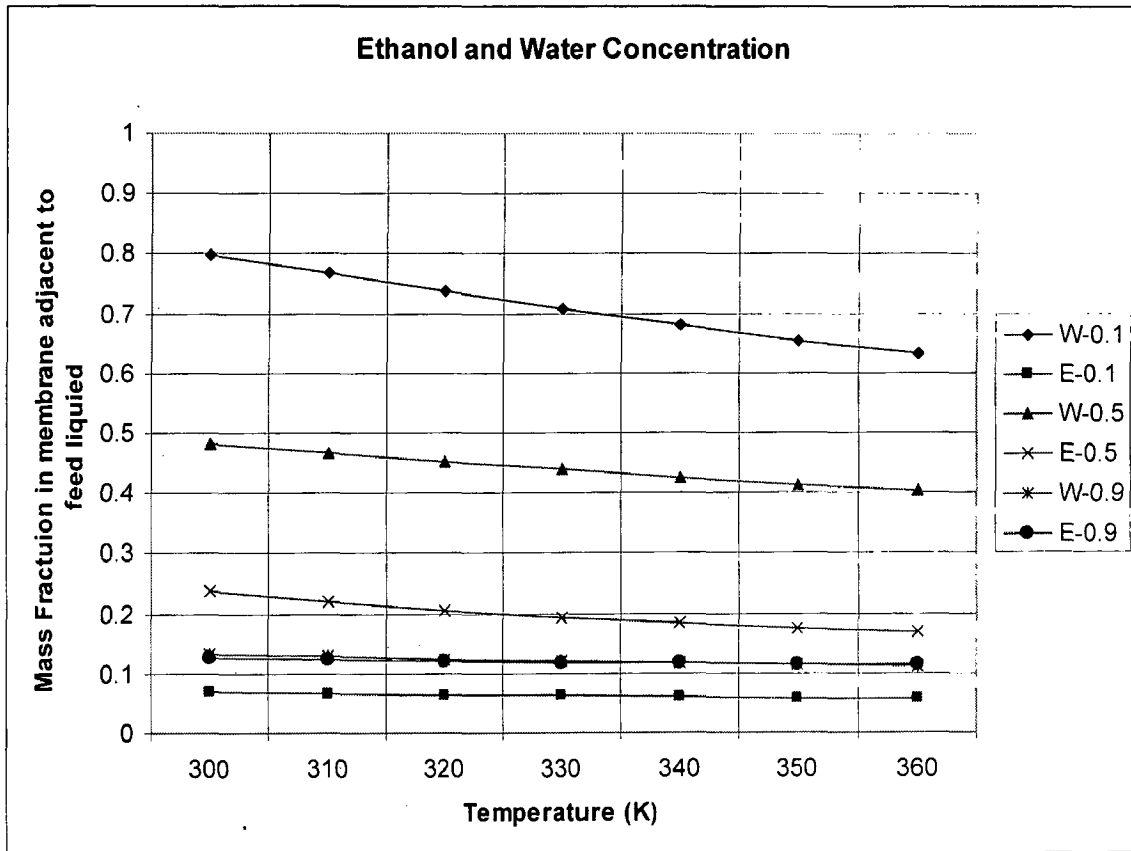
Fig. 5.3: Ethanol and Water mass fraction in membrane adjacent to feed liquid at different temperature;(W -0.1, W-0.5 and W-0.9 are the weight fraction of water in membrane for feed liquid contains 0.1, 0.5 and 0.9 weight fraction of ethanol; E - 0.1, E - 0.5 and E - 0.9 are the weight fraction of ethanol in membrane for feed liquid contains 0.1, 0.5 and 0.9 weight fraction of ethanol;)

Ethanol and water flux and weight fraction in permeate for different feed concentrations at 333 K temperature and 200 mbar pressure (Permeate Pressure) are calculated. Fig. 5.4 shows flux of ethanol and water for different feed composition and Fig. 5.5 shows the ethanol weight fractions in permeate at the pre mentioned process conditions. Predicted ethanol weight fraction verses Actual ethanol weight fraction is plotted in Fig. 5.6. From Fig. 5.6 shows that the model prediction deviates less than 10 % from actual value for corresponding ethanol weight fraction in feed, below 0.3 and above 0.6 respectively.

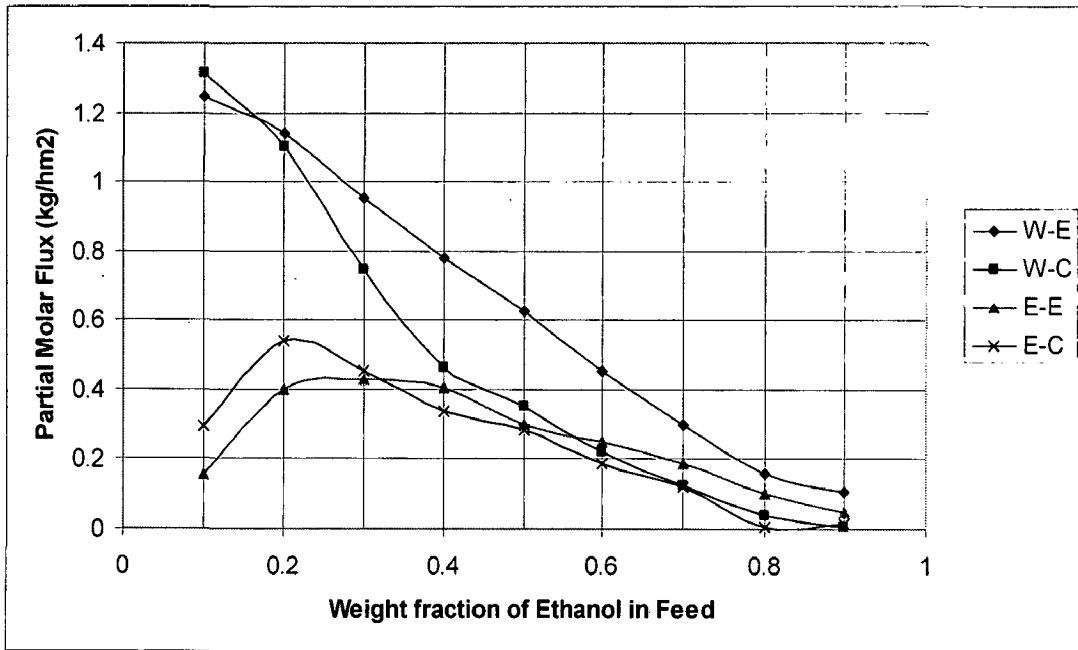Fig. 5.4: Partial Molar flux (kg/hm2) for different mass fraction of ethanol in feed liquid. W – E, Experimental Water Flux; W – C, Calculated Water Flux; E –E, Experimental Ethanol Flux; E – C, Calculated Ethanol Flux;
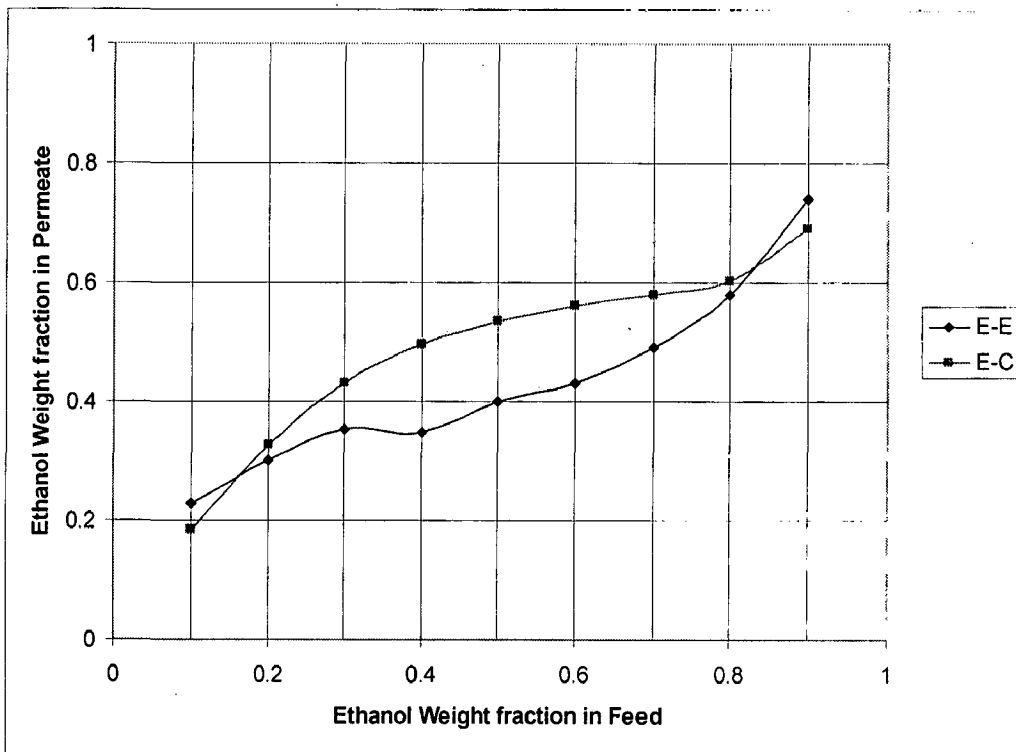

Fig. 5.5: Ethanol weight fraction in permeate for different concentration in feed liquid at 333K and 200 mbar Permeate Pressure. E – E, Experimental concentration; E – C calculated Concentration
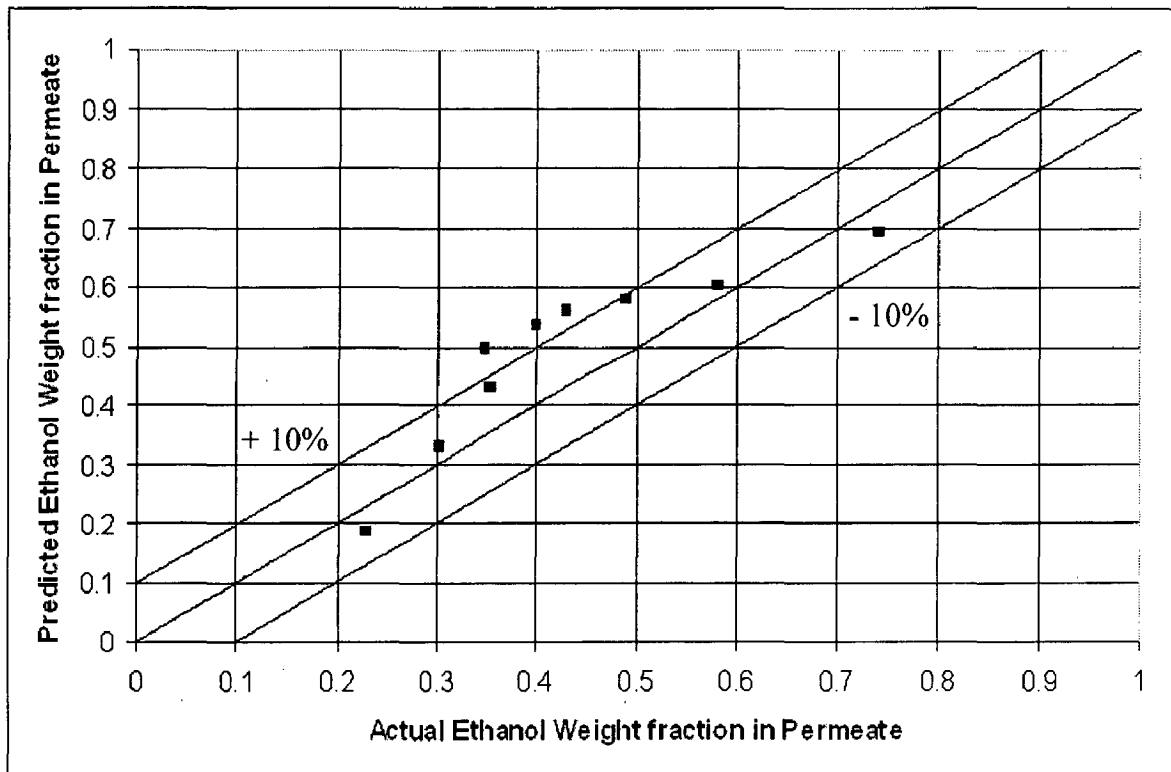
85

Fig. 5.6: Actual Ethanol Weight fraction verses Predicted Ethanol Weight fraction in Permeate.

Simulation in HYSYS is done by taking a saturated liquid feed mixture containing 20 wt% ethanol and rest water at 1.3 atm pressure. This mixture is separated by hybrid distillation in similar to I-211A except that permeate is not returning back to column (Fig.5.7). Feed process condition and compositions are given in Fig. 5.8 and Fig 5.9. Distillation column is simulated assuming column bottom and condenser pressure is 1.2 and 1.1 atm respectively. Using 200 kgmole/hr Over head liquid flow rate and top product composition as 80 wt% ethanol (active specification) column runner is stated and we get the converged solution. The overhead product is then separated in a pervaporation unit. Permeate flow rate and pressure is set at 80 kgmole/hr and 200 mbar. Over all process condition and composition are available in Fig. 5.7 and 5.8.
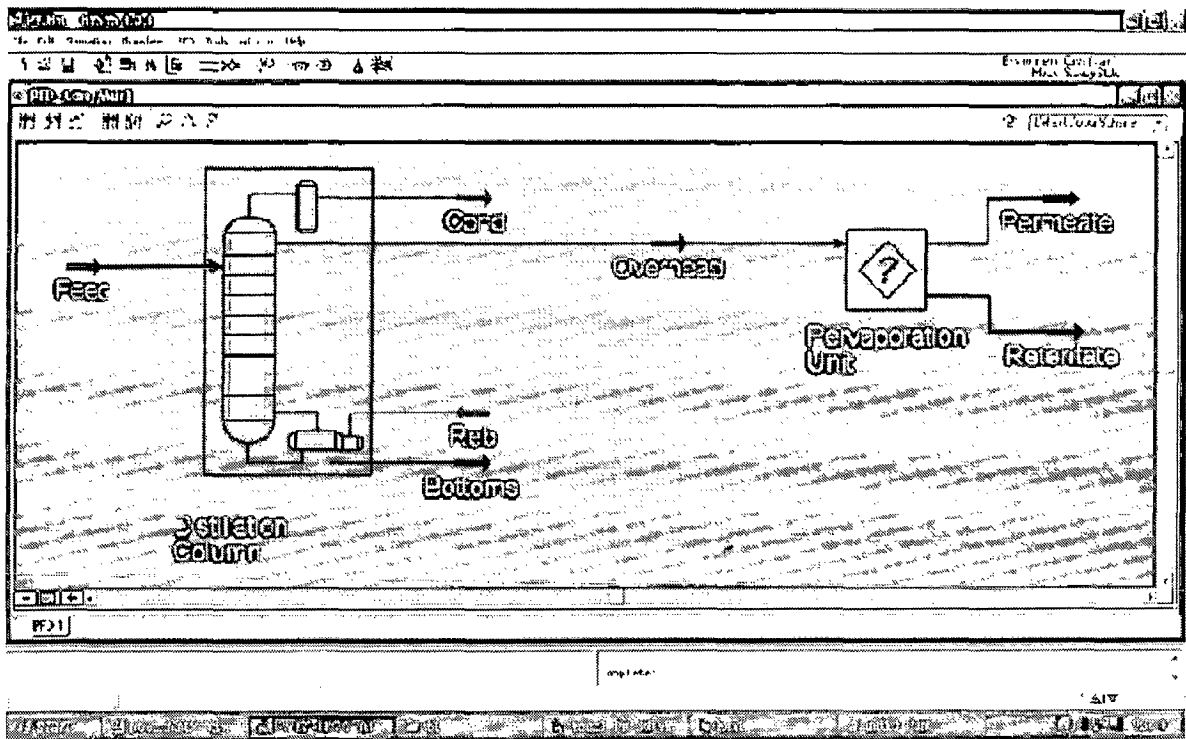
Fig. 5.7: PFD diagram of hybrid system for separation of ethanol – water mixture in HYSYS

Name	Feed	Overhead	Bottoms	Permeate	Retentate
Vapour Fraction	0.0000	0.0000	0.0000	1.0000	1.0000
Temperature [C]	90.07	79.02	97.85	79.02	79.02
Pressure [kPa]	131.7	101.3	152.0	20.00	101.3
Molar Flow [kgmole/h]	1000	200.0	800.0	80.00	120.0
Mass Flow [kg/h]	2.363e+004	7026	1.660e+004	1857	5168
Liquid Volume Flow [m3/h]	26.02	8.469	17.55	2.035	6.434
Heat Flow [kJ/h]	-2.775e+008	-5.480e+007	-2.225e+008	-1.901e+007	-2.785e+007
Name	** New **				
Vapour Fraction					
Temperature [C]					
Pressure [kPa]					
Molar Flow [kgmole/h]					
Mass Flow [kg/h]					
Liquid Volume Flow [m3/h]					
Heat Flow [kJ/h]					

Material Streams | Compositions | Energy Streams | Unit Ops

Distillation Column
FeederBlock_Feed

☐ Include Sub-Flowsheets
☐ Show Name Only
Number of Hidden Objects: 0

Fig. 5.8: Workbook – Case (Main): Material Tab for separation of ethanol – water mixture in HYSYS

87

Name	Feed	Bottom	Over Head	Permeate	Retentate
Comp Mole Frac (H2O)	0.8000	0.9025	0.3900	0.8146	0.1068
Comp Mole Frac (Ethanol)	0.2000	0.0975	0.6100	0.1854	0.8932
Comp Mass Frac (H2O)	0.6100	0.7835	0.2000	0.6322	0.0447
Comp Mass Frac (Ethanol)	0.3900	0.2165	0.8000	0.3678	0.9553
Name	** New **				
Comp Mole Frac (H2O)					
Comp Mole Frac (Ethanol)					
Comp Mass Frac (H2O)					
Comp Mass Frac (Ethanol)					

Material Streams | **Compositions** | Energy Streams | Unit Ops

Feed@Block Feed
T-100

☐ Include Sub-Flowsheets
☐ Show Name Only
Number of Hidden Objects: 0

Fig. 5.9: Workbook – Case (Main): Composition tab for separation of ethanol – water mixture in HYSYS

CHAPTER 6

CONCLUSION

In separation processes, hybrid distillation is slowly substituting the conventional distillation column as it exploits the advantages of distillation (lower capital cost) and membrane process (low energy consumption), while overcoming the disadvantages of both. in this thesis work a simple steady state model using log mean diffusivity coefficient is simulated in this work with Visual Basic 6.0 and HYSYS 3.0. From simulation results following conclusions can be drown:

1. This model is quite good for separation of mixture for ethanol weight fraction lower than 0.2 and above 0.7 weight fraction. Industrially hybrid distillation is used for azeotrope breaking in dehydration of ethanol. So for practical purpose this model can be used and it gives satisfactory results.

2. Weight fraction in membrane adjacent to feed liquid deviates from experimental results at high ethanol concentration (40 wt %)

3. The model predicted ethanol weight fraction deviates less than 10 % from Actual ethanol weight fraction in permeate, for corresponding ethanol weight fraction in feed below 0.3 and above 0.7 respectively. Accuracy of the model can be improved by taking the mass transfer resistance in concentration polarization layer and porous support layer.

4. This model is simulated for ethanol – water system but it can be used for dehydration of other organic provided that UNIQUAC model parameter and Maxwell – Stephan interaction parameter is known. It can be easily available from any simulation software like HYSYS, Pro-II, or Aspen Plus.

5. Simulation work is done in two different softwares namely Vissual Basic 6.0 and Micro Language Editor, but in between them programming in Micro Language Editor (HYSYS) is more reliable than Visual Basic as it is easy in Micro Language Editor to use directly physical properties from Fluid Property Package in HYSYS, where as, in Visual Basic it needs object linking which slows down the computation speed. But compare to Visual Basic it is less user friendly.

6. For hybrid distillation column simulations in Visual Basic 6.0 need to simulate distillation column model simultaneously but in HYSYS only need to develop the pervaporation model either as "user defined unit" or by creating "unit operation extension". It gives the model application not only for the hybrid distillation it can be used with other inbuilt unit operation.

7. Lastly if pervaporation "user defined unit" is developed it can be simulated with distillation column in different configuration and can be easily optimized in HYSYS using Optimizer option, but in other soft ware it needs separate programming for different configuration.

REFERENCES

1. Stankiewicz, A. & Moulijn, J.A. (2002). Process Intensification. *Industrial Engineering and Chemistry Research*, 41(8), 1920 – 1924.

2. Tsouris, C. & Porcelli, J.V. (2003). Process Intensification – Has Its Time Finally Come? *Chemical Engineering Progress*, 99 (10), 50 – 55.

3. Thomas G. Pressly and Ka M. Ng (1998). A Break – Even Analysis of Distillation – Membrane Hybrids. *Process System Engineering*, Vol. 44, No. 1, 93 – 105.

4. Frank Lipnizki, Robert W. Field, Po-Kiong Ten (1999). Pervaporation – based hybrid process: a review of process design, applications and economics. *Journal of Membrane Science*, 153,183 – 210.

5. P.M. Hoch, M.C. Daviou, A.M. Eliceche (2003). Optimization of the Operating Conditions of Azeotropic Distillation Columns with Pervaporation Membranes. *Latin American Applied Research*, 33, 177 – 183.

6. Jürgen Bausa, Wolfgang Marquardt. Detailaed Modeling of Stationary and Transient Mass Transfer Across Pervaporation Membranes, *AIChE Journal*, Vol. 47, No. 6 (2001)

7. H.E.A. Baüschke., *Membrane Technology in the chemical Industry*. Wiley – Vch.

8. J. Fontalvo, Design and performance of two- phase flow pervaporation and hybrid distillation process, Ph.D. Thesis, Geboren te Bogotá, Colombia,2006

9. J.D. Seader, Erbest J. Henley. *Separation Process Principle*. Wiley – India, (2006).

10. J. Fontalvo, P. Cuellar, J.M.K. Timmer, M.A.G. Vorstman, J.G. Wijers, J.T.F. Keurentjes (2005). Comparing Pervaporation and Vapor Permeation Hybrid Distillation Process. *Ind. Eng. Chem. Res*, 44, 5259 – 5266.

11. B. Smitha, D. Suhanya, S. Sridhar, M. Ramakrishna. Separation of organic–organic mixtures by pervaporation—a review. *Journal of Membrane Science*, 241, (2004), 1–21.

12. H.E.A. Brüschke, W.H. Schneider, G.F. Tusel. Pervaporation membrane for the separation of water and oxygen-containing simple organic solvents. *European Workshop on Pervaporation*. Nancy, France, Sept. 21 – 22, 1982.

13. A.H. Ballweg, H.E.A. Brüschke, W.H. Schneider, G.F. Tusel, K.W.Böddeker, A. Wenzlaff. Pervaporation membranes. An economical method to replace conventional dehydration and rectification columns in ethanol distilleries. *Fifth Intern. Sympos. On Alcohol Fuel Technology*. Auckland, New Zealand, May, 13 – 18, (1982).

14. H.E.A. Brüschke, Verwendung einer mehrschichtigen membran zur trennung von Flüssigkeitsgemischen nach dem Pervaporationsverfahren; *Europe Parent EP 096 339*, (1982).

15. Baker, R.W., E.L. Cussler, W. Eykamp, W.J. Koros, R.L. Riley and H. Strathmann. Membrane Separation Systems – A Research and Development Need Assessment. *Report DE 90 – 011770*, Department of commerce, NTIS, Springfield. VA (1990).

16. J. Néel, in: R.Y.M. Huang (Ed.), Pervaporation Membrane Processes, Elsevier, Amsterdam, 1991 (Chapter 1).

17. X. Feng, R.Y.M. Huang, in: R. Bakish (Ed.), Proceedings of the 6th International Conference on Pervaporation Processes in the Chemical Industry, Englewood, New Jersey, 1992, 305.

18. R.M. Waldburger, F. Widmer, Chem. Eng. Technol. 19 (1996) 117.

19. Travis C. Bowen1, Richard D. Noble, John L. Falconer. Fundamentals and applications of pervaporation through zeolite membranes. *Journal of Membrane Science* ,245 (2004) 1–33

20. Nazish Hoda, Satyanarayana V. Suggala , Prashant K. Bhattacharya, Pervaporation of hydrazine–water through hollow fiber module: Modeling and simulation. *Computers and Chemical Engineering*, 30 (2005) 202–214.

21. Michael Schleger, Stefan Sommer, Thomas Melin. Module arrangement for solvent dehydration with silica membranes. *Desalination*, 163 (2004) 281-286.

22. J. Fontalvo, E. Fourcade, P.C. Cuellar, J.G. Wijers, J.T.F. Keurentjes. Study of the hydrodynamics in a pervaporation module and implications for the design of multi-tubular systems. *Journal of Membrane Science*, 281 (2006) 219–227.

23. Leland M. Vane, Franklin R. Alvarez, Eugene L. Giroux. Reduction of concentration polarization in pervaporation using vibrating membrane module. *Journal of Membrane Science*, 153 (1999) 233 – 241.

24. Leland M. Vane, Franklin R. Alvarez. Vibrating pervaporation modules: Effect of module design on performance. *Journal of Membrane Science*, 255 (2005) 213–224.

25. R.C. Binning, F.E. James, Now separate by membrane permeation, *Pet. Refiner*, 37 (1958) 214 -215.

26. Anne Jonquières, Robert Clément, Pierre Lochon, Jean Néel, Marlène Dresch, Bruno Chrétien. Industrial state-of-the-art of pervaporation and vapour permeation in the western countries. *Journal of Membrane Science* 206 (2002) 87–117.

27. G.F. Tusel, A. Ballweg, Method and apparatus for dehydrating mixtures of organic liquids and water, US Patent 4 405 409 (1983).

28. G.F. Tusel, H.E.A. Brüschke, Use of Pervaporation systems in the chemical industry, *Desalination*, 53 (1985) 327 - 338.

29. P.O. Cogat, Dehydration of ethanol pervaporation compared with azeotropic distillation, in: R. Bakish (Ed.), Proceedings of the Third International Conference on Pervaporation Processes in the Chemical Industry, *Bakish Material Corporation, Englewood, NJ, USA*, 1988, 305 - 316.

30. H.L. Fleming, Membrane pervaporation: separation of organic/aqueous mixtures, Sep. Sci. Technol. 25 (1990) 1239 - 1255.

31. U. Sander, P. Soukup, Design and operation of a pervaporation plant for ethanol dehydration, *Journal of Membrane Science*. 36 (1988) 463 - 475.

32. M. Franke, Auslegung und Optimierung von Pervaporationsanlagen zur Entwässerung von Lösungsmitteln und Lö - sungsmittelgemischen. Ph.D. Thesis, RWTH, Aachen, Germany, 1990.

33. G. Guerreri, Membrane alcohol separation process-integrated pervaporation and fractional distillation, *Chem. Eng. Res. Des.* 70 (1992) 501 - 508.

34. H.E.A. Brüschke, G.F. Tusel, Economics of industrial pervaporation processes, in: Proceedings of the Conference on Membranes and Membrane Processes, 1986, 581 - 586.

35. Z. Szitkai, Z. Lelkes, E. Rev , Z. Fonyo. Optimization of hybrid ethanol dehydration systems. *Chemical Engineering and Processing*, 41 (2002),631–646.

36. C.H. Gooding, F.J. Bahouth, Membrane-aided distillation of azeotropic solutions, *Chem. Eng. Commun.* 35 (1985), 267 - 279.

37. M.E. Goldblatt, C.H. Gooding, An engineering analysis of membrane-aided distillation, *AIChE Symp. Ser.* 82 (1986), 51 - 69.

38. J. Stelmaszek, Untersuchungen der ökonomischen Effektivitaȅt von verschiedenen Wasserabscheidungsmethoden, *Chem.- Tech.* 8 (1979), 611 - 617.

39. T. Raiser, H. Steinhauser, Azeotrope ausgetrickst. Hybridverfahren - eine Kombination von Rektifikation und Pervaporation, *Chem.-Tech.* 23 (1994), 44 - 46.

40. A. Shanley, G. Ondrey, S. Moore, Pervaporation finds its niche, *Chem. Eng.* 101(9) (1994), 34 - 37.

41. H.E.A. Brüschke, Industrial application of membrane separation processes, *Pure Appl. Chem.* 67 (1995),993 - 1002.

42. V.M. Shah, C.R. Bartels, Engineering considerations in pervaporation applications, in: R. Bakish (Ed.), Proceedings of the Fifth International Conference on Pervaporation Processes in the Chemical Industry, *Bakish Material Corporation, Englewood*, NJ, USA, 1991, 331 - 337.

43. Veerle Van Hoof, Liesbet Van den Abeele, Anita Buekenhoudt, Chris Dotremont, Roger Leysen. Economic comparison between azeotropic distillation and different hybrid systems combining distillation with pervaporation for the dehydration of isopropanol. *Separation and Purification Technology*, 37 (2004) 33–49.

44. R. Chamberlain, C.P. Borges, A.C. Habert, R. Nobrega, Fractionation of fusel oil coupling pervaporation and distillation, in: R. Bakish (Ed.), Proceedings of the Seventh International Conference on Pervaporation Processes in the Chemical Industry, *Bakish Material Corporation, Englewood*, NJ, USA, 1995, 271 - 284.

45. D. Arnold, Optimierungsstrategie zur Einbindung von Pervaporationsnlagen bei der Entwässerung von Lösugsmitteln, Ph.D. Thesis, RWTH, Aachen, Germany, 1995.

46. H.J. Bart, H.O. Reisl, Der Hybridprozeß Reaktivdestillation/Pervaporation zur Herstellung von Carbonsäureester, *Chem.- Ing.-Tech.* 69 (1997), 824 - 827.

47. J. Bergdorf, Case study of solvent dehydration in hybrid processes with and without pervaporation, in: R. Bakish (Ed.), Proceedings of the Fifth International Conference on Pervaporation Processes in the Chemical Industry, *Bakish Material Corporation, Englewood*, NJ, USA, 1991, 362 - 382.

48. C. Staudt-Bickel, Thermodynamische Untersuchungen zum Einsatz der Pervaporation in technischen Prozessen, Ph.D. Thesis, Rupert-Karls-Universität, Heidelberg, Germany, 1995.

49. C. Staudt-Bickel, R.N. Lichtenthaler, Integration of pervaporation for the removal of water in the production process of methylisobutylketone, J. Membr. Sci. 111 (1996), 135 - 141.

50. C. Staudt-Bickel, R.N. Lichtenthaler, Integration of pervaporation for the removal of water in the production process of methylisobutylketone (MIBK), in: Proceedings of the International Congress on Membranes and Membrane Processes, ICOM'96, 1996, 394 - 395.

51. R. Rautenbach, J. Vier, Aufbereitung von Methanol/Diethylcarbonat - Ströme durch Kombination von Pervaporation und Rektifikation, Chem.-Ing.-Tech. 67 (1995) 1498 - 1501.

52. R. Rautenbach, J. Vier, Design and analysis of combined distillation/pervaporation processes, in: R. Bakish (Ed.), Proceedings of the Seventh International Conference on Pervaporation Processes in the Chemical Industry, Bakish Material Corporation, Englewood, NJ, USA, 1995, 70 - 85.

53. J. Vier, Pervaporation azeotroper wäßriger und rein organischer Stoffgemische - Verfarhrensentwicklung und - integration, Ph.D. Thesis, RWTH, Aachen, Germany, 1995.

54. J. Vier, Aufbereitung methanolhaliger organischer Mischungen durch Kombination von Pervaporation und Rektifikation, IVT-Information 25(1) (1995),38 -47.R.

55. J.C. Davis, R.J. Valus, R. Eshraghi and A.E. Velikoff, Facilitated transport membrane systems for oletin purification, Sep. Sci. Technol., 28 (1993) 463-476.

56. Srinivas Moganti, Richard D. Noble, Carl A. Kovalb, Analysis of a membrane/distillation column hybrid process. Journal of Membrane Science, 93 (1994), 31-44.

57. Rautenbach, R. Albrecht, The separation potential of pervaporation Part 2. Process design and economics, Journal of Membrane Science. 25 (1985) 25 - 54.

58. R. Albrecht, Pervaporation - Beiträge zur Verfahrensentwicklung, Ph.D. Thesis, RWTH, Aachen, Germany, 1983.

59. R. Rautenbach, R. Albrecht, Membrane Processes, Wiley, New York, 1989, 363 - 422.

60. M.S.K. Chen, G.S. Markiewicz, K.G. Venugopal, Development of membrane pervaporation Trim^{TM} process for methanol recovery from $CH_3OH/MTBE/C_4$ mixtures, *AIChE Symp.* Ser. 85 (1989), 82 - 88.

61. M.S. Chen, R.M. Eng, J.L. Glazer, C.G. Wensley, Pervaporation process for separating alcohols from ethers, US Patent 4 774 365 (1988).

62. N. Kanji, M. Makoto, Process for producing ether compound, US Patent 5 292 963 (1994).

63. C. Streicher, P. Kremer, V. Tomas, A. Hubner, G. Ellinghorst, Development of new pervaporation membranes, systems and processes to separate alcohols/ethers/hydrocarbons mixtures, in: R. Bakish (Ed.), Proceedings of the Seventh International Conference on Pervaporation Processes in the Chemical Industry, *Bakish Material Corporation, Englewood*, NJ, USA, 1995, 297 - 309.

64. U. Hömmerich, Integration der Pervaporation in den MTBE - Herstellungsprozeß, IVT-Information 26(2) (1996),2 - 13.

65. R. Rautenbach, U. Hömmerich, Design and optimization of combined pervaporation/distillation processes for the production of MTBE, in: Proceedings of the Gordon Research Conference, Andorer, USA, 1997.

66. R. Rautenbach, U. Hömmerich, Design and optimization of combined pervaporation/distillation processes for the production of MTBE, in: A.J.B. Kemperman, G.H. Koops (Eds.), Euromembrane '97, University of Twente, Netherlands, 1997, 356.

67. Uwe Hömmerich, Robert Rautenbach. Design and optimization of combined pervaporation/distillation processes for the production of MTBE. *Journal of Membrane Science*, 146 (1998), 53 – 64.

68. G.S. Luo, M. Niang, J. Schaetzel, Separation process of ethyl tert-butyl ether/ethanol by coupling pervaporation and distillation, in: A.J.B. Kemperman, G.H. Koops (Eds.), Proceedings of the Euromembrane '97, University of Twente, Netherlands, 1997, 353.

69. B.L. Yang, S. Goto, Pervaporation with reactive distillation for the production of ethyl tert-butyl-ether, *Sep. Sci. Technol.* 32 (1997),971 - 981.

70. Helget, A., M. Groebel, and E. D. Gilles, Dynamic Simulation for Plant and Control System Design, *Proc. PSE' 94*, Seoul, Korea, 1111(1994).

71. A.Heintz, W.Stephen, A generalized solution-diffusion model of the pervaporation process through composite membranes, Part I. Prediction of mixture solubilities in the dense active layer using UNIQAC model, *Journal of Membrane Science, 89(1994)143-151.*

72. Ping, z., Q. Nguyen, R. Clement, and J. Neel, Time – dependent Phenomena in Pervaporation: influence of the Crystallinity of Dense Poly(vinyl alcohol) Membranes on Their Pervaporation Performance, *Proc. Int. Conf. Pervaporation Processes in the Chem. Ind.*, T.Bakish, ed., Nancy, 1998.231.

73. R. Rautenbach, U. Hömmerich, Study of Dynamic Mass – Transfer Effects in Pervaporation, *AIChE J.*, 44, 1998,43.

74. Hömmerich, U., R. Rautenbach, J.Bausa., and W. Marquardt, Modellierung der Pervaporation als Gurndlage eines modelgestützten Entwurfs hybrider Trennpozesse am Beispiel der METB – production, *Tech. Rep., LTP – pro – 1998 – 04*, RWTH Aachen, Germany (1998); URL:http://www.lfpt.rwth–Aachen.de.

75. .Lonsdale, H.K., Merten, U. And Riley, transport properties of Cellulose Acetate, *J. Applied Polymer Sci.*, 9, 1965, 1341.

76. Merten, U., Transport Properties of Osmotic Membranes", in Desalination by Reverse Osmosis, *M.I.T. Press*, Cambridge, Mass., 1966, 15.

77. Mulder, M. H. V., Transport in Membranes, in Basic Principles of Membrane Technology, *Kluwer Academic Publishers*, Netherlands, 1991, 150

78. Krisna, R. and Wesselingh, J. A., The Maxwell – Stefan Approach to Mass Transfer, *Chem. Engg. Sci.*, 52(6), 1997, 889.

79. Lightfoot, E.N., Transport Phenomena and Living Systems., *McGraw – Hill*, New York, USA, 1974.

80. Maxwell, J. C., On the Dynamical Theory of Gases, *Phil. Trans. R. Soc.*,157,1866,49.

81. Stefan, J., Uber das Gleichgewicht und die Bewegung insbesondere die Diffusion von Gasmemegen, *Sitzber*. Akad. Wiss. Wein., 1971, 63 63

82. Fels, M. and Huang, R. Y. M., Diffusion Coefficient of Liquid in Polymer membranes by a Desorption Method, *J. Appl.Polym.Sci.*, 14,1970,523.

83. Heitz, A., Funke, H. and Lichtenthaler, R.N., Sorption and Diffusion in Pervaporation membranes, in Pervaporation Membrane Separation process, ed. Huang R. Y. M., *Elsevier Publishers*, Amsterdam, Netherlands, Chapter 10, 1991.

84. Paul, D. R., Further Comments on the Relation between Hydraulic Permeation and Diffusion, *J. Polym. Phys. Ed.*, 12, 1974, 1221.

85. Athayde, A.L., Baker, R.W., Daniels, R., Le, M.H. and J.H., Pervaporation for Wastewater treatment, *Chemtech*, January, 34, 1997.

86. Frenesson, I., Tragardh, G. and Hagerdahl, B. H., Pervaporation and Ethanol Upgrading – A Literature Review, *Chemical Engineering Communications*, 45, 1986, 277.

87. Mulder, M.H.V. and Smolders, C.A., Pervaporation, Solubility Aspects of the Solution – Diffusion Model, *Sep. and Purif. Methods*, 15 (1), 1986,1

88. Kataoka, T., Tsuru, T., Nakao, S., Permeation Equations Developed for Prediction of Membrane Performance in Pervaporation, Vapor Permeation and Reverse Osmosis Based on the Solution – Diffusion Model, *J. Chem. Eng. Japan*, 24(3), 1991, 323.

89. Aptel, P., Cury, J., Jozefowicz, J., Morel, G. and Neel., Liquid Transport through Membranes Prepared by grafting of Polar Monomers onto Poly (tetrafluroethylene) Films. 3. Steady State Distribution in Membrane during Pervaporation, *J. Appl. Polym. Sci.*, 18, 1974, 365.

90. Ghai, R.K., Ertl, H. and Dullien, F.A.L., Liquid Diffusion of Nonelectrolytes: Part I, *AIChE J.*, 19, 1987, 881.

91. Kim, S. N. and Kammermeyer, K., Actual Concentration Profiles in Membrane Separation, *Sep. Sci. and Technol.*, 5, 1970, 679

92. Nguyen, Q. T., Modeling of the Influence of Downstream Pressure for Highly Selective Pervaporation, *J. Membrane Sci.*, 27, 1987,11.

93. Sourirajan, S. and Matsuura, T., Reverse Osmosis/Ultrafiltration Process Principles, *National Research Council of Canada*, Ottawa, 1985.

94. Sourirajan, S., Bao,S and Matsuura, T., An Approach to Membrane Separation by Pervaporation, in *Proceedings of Second International Conference on Pervaporation Processes in the Chemical Industry*, ed. R.A. Bakish, Bakish Materials Corp., Englewood, NJ, 209, 1987.

95. Okada, T., Yoshikawa, M. and Matsuura,T., A study on the pervaporation of Ethanol/Water Mixtures on the Basis of Pore Flow Model, *J. Membrane Sci.*, 59,1991, 151.

96. Wijmans, J.A. and Krishna, R., Mass Transfer, *Ellis Horwood*, Chichester, UK, 1990.

97. Shieh, J. and Huang, R. Y.M., A Pseudophase – change Solution – Diffusion Model for Pervaporation. I. Single Component Permeation. *Sep. Sci. Technol.*, 33(6), 1998.767.

98. Karger, J. and Ruthven, D. M., Diffusion in Zeolites, Wiley, New York, USA, 1992.

99. Mason, E.A. and Malinaskas, A.P., Gas Transport in Porous media: The Dusty Gas Module, *Elsevier*, Amsterdam, Netherlands, 1983.

100. Wesselingh, J.A. and Krishna, R., Mass Transfer, *Ellis Horwood*, Chichester, UK, 1990.

101. Krishna, R., Multicomponent Surface Diffusion of Adsorbed Species. A Description Based on the Generalized Maxwell – Stefan Diffusion Equations, *Chem. Eng. Sci.*, 45, 1990, 1779.

102. Krishna, R., A Unified Approach to the Modeling of Intraparticle Diffusion in Adsorption Processes, *Gas Separation Purification*, 7, 1993b, 91.

103. Krishna, R., Problems and Pitfalls in the Use of Fick Formulation for IntraParticle Diffusion, *Chem. Eng. Sci.*, 48, 1993a, 845.

104. Lee, C. H., Theory of Reverse Osmosis and Some Other Membrane Permeation Operation, *J. Appl. Polym. Sci.*, 19, 1975, 83.

105. Flory, P. J., Principle of Polymer Chemistry, *Cornell University Press*, Ithaca, NY, 1953.

106. Favre, E., Nguyen, Q. T., Schaetzel, P., Chement, R and Neel, J., Sorption of Organic Solvents into Dense Silicone Membranes. Part I. Validity and Limitations of

Flory – Huggins and Related Theories. *J. Chem. Soc. Faraday Trans.*, 89 (24), 1993, 4339.

107. Casassa, E. F. and Berry, G. C., in comprehensive Polymer Science, ed. Allen, S.G. and Bevington, J.C., *Pergamon Press*, Oxford, 2, 1989,77.

108. Bueche, A. M., J. Poly. Sci, 15, 1955, 97.

109. Kennedy, J. M., *Macromol. Chem.*, 1, 1980, 296.

110. Koningsveld, R. and Kleintjens, L. A., Liquid – Liquid Phase Separation in Multicomponent Polymer Systems. X. Concentration Dependence of the Pair – Interaction Parameter in the System Cyclohexane – Polystyrene, *Macromolecules*, 4, 1971, 637.

111. Flory, P.J. and Tehner, J., Statistical Mechanics of Cross – Linked Polymer Networks. II. Swelling, *J. Chem. Phys.*, 11, 1943,523.

112. Doong, S. J. and Ho, W. S., Sorption of Organic Vapors in Polyethylene, *Ind. Eng. Chem. Res.*, 30, 1991, 1351.

113. Gundert, F. and Wolf, B.A., Polymer Handbook VII, 3rd ed., *Wiley Interscience*, New York, USA, 1989.

114. Adrams, D. S. and Prausnitz, J.M., Statistical Thermodynamics of the Liquid Mixtures: A New Expression for the Excess Gibbs Energy of Partly or Completely Miscible System. *AIChE J.*, 21, 1975, 116.

115. Grant, D. W. and Takeru, H., Solubility Behavior of Organic Compounds, Techniques of Chemistry, Vol. XXI, *John Wiley & Sons*, New York, USA, June 1989.

116. Yalkowsky, S. H. and Banerjee, S., Aqueous Solubility – Methods of Estimation for Organic Compounds, *Marcel Dekker Inc.*, New York, USA, 1992.

117. Oishi, T. and Prausnitz, J. M., Estimation of Solvent Activities in Polymer Solutions using a Group Contribution Method, *Ind. Eng. Chem. Proc. Des. Dev.*, 17, 1978,333.

118. Goydan, R., Reid, R. C. and Tseng, H. S., Estimation of Solubilities of Organic Compounds in Polymers by Group Contribution Methods, *Ind. Eng. Chem. Res.*, 28, 1989, 445.

119. Heintz, A. and Stephan, W., Separation of Aliphatic/Aromatic Mixtures by Pervaporation using Polyurethene Membranes. Model Calculations and Comparison

with Experimental Reasults, in *Proceedings of Sixth International Conference on Pervaporation Processes in the Chemical Industry*, Ottawa, Canada, September 27 - 30, 1992, 292.

120. Heintz, A. and Stephan, W., A Generalized Solution – Diffusion Model of the Pervaporation Process through Composite Membranes. Part I. Prediction of Mixture Solubilities in the Dense Active Layer using the UNIQUAC MODEL, *J. Membrane Sci.* **89**, 1994, 143.

121. Anderson, T. F. and Prausnitz, J. M., Application to the UNIQUAC Equation to Calculation of Multicomponent Equilibria. I. Vapor – Liquid Equilibria, *Ind. Eng. Chem. Process Des. Dev.*, 17, 1978, 552.

122. Prausnitz, J. M., Lichenthaler, R. N. and Azeovado, E. G., *Molecular Thermodynamics of Fluid – Phase Equilibria, 2nd ed.*, Prentice Hall, Wnglewoods Cliffs, NJ, 1986.

123. Jonquieres, A., Perrin, L., Arnold, S., Clement, R. and Lochon, P., From Binary to Ternary Systems: General Behavior and Modeling of Membrane Sorption in Purely Organic Systems Strongly Deviating from Ideality by UNIQUAC and Related Models, *J. Membrane Sci.*, 174, 2000, 255.

124. Enneking, L., Stephan, W. and Heintz, A., Sorption and Diffusivity Measurements of Cyclohexane/Benzene and Cyclohexane/Toluene Mixtures in Polyurethane Membranes and Modeling the Pervaporation Process, *Ber. Bunsenges. Phys. Chem.*, 97, 1993, 773.

125. Favre, E., Nguyen, Q. T., Clement, R. and Neel, J., The Engaged Species Induced Clustering (ENSIC) Model: A Unified Mechanistic Approach of Sorption Phenomena in Polymers, *J. Membrane Sci.*, 117, 1996, 227.

126. Favre, E., Clement, R. Nguyen, Q. T., Schaetzel, P. and Neel, J., Sorption of Organic Solvents into Dense Silicone Membranes. Part 2. Development of a New Approach Based on a Clustering Hypothesis, *J. Chem. Soc. Faraday Trans.*, 89, 1993, 4339.

127. Yasuda, H. and Stanett, V., Pervaporation, Solution and Diffusion of Water in Some High Polymers, *J. Polym. Sci.*, 57, 1962, 907.

128. Nguyen, Q. T., Favre, E., Clement, R. and Neel, J., Clustering of Solvents in Membranes and its Influence on Membrane Transport Properties, *J. Membrane Sci.*, 113, 1996, 137.

129. Rogers, C. E., Solubility and Diffusivity, in *Physics and Chemistry of the Organic Solid Sate Vol. 2*, eds. Fox, D., Labes M. M. and Weissberger, A., Interscience, New York, 1965.

130. Favre, E., Schaetzel, P., Nguyen, Q.T., Clement, R. and Neel, J., Sorption, Diffusion and Vapor Permeation of Various Penetrants through Dense Poly (dimthylsiloxane) Membranes: A Transport Analysis, *J. Membrane Sci.*, 92, 1994, 169.

131. Jonquieres, A., Perrin, L., Durand, A., Arnold, S., Clement, R. and Lochon, P., Modelling of Vapor Sorption in Polar Materials: Comparison of Flory – Huggins and Related Models with the ENSIC Mechanistic Approach, *J. Membrane Sci.*, 147, 1998, 59.

132. Ruthven, D. M., Principles of Adsorption and Adsorption Processes, *John Wiley and Sons*, NY, 30, 1984.

133. Kiselev, A. V., Vapor Adsorption on Zeolites Considered as Crystalline Specific Adsorbents, *Adv. Chem.*, 102, 1971, 37.

134. Ruthven, D. M., Sorption and Diffusion in Molecular Sieve Zeolites, *Sep. and Purif. Methods*, 5(2), 1976, 189.

135. Derrah, R. I. and Ruthven, D. M., *Canad. J. Chem.*, 543, 1975, 53.

136. Barrer, R. M. and Reucroft, P. J., in *Proceedings of Royal Society of London*, A258, 1960, 431.

137. Rees, L. V. C. and Williams, C. J., Trans. Faraday Soc., 60, 1964, 1973.

138. Barrer, R. M. and Sutherland, J. W., *Proceedings of Royal Society of London*, A237, 1956, 439.

139. Barrer, R. M. Bultitude, F. W. and Sutherland, J. W., *Trans. Faraday Soc.*, 52, 1957, 1111.

140. Breck, D.W. and Grose, R. W., *Adv. In Chem.*, 121, 1973, 319.

141. Ruthven, D. M., *Nature, Phys. Sci.*, 232, 1971, 70.

142. Ruthven, D. M. and Loughlin, K. K ., *J. Chem. Soc. Faraday Trans.*, 68, 1972, 696.

143. Coughlan, B., Kilmartin, S., McEntee and Shaw, R.G., *J. Colloid Interface Sci.*, 52, 1975, 386.

144. Dubinin, M. M., *Chem. Revs.*, 60, 1960, 235.

145. Cointot, A., Couchaudet, J. and Simonot – Grange, M. H., *Bull. Soc. Chem., France*, 1970, 497.

146. Fujita, H., Kishimoto, A. and Matsumoto, K., Concentration and Temperature Dependence of Diffusion Coefficients for Systems – PolymethylAcrylate and N – Alkyl acetates, *Trans. Faraday Soc.*, 56, 1960, 424.

147. Fujita, H., Diffusion in Polymer – Diluents System, *Adv. Polym. Sci.*, 3, 1961, 1.

148. Kreituss, A. and Frisch, H. L., Free – Volume Estimates in Heterogeneous Polymer Systems. I. Diffusion in Crystalline Ethylene – Propylene Copolymers, *J. Polym. Sci. Phys. Ed.*, 19, 1981, 889.

149. Yeom, C. K. and Huang, R. Y. M., A New Method for Determining the Diffusion Coefficients of Penetrants through Polymeric Films from Steady State Pervaporation Experiments, *J. Membrane Sci.*, 68, 1992a, 11.

150. Fang, S. M., Stern, S. A. and Frisch H. L., A Free Volume Model of Permeation of Gas and Liquid Mixtures through Polymeric Membranes, *Chem. Eng. Sci.*, 30, 1975, 773.

151. Yeom, C. K. and Huang, R. Y. M., Modellling of the Pervapotation Separation of Ethanol – Water mixtures through Crosslinked Poly (Vinylalcohol) Membrane, *J. Membrane Sci.*, 67, 1992b.

152. de Pinho, M. N., Rautenbach, R.and Heropm, C., Mass Transfer in Radiation – Grafted Pervaporation Membranes, *J. Membrane Sci.*, 54, 1990, 131.

153. Jeon, E. J. and Kim, S. C., Computer Simulation for the Pervaporation Process of Water/Ethanol Mixture through Interpenetrating Polymer Network (IPN) Membranes, *J. Membrane Sci.*, 80, 1992, 1124.

154. Sferraza, R. A. and Gooding, C. H., Prediction of Sorption Selectivity in Pervaporation Membranes, *in Proceedings of Third International Conference on Pervaporation Processes in Chemical Industry*, Nancy, France, 54, 1988.

155. Doong, D. J. and Ho, W. S., Diffusion of Hydrocarbons in Polyethylene, *Ind. Eng. Chem. Res.*, 31, 1992, 1050.

156. Doong, D. J. and Ho, W. S. and Mastondrea, R. P., Predoctopm pf Flux and Selectivity in Pervaporation through a Membrane, *J. Membrane Sci.*, 107, 1995,129.

157. Dutta, B. K. and Sikdar, S. K., Separation of Azeotropic Organic Liquid Mixtures by Pervaporation, *AIChE J.*, 37 (4), 1991,581.

158. Greenlaw, F. W., Shelden, R. A. and Thompson, E. V., Dependence of Diffusive Permeation Rates on Upstream and Downstream Pressures. II. Two Component Permeation, *J. Membrane Sci.*, 36, 1998, 331.

159. Suzuki, F. and Onozato, K., Pervaporation of Benzene – Cuclohexane Mixtures by Polymethyl – glutamate Membrane and Synergistic Effect of their Mixture on Diffusion Rate, *J. Applied Polymer Sci.*, 27, 1982,4229.

160. Brun, J. P., Larchet, C., Bulvestre, G. And Auclair, B., Sorption and Pervaporation of Dilute Aqueous Solutions of Organic Compounds through Polymer Membranes, *J. Membrane Sci.*, 25, 1985, 55.

161. Brun, J. P., Larchet, C., Melet, R. and Bulvestre, G., Modeling of the Pervaporation of Binary Mixtures through Moderately Swelling, Non – interacting Membranes, *J. Membrane Sci.*, 23, 1985, 257.

162. Bitter, J. G. A., Effect of Crystallinity and Swelling on the Permeability and Selectivity of Polymer Membranes, *Desalination*, 51, 1984, 19.

163. Bitter, J. G. A., Transport Mechanisms in Membrane Separation Processes, *Plenum Press*, New York, 1991.

164. Aust, E., Dahlke, K. and Emig, G., Simulation of Transport and Self – diffusion in Zeolites with the Monte Carlo Method, J. Cata;., 115, 1989, 86.

165. Barrer, R. M., Zeolites and Clay Minerals as Sorbents and Molecular Sieves, *Academic Press*, London, UK, 1978.

166. Riekert, L., Rates of Sorption and Diffusion of Hydrocarbons in Zeolites, *AIChE*, 17, 1971, 446.

167. van den Broeke, L. J. P., Simulation of Diffusion in Zeolitic Structures, *AIChE*, 41, 1995, 2399.

168. Dhaval S. Shah, Pervaporation of Solvent Mixtures Using Polymeric and Zeolitic Membranes: Separation Studies and Modeling, *PhD Thesis*, The Graduate School, University of Kentucky, 2001.

169. Heintz, A. and Stephan, W., A Generalized Solution – Diffusion Model of the Pervaporation Process through Composite Membranes. Part I. Concentration polarization, coupled diffusion and influence of the porous support layer, *J. Membrane Sci.* 89, 1994, 153.

170. Jurgen Baüsa and Wolfgang Marquardt, Detailed Modeling of Stationary and Transient Mass Transfer Across Pervaporation Membranes, *AIChE Journal,* June 2001, Vol. 47, No.6, 1318-1332.

APPINDIX-A

Visual Basic 6.0 Programming for Pervaporation unit:

```
Option Explicit
Const rw As Double = 0.92
Const re As Double = 2.11
Const qw As Double = 1.47
Const qe As Double = 1.97
Const qws As Double = 1
Const qes As Double = 0.92
Const a12 As Double = -2.4936
Const b12 As Double = 756.947
Const a21 As Double = 2.0046
Const b21 As Double = -728.97
Const QR As Double = 0.934
Const QRS As Double = 0.434
Const u1MR As Double = 539.5
Const uM1R As Double = -366.01
Const u2MR As Double = 632.044
Const uM2R As Double = 230.93
Const Dw As Double = 1
Const De As Double = 0.785
Const Dm As Double = 1.2 .
Dim T1M As Double
Dim TM1 As Double
Dim T2M As Double
Dim TM2 As Double
Dim T12 As Double
Dim T21 As Double
Dim lw As Double
Dim le As Double
Dim Tw As Double
Dim Te As Double
Dim Tws As Double
Dim Tes As Double
Dim fr As Double
Dim s As Double
Dim th As Double
Dim fo As Double
Dim fi As Double
Dim six As Double
Dim total As Double
Dim Tm As Double
Dim Tms As Double
```

```vb
Dim ww As Double
Dim we As Double
Dim wwfm As Double
Dim wefm As Double
Dim wwpm As Double
Dim wepm As Double
Dim t As Double
Dim x0 As Double
Dim y0 As Double
Dim Fun1 As Double
Dim Fun2 As Double
Dim F1x As Double
Dim F1y As Double
Dim F2x As Double
Dim F2y As Double
Dim D As Double
Dim x As Double
Dim y As Double
Dim i As Boolean
Dim j As Boolean
Dim Error As Double
Dim m As Double
Dim n As Double

Private Sub Form_Load()
Text8.Text = ""
Text9.Text = ""
Text6.Text = ""
Text7.Text = ""
Text10.Text = ""
Text11.Text = ""
Text12.Text = ""
Text13.Text = ""
Text14.Text = ""
End Sub

Private Sub Command1_Click()
Dim aw As Double
Dim ae As Double
Dim m As Double
Dim n As Double

t = Val(Text3.Text)
m = Val(Text1.Text)
n = 1 - m
ww = (m / 18) / (m / 18 + n / 44)
```

```
we = 1 - ww
Text2.Text = CStr(n)
aw = Activity1(ww, we, t)
ae = Activity2(ww, we, t)
Error = 0.000001
x0 = 0.001
y0 = 0.001
Phase1:
Fun1 = f(x0, y0, t, aw)
Fun2 = g(x0, y0, t, ae)
F1x = f1(x0, y0, t, aw)
F1y = f2(x0, y0, t, aw)
F2x = g1(x0, y0, t, ae)
F2y = g2(x0, y0, t, ae)
D = F1x * F2y - F1y * F2x
x = x0 - (Fun1 * F2y - Fun2 * F1y) / D
y = y0 - (Fun2 * F1x - Fun1 * F2x) / D
If (Abs(x - x0) > Error) Then
    i = True
ElseIf (Abs(y - y0) > Error) Then
    i = True
Else
    i = False
End If
If i = True Then
    x0 = x
    y0 = y
    GoTo Phase1
Else
wefm = y
wwfm = x
Text4.Text = CStr(wwfm)
Text5.Text = CStr(wefm)
Text12.Text = CStr(wwfm / m)
Text13.Text = CStr(wefm / n)
End If
End Sub

Private Sub Command2_Click()
Dim aw As Double
Dim ae As Double
Dim Jw As Double
Dim Je As Double
Dim Ww0 As Double
Dim We0 As Double
Dim Pt As Double
```

```
Dim pw As Double
Dim pe As Double
Dim Pw0 As Double
Dim Pe0 As Double
t = Val(Text3.Text)
ww = Val(Text8.Text)
Pt = Val(Text14.Text)
we = 1 - ww
Text9.Text = CStr(we)
phase3:
pw = ((ww / 18) / (ww / 18 + we / 44)) * Pt
pe = Pt - pw
Pw0 = (10 ^ (8.07131 - 1730.63 / (t + (233.426 - 273.16)))) * 1.33224
aw = pw / Pw0
Pe0 = (10 ^ (8.1122 - 1592.864 / (t + (226.184 - 273.16)))) * 1.33224
ae = pe / Pe0
Error = 0.001
x0 = 0.001
y0 = 0.001
Phase2:
Fun1 = f(x0, y0, t, aw)
Fun2 = g(x0, y0, t, ae)
F1x = f1(x0, y0, t, aw)
F1y = f2(x0, y0, t, aw)
F2x = g1(x0, y0, t, ae)
F2y = g2(x0, y0, t, ae)
D = F1x * F2y - F1y * F2x
x = x0 - (Fun1 * F2y - Fun2 * F1y) / D
y = y0 - (Fun2 * F1x - Fun1 * F2x) / D
If (Abs(x - x0) > Error) Then
    i = True
ElseIf (Abs(y - y0) > Error) Then
    i = True
Else
    i = False
End If
If i = True Then
    x0 = x
    y0 = y
    GoTo Phase2
Else
wwpm = x
wepm = y
End If
Jw = j1(wefm, wepm, wwfm, wwpm)
Je = j2(wefm, wepm, wwfm, wwpm)
```

```
Ww0 = 1 / (1 + (Je * 44 ) / (Jw * 18 ))
We0 = 1 - Ww0
If Abs(Ww0 - ww) > 0.001 Then
j = True
ElseIf Abs(We0 - we) > 0.001 Then
j = True
Else
j = False
End If
If j = True Then
ww = Ww0
we = We0
GoTo phase3
Else
Text8.Text = CStr(ww)
Text9.Text = CStr(we)
Text6.Text = CStr(wwpm)
Text7.Text = CStr(wepm)
Text10.Text = CStr(Jw * 18 )
Text11.Text = CStr(Je * 44 )
End If
End Sub


Public Function Activity1(ww As Double, we As Double, t As Double) As Double


Dim pw As Double
Dim pe As Double

T12 = Exp(a12 + b12 / t)
T21 = Exp(a21 + b21 / t)
lw = 5 * (rw - qw) - (rw - 1)
le = 5 * (re - qe) - (re - 1)
pw = (rw * ww) / (rw * ww + re * we)
pe = 1 - pw
Tw = (qw * pw / rw) / ((qw * pw / rw) + (qe * pe / re))
Te = 1 - Tw
Tws = (qws * pw / rw) / ((qws * pw / rw) + (qes * pe / re))
Tes = 1 - Tws
fr = Log(pw)
s = 5 * qw * Log(Tw / pw)
th = pw * lw + pe * rw * le / re
fo = qws * Log(Tws + Tes * T21)
fi = qws * ((Tws / (Tws + Tes * T21)) + (Tes * T12 / (Tws * T12 + Tes)))
six = fr + s + lw - th - fo + qws - fi
```

```
Activity1 = Exp(six)
End Function
Public Function Activity2(ww As Double, we As Double, t As Double) As Double

Dim pw As Double
Dim pe As Double

T12 = Exp(a12 + b12 / t)
T21 = Exp(a21 + b21 / t)
lw = 5 * (rw - qw) - (rw - 1)
le = 5 * (re - qe) - (re - 1)
pw = (rw * ww) / (rw * ww + re * we)
pe = 1 - pw
Tw = (qw * pw / rw) / ((qw * pw / rw) + (qe * pe / re))
Te = 1 - Tw
Tws = (qws * pw / rw) / ((qws * pw / rw) + (qes * pe / re))
Tes = 1 - Tws
fr = Log(pe)
s = 5 * qe * Log(Te / pe)
th = pw * re * lw / rw + pe * le
fo = qes * Log(Tws * T12 + Tes)
fi = qws * ((Tws * T21 / (Tws + Tes * T21)) + (Tes / (Tws * T12 + Tes)))
six = fr + s + le - th - fo + qes - fi
Activity2 = Exp(six)
End Function


Public Function f(x As Double, y As Double, t As Double, aw As Double) As Double

Dim pw As Double
Dim pe As Double
Dim pm As Double

pw = (x / Dw) / (x / Dw + y / De + (1 - x - y) / Dm)
pe = (y / De) / (x / Dw + y / De + (1 - x - y) / Dm)
pm = 1 - pw - pe
T12 = Exp(a12 + b12 / t)
T21 = Exp(a21 + b21 / t)
T1M = Exp(-u1MR / t)
TM1 = Exp(-uM1R / t)
T2M = Exp(-u2MR / t)
TM2 = Exp(-uM2R / t)
lw = 5 * (rw - qw) - (rw - 1)
le = 5 * (re - qe) - (re - 1)
Tw = (qw * pw / rw) / ((qw * pw / rw) + (qe * pe / re) + QR * pm)
Te = (qe * pe / re) / ((qw * pw / rw) + (qe * pe / re) + QR * pm)
```

```
Tm = 1 - Te - Tw
Tws = (qws * pw / rw) / ((qws * pw / rw) + (qes * pe / re) + QRS * pm)
Tes = (qes * pe / re) / ((qws * pw / rw) + (qes * pe / re) + QRS * pm)
Tms = 1 - Tws - Tes
fr = Log(pw)
s = 5 * qw * Log(Tw / pw)
th = pw * lw + pe * le * rw / re
fo = qws * Log(Tws + Tes * T21 + Tms * TM1)
fi = qws * ((Tws / (Tws + Tes * T21 + Tms * TM1)) + (Tes * T12 / (Tws * T12 + Tes +
Tms * TM2)) + (Tms * T1M / (Tws * T1M + Tes * T2M + Tms)))
six = rw * pm * (5 * (1 - QR) - 1)
f = Exp(fr + s + lw - th - six - fo + qws - fi) - aw
End Function


Public Function g(x As Double, y As Double, t As Double, ae As Double) As Double

Dim pw As Double
Dim pe As Double
Dim pm As Double


pw = (x / Dw) / (x / Dw + y / De + (1 - x - y) / Dm)
pe = (y / De) / (x / Dw + y / De + (1 - x - y) / Dm)
pm = 1 - pw - pe
T12 = Exp(a12 + b12 / t)
T21 = Exp(a21 + b21 / t)
T1M = Exp(-u1MR / t)
TM1 = Exp(-uM1R / t)
T2M = Exp(-u2MR / t)
TM2 = Exp(-uM2R / t)
lw = 5 * (rw - qw) - (rw - 1)
le = 5 * (re - qe) - (re - 1)
Tw = (qw * pw / rw) / ((qw * pw / rw) + (qe * pe / re) + QR * pm)
Te = (qe * pe / re) / ((qw * pw / rw) + (qe * pe / re) + QR * pm)
Tm = 1 - Te - Tw
Tws = (qws * x / rw) / ((qws * x / rw) + (qes * y / re) + QRS * pm)
Tes = (qes * y / re) / ((qws * x / rw) + (qes * y / re) + QRS * pm)
Tms = 1 - Tws - Tes
fr = Log(pe)
s = 5 * qe * Log(Te / pe)
th = pw * re * lw / rw + pe * le
fo = qes * Log(Tws * T12 + Tes + Tms * TM2)
fi = qws * ((Tws * T21 / (Tws + Tes * T21 + Tms * TM1)) + (Tes / (Tws * T12 + Tes +
Tms * TM2)) + (Tms * T2M / (Tws * T1M + Tes * T2M + Tms)))
six = re * pm * (5 * (1 - QR) - 1)
```

g = Exp(fr + s + le - th - six - fo + qes - fi) - ae
End Function

Public Function f1(x As Double, y As Double, t As Double, aw As Double) As Double
f1 = (f(x + 0.0000001, y, t, aw) - f(x - 0.0000001, y, t, aw)) / (2 * 0.0000001)
End Function

Public Function f2(x As Double, y As Double, t As Double, aw As Double) As Double
f2 = (f(x, y + 0.0000001, t, aw) - f(x, y - 0.0000001, t, aw)) / (2 * 0.0000001)
End Function

Public Function g1(x As Double, y As Double, t As Double, ae As Double) As Double
g1 = (g(x + 0.0000001, y, t, ae) - g(x - 0.0000001, y, t, ae)) / (2 * 0.0000001)
End Function

Public Function g2(x As Double, y As Double, t As Double, ae As Double) As Double
g2 = (g(x, y + 0.0000001, t, ae) - g(x, y - 0.0000001, t, ae)) / (2 * 0.0000001)
End Function

Public Function j1(wefm As Double, wepm As Double, wwfm As Double, wwpm As Double) As Double
Dim Di12f As Double
Dim Di13f As Double
Dim Di23f As Double
Dim Di12p As Double
Dim Di13p As Double
Dim Di23p As Double
Dim pwf As Double
Dim pef As Double
Dim pmf As Double
Dim pwp As Double
Dim pep As Double
Dim pmp As Double
Dim Der1f As Double
Dim Der2f As Double
Dim Der1p As Double
Dim Der2p As Double
Dim Diff12f As Double
Dim Diff13f As Double
Dim Diff23f As Double
Dim Diff12p As Double
Dim Diff13p As Double
Dim Diff23p As Double
Dim Diff12 As Double
Dim Diff1M As Double

113

```
Dim Diff2M As Double
Dim Wwa As Double
Dim Wea As Double
Wwa = (wwfm + wwpm) / 2
Wea = (wefm + wepm) / 2
Di12f = d12(t)
Di13f = d13(wwfm, t)
Di23f = d23(wwfm, t)
Di12p = d12(t)
Di13p = d13(wwpm, t)
Di23p = d23(wwpm, t)
pwf = pw(wwfm, wefm)
pef = pe(wwfm, wefm)
pmf = 1 - pwf - pef
pwp = pw(wwpm, wepm)
pep = pe(wwpm, wepm)
pmp = 1 - pwp - pep
Der1f = Derivative1(pwf, pef, pmf, t)
Der2f = Derivative2(pwf, pef, pmf, t)
Der1p = Derivative1(pwp, pep, pmp, t)
Der2p = Derivative2(pwp, pep, pmp, t)
Diff12f = Der1f * Di12f / pmf
Diff13f = Der1f * Di13f / pmf
Diff23f = Der2f * Di23f / pmf
Diff12p = Der1p * Di12p / pmp
Diff13p = Der1p * Di13p / pmp
Diff23p = Der2p * Di23f / pmp
Diff12 = ((Diff12f - Diff12p) / (Log(Diff12f / Diff12p))) * 3600
Diff1M = ((Diff13f - Diff13p) / (Log(Diff13f / Diff13p))) * 3600
Diff2M = ((Diff23f - Diff23p) / (Log(Diff23f / Diff23p))) * 3600
'j1 = 1200 * Diff1M * wwfm / (1.3 * 10 ^ (-7))
j1 = Diff1M * ((Diff2M * Wwa + Diff12) / (Diff12 + Wwa * Diff2M + Wea * Diff1M))
* (1200 * (wwfm - wwpm) / (1.3 * 18 * 10 ^ (-7))) + Diff1M * ((Diff2M * Wwa) /
(Diff12 + Wwa * Diff2M + Wea * Diff1M)) * (1200 * (wefm - wepm) / (1.3 * 18 * 10 ^
(-7)))
End Function


Public Function j2(wefm As Double, wepm As Double, wwfm As Double, wwpm As
Double) As Double
Dim Di12f As Double
Dim Di13f As Double
Dim Di23f As Double
Dim Di12p As Double
Dim Di13p As Double
Dim Di23p As Double
Dim pwf As Double
```

```
Dim pef As Double
Dim pmf As Double
Dim pwp As Double
Dim pep As Double
Dim pmp As Double
Dim Der1f As Double
Dim Der2f As Double
Dim Der1p As Double
Dim Der2p As Double
Dim Diff12f As Double
Dim Diff13f As Double
Dim Diff23f As Double
Dim Diff12p As Double
Dim Diff13p As Double
Dim Diff23p As Double
Dim Diff12 As Double
Dim Diff1M As Double
Dim Diff2M As Double
Dim Wwa As Double
Dim Wea As Double
Wwa = (wwfm + wwpm) / 2
Wea = (wefm + wepm) / 2
Di12f = d12(t)
Di13f = d13(wwfm, t)
Di23f = d23(wwfm, t)
Di12p = d12(t)
Di13p = d13(wwpm, t)
Di23p = d23(wwpm, t)
pwf = pw(wwfm, wefm)
pef = pe(wwfm, wefm)
pmf = 1 - pwf - pef
pwp = pw(wwpm, wepm)
pep = pe(wwpm, wepm)
pmp = 1 - pwp - pep
Der1f = Derivative1(pwf, pef, pmf, t)
Der2f = Derivative2(pwf, pef, pmf, t)
Der1p = Derivative1(pwp, pep, pmp, t)
Der2p = Derivative2(pwp, pep, pmp, t)
Diff12f = Der1f * Di12f / pmf
Diff13f = Der1f * Di13f / pmf
Diff23f = Der2f * Di23f / pmf
Diff12p = Der1p * Di12p / pmp
Diff13p = Der1p * Di13p / pmp
Diff23p = Der2p * Di23f / pmp
Diff12 = ((Diff12f - Diff12p) / (Log(Diff12f / Diff12p))) * 3600
Diff1M = ((Diff13f - Diff13p) / (Log(Diff13f / Diff13p))) * 3600
```

115

Diff2M = ((Diff23f - Diff23p) / (Log(Diff23f / Diff23p))) * 3600
'j2 = 1200 * Diff2M * wefm / (1.3 * 10 ^ (-7))

j2 = Diff2M * ((Diff1M * Wea + Diff12) / (Diff12 + Wwa * Diff2M + Wea * Diff1M)) *
(1200 * (wefm - wepm) / (1.3 * 44 * 10 ^ (-7))) + Diff2M * ((Diff1M * Wea) / (Diff12 +
Wwa * Diff2M + Wea * Diff1M)) * (1200 * (wwfm - wwpm) / (1.3 * 44 * 10 ^ (-7)))
End Function
Public Function d12(t As Double) As Double
d12 = (4.2426 * 10 ^ (-11)) * Exp(22041.4 * (1 / 363.15 - 1 / t))
End Function
Public Function d13(ww As Double, t As Double) As Double
d13 = (2.1786 * 10 ^ (-11)) * (1 + 52.2465 * ww) * Exp(1381.1 * (1 / 363.15 - 1 / t))
End Function
Public Function d23(ww As Double, t As Double) As Double
d23 = (9.5246 * 10 ^ (-13)) * (1 + 33.0635 * ww) * Exp(2994.8 * (1 / 363.15 - 1 / t))
End Function
Public Function pw(ww As Double, we As Double) As Double
pw = (ww / Dw) / (ww / Dw + we / De + (1 - ww - we) / Dm)
End Function
Public Function pe(ww As Double, we As Double) As Double
pe = (we / De) / (ww / Dw + we / De + (1 - ww - we) / Dm)
End Function
Public Function lnaw(pw As Double, pe As Double, pm As Double, t As Double) As
Double
T12 = Exp(a12 + b12 / t)
T21 = Exp(a21 + b21 / t)
T1M = Exp(-u1MR / t)
TM1 = Exp(-uM1R / t)
T2M = Exp(-u2MR / t)
TM2 = Exp(-uM2R / t)
lw = 5 * (rw - qw) - (rw - 1)
le = 5 * (re - qe) - (re - 1)
Tw = (qw * pw / rw) / ((qw * pw / rw) + (qe * pe / re) + QR * pm)
Te = (qe * pe / re) / ((qw * pw / rw) + (qe * pe / re) + QR * pm)
Tm = 1 - Te - Tw
Tws = (qws * pw / rw) / ((qws * pw / rw) + (qes * pe / re) + QRS * pm)
Tes = (qes * pe / re) / ((qws * pw / rw) + (qes * pe / re) + QRS * pm)
Tms = 1 - Tws - Tes
fr = Log(pw)
s = 5 * qw * Log(Tw / pw)
th = pw * lw + pe * le * rw / re
fo = qws * Log(Tws + Tes * T21 + Tms * TM1)
fi = qws * ((Tws / (Tws + Tes * T21 + Tms * TM1)) + (Tes * T12 / (Tws * T12 + Tes +
Tms * TM2)) + (Tms * T1M / (Tws * T1M + Tes * T2M + Tms)))
six = rw * pm * (5 * (1 - QR) - 1)
lnaw = Exp(fr + s + lw - th - six - fo + qws - fi)

End Function

Public Function lnae(pw As Double, pe As Double, pm As Double, t As Double) As Double
T12 = Exp(a12 + b12 / t)
T21 = Exp(a21 + b21 / t)
T1M = Exp(-u1MR / t)
TM1 = Exp(-uM1R / t)
T2M = Exp(-u2MR / t)
TM2 = Exp(-uM2R / t)
lw = 5 * (rw - qw) - (rw - 1)
le = 5 * (re - qe) - (re - 1)
Tw = (qw * pw / rw) / ((qw * pw / rw) + (qe * pe / re) + QR * pm)
Te = (qe * pe / re) / ((qw * pw / rw) + (qe * pe / re) + QR * pm)
Tm = 1 - Te - Tw
Tws = (qws * pw / rw) / ((qws * pw / rw) + (qes * pe / re) + QRS * pm)
Tes = (qes * pe / re) / ((qws * pw / rw) + (qes * pe / re) + QRS * pm)
Tms = 1 - Tws - Tes
fr = Log(pe)
s = 5 * qe * Log(Te / pe)
th = pw * re * lw / rw + pe * le
fo = qes * Log(Tws * T12 + Tes + Tms * TM2)
fi = qws * ((Tws * T21 / (Tws + Tes * T21 + Tms * TM1)) + (Tes / (Tws * T12 + Tes + Tms * TM2)) + (Tms * T2M / (Tws * T1M + Tes * T2M + Tms)))
six = re * pm * (5 * (1 - QR) - 1)
lnae = Exp(fr + s + le - th - six - fo + qes - fi)
End Function
Public Function Derivative1(pw As Double, pe As Double, pm As Double, t As Double) As Double
Derivative1 = ((lnaw(pw + 10 ^ (-15), pe - 10 ^ (-15), pm, t) - lnaw(pw - 10 ^ (-15), pe + 10 ^ (-15), pm, t)) / (2 * 10 ^ (-15))) * pw / lnaw(pw, pe, pm, t)
End Function
Public Function Derivative2(pw As Double, pe As Double, pm As Double, t As Double) As Double
Derivative2 = ((lnae(pw - 10 ^ (-15), pe + 10 ^ (-15), pm, t) - lnae(pw + 10 ^ (-15), pe - 10 ^ (-15), pm, t)) / (2 * 10 ^ (-15))) * pe / lnae(pw, pe, pm, t)
End Function

Visual – Basic 6.0 for Pervaporation unit: Form Design

APPINDIX-B

Micro Language Editor (HYSYS) for Pervaporation unit

```
Option Explicit
Const rw As Double = 0.92
Const re As Double = 2.11
Const qw As Double = 1.47
Const qe As Double = 1.97
Const qws As Double = 1
Const qes As Double = 0.92
Const a12 As Double = -2.4936
Const b12 As Double = 756.947
Const a21 As Double = 2.0046
Const b21 As Double = -728.97
Const QR As Double = 0.934
Const QRS As Double = 0.434
Const u1MR As Double = 539.5
Const uM1R As Double = -366.01
Const u2MR As Double = 632.044
Const uM2R As Double = 230.93
Const Dw As Double = 1
Const De As Double = 0.785
Const Dm As Double = 1.2
Dim T1M As Double
Dim TM1 As Double
Dim T2M As Double
Dim TM2 As Double
Dim T12 As Double
Dim T21 As Double
Dim lw As Double
Dim le As Double
Dim Tw As Double
Dim Te As Double
Dim Tws As Double
Dim Tes As Double
Dim fr As Double
Dim s As Double
Dim th As Double
Dim fo As Double
Dim fi As Double
Dim six As Double
Dim total As Double
Dim Tm As Double
Dim Tms As Double
```

```
Dim ww As Double
Dim we As Double
Dim wwfm As Double
Dim wefm As Double
Dim wwpm As Double
Dim wepm As Double
Const rw As Double = 0.92
Const re As Double = 2.11
Const qw As Double = 1.47
Const qe As Double = 1.97
Const qws As Double = 1
Const qes As Double = 0.92
Const a12 As Double = -2.4936
Const b12 As Double = 756.947
Const a21 As Double = 2.0046
Const b21 As Double = -728.97
Const QR As Double = 0.934
Const QRS As Double = 0.434
Const u1MR As Double = 539.5
Const uM1R As Double = -366.01
Const u2MR As Double = 632.044
Const uM2R As Double = 230.93
Const Dw As Double = 1
Const De As Double = 0.785
Const Dm As Double = 1.2
Dim T1M As Double
Dim TM1 As Double
Dim T2M As Double
Dim TM2 As Double
Dim T12 As Double
Dim T21 As Double
Dim lw As Double
Dim le As Double
Dim Tw As Double
Dim Te As Double
Dim Tws As Double
Dim Tes As Double
Dim fr As Double
Dim s As Double
Dim th As Double
Dim fo As Double
Dim fi As Double
Dim six As Double
Dim total As Double
Dim Tm As Double
Dim Tms As Double
```

```vba
Dim ww As Double
Dim we As Double
Dim wwfm As Double
Dim wefm As Double
Dim wwpm As Double
Dim wepm As Double
Dim t As Double
Dim x0 As Double
Dim y0 As Double
Dim Fun1 As Double
Dim Fun2 As Double
Dim F1x As Double
Dim F1y As Double
Dim F2x As Double
Dim F2y As Double
Dim D As Double
Dim x As Double
Dim y As Double
Dim i As Boolean
Dim j As Boolean
Dim Errorv As Double
Dim m As Double
Dim n As Double
Dim aw As Double
Dim ae As Double


Sub Initialize()
        ' Of the four optional nozzles, we only want the second products:
        ActiveObject.Feeds1Name="Feed"
        ActiveObject.Products1Name="Permeate"
        ActiveObject.Products2Name="Rentate"
        ActiveObject.EnergyFeedsName="Inactive Energy In"
        ActiveObject.EnergyProductsName="Inactive Energy Out"
        ActiveObject.Feeds2Active=False
        ActiveObject.EnergyFeedsActive=False
        ActiveObject.EnergyProductsActive=False

End Sub

Sub Execute()
        On Error GoTo EarlyExit
        ' get the feed stream
        Dim feed As Object
        Set feed= ActiveObject.Feeds1.Item(0)
        If feed Is Nothing Then GoTo EarlyExit
        'get the permeate stream
```

121

```vb
Dim perm As Object
Set perm = ActiveObject.Products1.Item(0)
If perm Is Nothing Then GoTo EarlyExit
'get the retentate stream
Dim rete As Object
Set rete= ActiveObject.Products2.Item(0)
If rete Is Nothing Then GoTo EarlyExit
t = feed.TemperatureValue
perm.Temperature.Calculate(t)
rete.Temperature.Calculate(t)
rete.Pressure.Calculate(feed.PressureValue)
Dim theComps As Object
Dim WaterPosn As Integer
Dim EthanolPosn As Integer
Set theComps= ActiveObject.Flowsheet.FluidPackage.Components
WaterPosn= theComps.index("H2O")
EthanolPosn= theComps.index("Ethanol")
Dim CMFs As Variant
CMFs= feed.ComponentMassFractionValue
ww= CMFs(WaterPosn)
we=CMFs(EthanolPosn)
' Calculation of Feed side activity
aw = Activity1(ww, we, t)
ae = Activity2(ww, we, t)
'First trial
Errorv = 0.000001
x0 = 0.001
y0 = 0.001
Phase1:
        Fun1 = f(x0, y0, t, aw)
        Fun2 = g(x0, y0, t, ae)
        F1x = f1(x0, y0, t, aw)
        F1y = f2(x0, y0, t, aw)
        F2x = g1(x0, y0, t, ae)
        F2y = g2(x0, y0, t, ae)
        D = F1x * F2y - F1y * F2x
        x = x0 - (Fun1 * F2y - Fun2 * F1y) / D
        y = y0 - (Fun2 * F1x - Fun1 * F2x) / D
        If (Abs(x - x0) > Errorv) Then
                i = True
        ElseIf (Abs(y - y0) > Errorv) Then
                i = True
        Else
                i = False
        End If
        If i = True Then
```

```
                    x0 = x
                    y0 = y
                    GoTo Phase1
        Else
                    wefm = y
                    wwfm = x
        End If
'Calculation of mass fraction in membrane phase adjacent to permeate
Dim Jw As Double
Dim Je As Double
Dim Ww0 As Double
Dim We0 As Double
Dim Pt As Double
Dim pvw As Double
Dim pve As Double
Dim Pvw0 As Double
Dim Pve0 As Double
Pt= Permeate.PressureValue
ww=0.9
we= 1-ww
phase3:
        pvw = ((ww / 18) / (ww / 18 + we / 44)) * Pt
        pve = Pt - pvw
        Pvw0 = (10 ^ (8.07131 - 1730.63 / (t + (233.426 - 273.16)))) * 1.33224
        aw = pvw / Pvw0
        Pve0 = (10 ^ (8.1122 - 1592.864 / (t + (226.184 - 273.16)))) * 1.33224
        ae = pve / Pve0
        Errorv = 0.00001
        x0 = 0.001
        y0 = 0.001
Phase2:
        Fun1 = f(x0, y0, t, aw)
        Fun2 = g(x0, y0, t, ae)
        F1x = f1(x0, y0, t, aw)
        F1y = f2(x0, y0, t, aw)
        F2x = g1(x0, y0, t, ae)
        F2y = g2(x0, y0, t, ae)
        D = F1x * F2y - F1y * F2x
        x = x0 - (Fun1 * F2y - Fun2 * F1y) / D
        y = y0 - (Fun2 * F1x - Fun1 * F2x) / D
        If (Abs(x - x0) > Errorv) Then
                i = True
        ElseIf (Abs(y - y0) > Errorv) Then
                i = True
        Else
                i = False
```

123

```
End If
If i = True Then
        x0 = x
        y0 = y
        GoTo Phase2
Else
        wwpm = x
        wepm = y
End If
Jw = j1(wefm, wepm, wwfm, wwpm)
Je = j2(wefm, wepm, wwfm, wwpm)
Ww0 = 1 / (1 + (Je * 44) / (Jw * 18))
We0 = 1 - Ww0
If Abs(Ww0 - ww) > 0.001 Then
        j = True
ElseIf Abs(We0 - we) > 0.001 Then
        j = True
Else
        j = False
End If
If j = True Then
        ww = Ww0
        we = We0
GoTo phase3
End If


CMFs = perm.ComponentMassFraction
For k =0 To theComps.Count - 1
CMFs(k)=0.0
Next k
CMFs(WaterPosn)=Ww0
CMFs(EthanolPosn)=We0
perm.ComponentMassFraction.Calculate(CMFs)
FlowR= feed.MassFlowValue-perm.MassFlowValue
rete.MassFlow.Calculate(FlowR)
CMFs= rete.ComponentMassFraction
For k = 0 To theComps.Count-1
CMFs(k)=0
Next k
CMFs(WaterPosn)=(feed.ComponentMassFlowValue(WaterPosn)-
perm.ComponentMassFlowValue(WaterPosn))/FlowR
        CMFs(EthanolPosn)=(feed.ComponentMassFlowValue(EthanolPosn)-
perm.ComponentMassFlowValue(EthanolPosn))/FlowR
        rete.ComponentMassFraction.Calculate(CMFs)
        ActiveObject.SolveComplete
        EarlyExit:
```

124

```
End Sub

Sub StatusQuery()
        On Error GoTo ThatsAll
        Dim GotOne As Boolean
        GotOne=False
        If ActiveObject.Feeds1.Count=0 Then
        GotOne=True
        ActiveObject.AddStatusCondition(slMissingRequiredInformation,1,"Feed Stream
Required")
        End If
        If ActiveObject.Products1.Count=0 Then
        GetOne = True
        ActiveObject.AddStatusCondition(slMissingRequiredInformation,2, "Permeate
Stream Required")
        End If
        If ActiveObject.Products2.Count=0 Then
        GetOne=True
        ActiveObject.AddStatusCondition(slMissingRequiredInformation,3,"Rentate
Stream Required")
        End If
        If GetOne=True Then GoTo ThatsAll
        Dim Feed As Object
        Set feed= ActiveObject.Feeds1.Item(0)
        If Not feed.Temperature.IsKnown Then
                ActiveObject.AddStatusCondition(slMissingOptionalInformation,4,"Feed
Temperature Unknown")
                GetOne= True
        End If
        If Not feed.Pressure.IsKnown Then
                ActiveObject.AddStatusCondition(slMissingOptionalInformation,5,"Feed
Pressure Unknown")
                GetOne= True
        End If
        If Not feed.MolarFlow.IsKnown Then
                ActiveObject.AddStatusCondition(slMissingOptionalInformation,6,"Feed
Flow Rate Unknown")
                GetOne= True
        End If
        CMFsknown= feed.ComponentMolarFraction.IsKnown
        If Not CMFsknown(0) Then
                ActiveObject.AddStatusCondition(slMissingOptionalInformation,7,"Feed
Composition Unknown")
                GetOne= True
        End If
        If GetOne=True Then GoTo ThatsAll
```

ThatsAll:

End Sub
Public Function Activity1(ww As Double, we As Double, t As Double) As Double

Dim pw As Double
Dim pe As Double

```
T12 = Exp(a12 + b12 / t)
T21 = Exp(a21 + b21 / t)
lw = 5 * (rw - qw) - (rw - 1)
le = 5 * (re - qe) - (re - 1)
pw = (rw * ww) / (rw * ww + re * we)
pe = 1 - pw
Tw = (qw * pw / rw) / ((qw * pw / rw) + (qe * pe / re))
Te = 1 - Tw
Tws = (qws * pw / rw) / ((qws * pw / rw) + (qes * pe / re))
Tes = 1 - Tws
fr = Log(pw)
s = 5 * qw * Log(Tw / pw)
th = pw * lw + pe * rw * le / re
fo = qws * Log(Tws + Tes * T21)
fi = qws * ((Tws / (Tws + Tes * T21)) + (Tes * T12 / (Tws * T12 + Tes)))
six = fr + s + lw - th - fo + qws - fi
Activity1 = Exp(six)
End Function
Public Function Activity2(ww As Double, we As Double, t As Double) As Double
```

Dim pw As Double
Dim pe As Double

```
T12 = Exp(a12 + b12 / t)
T21 = Exp(a21 + b21 / t)
lw = 5 * (rw - qw) - (rw - 1)
le = 5 * (re - qe) - (re - 1)
pw = (rw * ww) / (rw * ww + re * we)
pe = 1 - pw
Tw = (qw * pw / rw) / ((qw * pw / rw) + (qe * pe / re))
Te = 1 - Tw
Tws = (qws * pw / rw) / ((qws * pw / rw) + (qes * pe / re))
Tes = 1 - Tws
fr = Log(pe)
s = 5 * qe * Log(Te / pe)
th = pw * re * lw / rw + pe * le
fo = qes * Log(Tws * T12 + Tes)
```

```vb
fi = qws * ((Tws * T21 / (Tws + Tes * T21)) + (Tes / (Tws * T12 + Tes)))
six = fr + s + le - th - fo + qes - fi
Activity2 = Exp(six)
End Function




Public Function f(x As Double, y As Double, t As Double, aw As Double) As Double

Dim pw As Double
Dim pe As Double
Dim pm As Double

pw = (x / Dw) / (x / Dw + y / De + (1 - x - y) / Dm)
pe = (y / De) / (x / Dw + y / De + (1 - x - y) / Dm)
pm = 1 - pw - pe
T12 = Exp(a12 + b12 / t)
T21 = Exp(a21 + b21 / t)
T1M = Exp(-u1MR / t)
TM1 = Exp(-uM1R / t)
T2M = Exp(-u2MR / t)
TM2 = Exp(-uM2R / t)
lw = 5 * (rw - qw) - (rw - 1)
le = 5 * (re - qe) - (re - 1)
Tw = (qw * pw / rw) / ((qw * pw / rw) + (qe * pe / re) + QR * pm)
Te = (qe * pe / re) / ((qw * pw / rw) + (qe * pe / re) + QR * pm)
Tm = 1 - Te - Tw
Tws = (qws * pw / rw) / ((qws * pw / rw) + (qes * pe / re) + QRS * pm)
Tes = (qes * pe / re) / ((qws * pw / rw) + (qes * pe / re) + QRS * pm)
Tms = 1 - Tws - Tes
fr = Log(pw)
s = 5 * qw * Log(Tw / pw)
th = pw * lw + pe * le * rw / re
fo = qws * Log(Tws + Tes * T21 + Tms * TM1)
fi = qws * ((Tws / (Tws + Tes * T21 + Tms * TM1)) + (Tes * T12 / (Tws * T12 + Tes +
Tms * TM2)) + (Tms * T1M / (Tws * T1M + Tes * T2M + Tms)))
six = rw * pm * (5 * (1 - QR) - 1)
f = Exp(fr + s + lw - th - six - fo + qws - fi) - aw
End Function




Public Function g(x As Double, y As Double, t As Double, ae As Double) As Double

Dim pw As Double
Dim pe As Double
Dim pm As Double
```

```
pw = (x / Dw) / (x / Dw + y / De + (1 - x - y) / Dm)
pe = (y / De) / (x / Dw + y / De + (1 - x - y) / Dm)
pm = 1 - pw - pe
T12 = Exp(a12 + b12 / t)
T21 = Exp(a21 + b21 / t)
T1M = Exp(-u1MR / t)
TM1 = Exp(-uM1R / t)
T2M = Exp(-u2MR / t)
TM2 = Exp(-uM2R / t)
lw = 5 * (rw - qw) - (rw - 1)
le = 5 * (re - qe) - (re - 1)
Tw = (qw * pw / rw) / ((qw * pw / rw) + (qe * pe / re) + QR * pm)
Te = (qe * pe / re) / ((qw * pw / rw) + (qe * pe / re) + QR * pm)
Tm = 1 - Te - Tw
Tws = (qws * x / rw) / ((qws * x / rw) + (qes * y / re) + QRS * pm)
Tes = (qes * y / re) / ((qws * x / rw) + (qes * y / re) + QRS * pm)
Tms = 1 - Tws - Tes
fr = Log(pe)
s = 5 * qe * Log(Te / pe)
th = pw * re * lw / rw + pe * le
fo = qes * Log(Tws * T12 + Tes + Tms * TM2)
fi = qws * ((Tws * T21 / (Tws + Tes * T21 + Tms * TM1)) + (Tes / (Tws * T12 + Tes +
Tms * TM2)) + (Tms * T2M / (Tws * T1M + Tes * T2M + Tms)))
six = re * pm * (5 * (1 - QR) - 1)
g = Exp(fr + s + le - th - six - fo + qes - fi) - ae
End Function


Public Function f1(x As Double, y As Double, t As Double, aw As Double) As Double
f1 = (f(x + 0.0000001, y, t, aw) - f(x - 0.0000001, y, t, aw)) / (2 * 0.0000001)
End Function


Public Function f2(x As Double, y As Double, t As Double, aw As Double) As Double
f2 = (f(x, y + 0.0000001, t, aw) - f(x, y - 0.0000001, t, aw)) / (2 * 0.0000001)
End Function


Public Function g1(x As Double, y As Double, t As Double, ae As Double) As Double
g1 = (g(x + 0.0000001, y, t, ae) - g(x - 0.0000001, y, t, ae)) / (2 * 0.0000001)
End Function


Public Function g2(x As Double, y As Double, t As Double, ae As Double) As Double
g2 = (g(x, y + 0.0000001, t, ae) - g(x, y - 0.0000001, t, ae)) / (2 * 0.0000001)
End Function
```

```
Public Function j1(wefm As Double, wepm As Double, wwfm As Double, wwpm As
Double) As Double
Dim Di12f As Double
Dim Di13f As Double
Dim Di23f As Double
Dim Di12p As Double
Dim Di13p As Double
Dim Di23p As Double
Dim pwf As Double
Dim pef As Double
Dim pmf As Double
Dim pwp As Double
Dim pep As Double
Dim pmp As Double
Dim Der1f As Double
Dim Der2f As Double
Dim Der1p As Double
Dim Der2p As Double
Dim Diff12f As Double
Dim Diff13f As Double
Dim Diff23f As Double
Dim Diff12p As Double
Dim Diff13p As Double
Dim Diff23p As Double
Dim Diff12 As Double
Dim Diff1M As Double
Dim Diff2M As Double
Dim Wwa As Double
Dim Wea As Double
Wwa = (wwfm + wwpm) / 2
Wea = (wefm + wepm) / 2
Di12f = d12(t)
Di13f = d13(wwfm, t)
Di23f = d23(wwfm, t)
Di12p = d12(t)
Di13p = d13(wwpm, t)
Di23p = d23(wwpm, t)
pwf = pww(wwfm, wefm)
pef = pee(wwfm, wefm)
pmf = 1 - pwf - pef
pwp = pww(wwpm, wepm)
pep = pee(wwpm, wepm)
pmp = 1 - pwp - pep
Der1f = Derivative1(pwf, pef, pmf, t)
Der2f = Derivative2(pwf, pef, pmf, t)
Der1p = Derivative1(pwp, pep, pmp, t)
```

```
Der2p = Derivative2(pwp, pep, pmp, t)
Diff12f = Der1f * Di12f / pmf
Diff13f = Der1f * Di13f / pmf
Diff23f = Der2f * Di23f / pmf
Diff12p = Der1p * Di12p / pmp
Diff13p = Der1p * Di13p / pmp
Diff23p = Der2p * Di23f / pmp
Diff12 = ((Diff12f - Diff12p) / (Log(Diff12f / Diff12p))) * 3600
Diff1M = ((Diff13f - Diff13p) / (Log(Diff13f / Diff13p))) * 3600
Diff2M = ((Diff23f - Diff23p) / (Log(Diff23f / Diff23p))) * 3600
'j1 = 1200 * Diff1M * wwfm / (1.3 * 10 ^ (-7))
j1 = Diff1M * ((Diff2M * Wwa + Diff12) / (Diff12 + Wwa * Diff2M + Wea * Diff1M))
* (1200 * (wwfm - wwpm) / (1.3 * 18 * 10 ^ (-7))) + Diff1M * ((Diff2M * Wwa) /
(Diff12 + Wwa * Diff2M + Wea * Diff1M)) * (1200 * (wefm - wepm) / (1.3 * 18 * 10 ^
(-7)))
End Function


Public Function j2(wefm As Double, wepm As Double, wwfm As Double, wwpm As
Double) As Double
Dim Di12f As Double
Dim Di13f As Double
Dim Di23f As Double
Dim Di12p As Double
Dim Di13p As Double
Dim Di23p As Double
Dim pwf As Double
Dim pef As Double
Dim pmf As Double
Dim pwp As Double
Dim pep As Double
Dim pmp As Double
Dim Der1f As Double
Dim Der2f As Double
Dim Der1p As Double
Dim Der2p As Double
Dim Diff12f As Double
Dim Diff13f As Double
Dim Diff23f As Double
Dim Diff12p As Double
Dim Diff13p As Double
Dim Diff23p As Double
Dim Diff12 As Double
Dim Diff1M As Double
Dim Diff2M As Double
Dim Wwa As Double
Dim Wea As Double
```

```
Wwa = (wwfm + wwpm) / 2
Wea = (wefm + wepm) / 2
Di12f = d12(t)
Di13f = d13(wwfm, t)
Di23f = d23(wwfm, t)
Di12p = d12(t)
Di13p = d13(wwpm, t)
Di23p = d23(wwpm, t)
pwf = pww(wwfm, wefm)
pef = pee(wwfm, wefm)
pmf = 1 - pwf - pef
pwp = pww(wwpm, wepm)
pep = pee(wwpm, wepm)
pmp = 1 - pwp - pep
Der1f = Derivative1(pwf, pef, pmf, t)
Der2f = Derivative2(pwf, pef, pmf, t)
Der1p = Derivative1(pwp, pep, pmp, t)
Der2p = Derivative2(pwp, pep, pmp, t)
Diff12f = Der1f * Di12f / pmf
Diff13f = Der1f * Di13f / pmf
Diff23f = Der2f * Di23f / pmf
Diff12p = Der1p * Di12p / pmp
Diff13p = Der1p * Di13p / pmp
Diff23p = Der2p * Di23f / pmp
Diff12 = ((Diff12f - Diff12p) / (Log(Diff12f / Diff12p))) * 3600
Diff1M = ((Diff13f - Diff13p) / (Log(Diff13f / Diff13p))) * 3600
Diff2M = ((Diff23f - Diff23p) / (Log(Diff23f / Diff23p))) * 3600
'j2 = 1200 * Diff2M * wefm / (1.3 * 10 ^ (-7))

j2 = Diff2M * ((Diff1M * Wea + Diff12) / (Diff12 + Wwa * Diff2M + Wea * Diff1M)) *
(1200 * (wefm - wepm) / (1.3 * 44 * 10 ^ (-7))) + Diff2M * ((Diff1M * Wea) / (Diff12 +
Wwa * Diff2M + Wea * Diff1M)) * (1200 * (wwfm - wwpm) / (1.3 * 44 * 10 ^ (-7)))
End Function
Public Function d12(t As Double) As Double
d12 = (4.2426 * 10 ^ (-11)) * Exp(22041.4 * (1 / 363.15 - 1 / t))
End Function
Public Function d13(ww As Double, t As Double) As Double
d13 = (2.1786 * 10 ^ (-11)) * (1 + 52.2465 * ww) * Exp(1381.1 * (1 / 363.15 - 1 / t))
End Function
Public Function d23(ww As Double, t As Double) As Double
d23 = (9.5246 * 10 ^ (-13)) * (1 + 33.0635 * ww) * Exp(2994.8 * (1 / 363.15 - 1 / t))
End Function
Public Function pww(ww As Double, we As Double) As Double
pww = (ww / Dw) / (ww / Dw + we / De + (1 - ww - we) / Dm)
End Function
Public Function pee(ww As Double, we As Double) As Double
```

pee = (we / De) / (ww / Dw + we / De + (1 - ww - we) / Dm)
End Function
Public Function lnaw(pw As Double, pe As Double, pm As Double, t As Double) As Double
T12 = Exp(a12 + b12 / t)
T21 = Exp(a21 + b21 / t)
T1M = Exp(-u1MR / t)
TM1 = Exp(-uM1R / t)
T2M = Exp(-u2MR / t)
TM2 = Exp(-uM2R / t)
lw = 5 * (rw - qw) - (rw - 1)
le = 5 * (re - qe) - (re - 1)
Tw = (qw * pw / rw) / ((qw * pw / rw) + (qe * pe / re) + QR * pm)
Te = (qe * pe / re) / ((qw * pw / rw) + (qe * pe / re) + QR * pm)
Tm = 1 - Te - Tw
Tws = (qws * pw / rw) / ((qws * pw / rw) + (qes * pe / re) + QRS * pm)
Tes = (qes * pe / re) / ((qws * pw / rw) + (qes * pe / re) + QRS * pm)
Tms = 1 - Tws - Tes
fr = Log(pw)
s = 5 * qw * Log(Tw / pw)
th = pw * lw + pe * le * rw / re
fo = qws * Log(Tws + Tes * T21 + Tms * TM1)
fi = qws * ((Tws / (Tws + Tes * T21 + Tms * TM1)) + (Tes * T12 / (Tws * T12 + Tes + Tms * TM2)) + (Tms * T1M / (Tws * T1M + Tes * T2M + Tms)))
six = rw * pm * (5 * (1 - QR) - 1)
lnaw = Exp(fr + s + lw - th - six - fo + qws - fi)
End Function

Public Function lnae(pw As Double, pe As Double, pm As Double, t As Double) As Double
T12 = Exp(a12 + b12 / t)
T21 = Exp(a21 + b21 / t)
T1M = Exp(-u1MR / t)
TM1 = Exp(-uM1R / t)
T2M = Exp(-u2MR / t)
TM2 = Exp(-uM2R / t)
lw = 5 * (rw - qw) - (rw - 1)
le = 5 * (re - qe) - (re - 1)
Tw = (qw * pw / rw) / ((qw * pw / rw) + (qe * pe / re) + QR * pm)
Te = (qe * pe / re) / ((qw * pw / rw) + (qe * pe / re) + QR * pm)
Tm = 1 - Te - Tw
Tws = (qws * pw / rw) / ((qws * pw / rw) + (qes * pe / re) + QRS * pm)
Tes = (qes * pe / re) / ((qws * pw / rw) + (qes * pe / re) + QRS * pm)
Tms = 1 - Tws - Tes
fr = Log(pe)
s = 5 * qe * Log(Te / pe)

th = pw * re * lw / rw + pe * le

fo = qes * Log(Tws * T12 + Tes + Tms * TM2)

fi = qws * ((Tws * T21 / (Tws + Tes * T21 + Tms * TM1)) + (Tes / (Tws * T12 + Tes + Tms * TM2)) + (Tms * T2M / (Tws * T1M + Tes * T2M + Tms)))

six = re * pm * (5 * (1 - QR) - 1)

lnae = Exp(fr + s + le - th - six - fo + qes - fi)

End Function

Public Function Derivative1(pw As Double, pe As Double, pm As Double, t As Double) As Double

Derivative1 = ((lnaw(pw + 10 ^ (-15), pe - 10 ^ (-15), pm, t) - lnaw(pw - 10 ^ (-15), pe + 10 ^ (-15), pm, t)) / (2 * 10 ^ (-15))) * pw / lnaw(pw, pe, pm, t)

End Function

Public Function Derivative2(pw As Double, pe As Double, pm As Double, t As Double) As Double

Derivative2 = ((lnae(pw - 10 ^ (-15), pe + 10 ^ (-15), pm, t) - lnae(pw + 10 ^ (-15), pe - 10 ^ (-15), pm, t)) / (2 * 10 ^ (-15))) * pe / lnae(pw, pe, pm, t)

End Function